STRUCTURAL AND QUANTITATIVE STUDIES ON THE NORMAL C3H AND LURCHER MUTANT MOUSE

By K. W. T. CADDY† and T. J. BISCOE‡
Department of Physiology, University of Bristol, Bristol BS8 1TD, U.K.

(*Communicated by B. D. Burns, F.R.S. – Received 1 September* 1978)

[Plates 1–15]

CONTENTS

PAGE

I. Introduction 170

II. Methods 170
1. Breeding 170
2. Light microscopy 171
3. Quantification 171
(*a*) General comments on the counting methods 171
(*b*) The number of Purkinje cells 173
(*c*) The number of granule cells 174
(*d*) The number of inferior olivary neurons 174
(*e*) The number of neurons in the deep cerebellar nuclei 174
(*f*) Electron microscopy 175
(*g*) Golgi–Cox technique 175

III. Results 175
1. Qualitative 175
(*a*) The structure of the cerebellum of the normal mouse 175
(i) The Purkinje cell 176
(*b*) The structure of the cerebellum of the heterozygote Lurcher mouse (*Lc*/+) 176
(i) The Purkinje cell 176
(*c*) The interneurons of the cerebellum in the normal and Lurcher mouse 178
(i) The Golgi cell 178
(ii) The basket cell 178
(iii) The stellate cell 178
(iv) The granule cell 178

† Present address: Department of Neuroscience, Children's Hospital Medical Center, 300 Longwood Avenue, Boston, Massachusetts 02115, U.S.A.
‡ Present address: Department of Physiology, University College London, Gower Street, London WC1E 6BT, U.K.

PAGE

(*d*) The structure of the inferior olivary nucleus from the normal and Lurcher mouse 179
(*e*) The mossy and climbing fibres of the normal and Lurcher mouse 179
(*f*) The structure of the deep cerebellar nuclei from the normal and Lurcher mouse 180
2. Quantitative results in the normal mouse 181
(*a*) Purkinje cells 181
(*b*) Granule cells 182
(*c*) Olive neurons 183
(*d*) Deep cerebellar nuclei 183
(*e*) Ratio of neuron numbers 184
3. Quantitative results in the Lurcher mouse 185
(*a*) Purkinje cells 185
(*b*) Granule cells 185
(*c*) Olive neurons 185
(*d*) Deep cerebellar nuclei 186
(*e*) Ratio of neuron numbers 186

IV. Discussion 187
1. Qualitative results in the normal mouse 187
2. Quantitative results in the normal mouse 187
(*a*) Purkinje cells 187
(*b*) Granule cells 190
(*c*) Olive neurons 191
(*d*) Deep cerebellar nuclei neurons 191
3. Qualitative results in the Lurcher mouse 191
(*a*) Purkinje cell changes and other cerebellar mutants 191
(*b*) Granule cells 193
(*c*) Olive neurons 193
(*d*) Deep cerebellar nuclei neurons 194
4. Quantitative results in the Lurcher mouse 194
(*a*) Purkinje cells 194
(*b*) Granule cells 194
(*c*) Olive neurons 195
(*d*) Deep cerebellar nuclei neurons 195
5. Experimentally produced lesions and the Lurcher mutation 195
6. Ratio of neuron numbers 197
7. Concluding remarks 197

References 198

The cerebellum, the deep cerebellar nuclei, and the inferior olivary nucleus of the heterozygote Lurcher mutant mouse have been compared with the same structures in normal littermates. The comparison was made using light and electron microscopic methods for qualitative observations and light microscopic methods for quantitative observations. The study included the newborn period from 4 days of age up to 730 days, which is old age for a mouse.

The cerebellum of the normal mouse is similar to that of many other species though apparently minor structural differences are seen. Amongst these was the similarity between the mouse climbing fibre and mossy fibre glomeruli which contrasts with the rat where they can be distinguished by the high density of synaptic vesicles and central cluster of mitochondria in the climbing fibres. In Golgi stained material the inferior olivary nucleus of the normal mouse showed cells with highly ramified dendrites and cells with simple dendrite patterns.

In the adult Lurcher mouse the cerebellum is much smaller than is normal. There are no Purkinje cells and the internal granule cell layer is reduced in thickness and density. Examination of younger animals shows that Purkinje cells are present and that they undergo degeneration. In Golgi stained material from younger animals Purkinje cells often show more than one primary dendrite, sometimes as many as five, and somatic spines persist well beyond the first week of life. Cytoplasmic organelles often have a random orientation and the mitochondria are rounded rather like those seen in the nervous mutant. Granule cells in the adult Lurcher mutant are reduced in number and during the developmental period degenerative changes are seen. The Golgi cells and stellate cells are relatively normal and some cells, identified as basket cells, are seen.

The inferior olivary nucleus is found with ease in the Lurcher mutant and is as extensive as in the normal mouse. However, in Golgi stained material only cells with highly ramified dendrites are seen. In addition the total number of neurons is reduced. It is possible that the neurons with a simple dendrite pattern have climbing fibres which pass only to the Purkinje cells.

The deep cerebellar nuclei in the normal mouse cannot be separated easily into their three subdivisions, lateral, interpositus and medial. In the Lurcher mutant the neurons are of similar size to those of the normal mouse but they are crowded more closely together than is normal. In the Lurcher mutant as in the normal adult the neuronal cell bodies are covered with synapses and not with glial cells.

Estimates of total cell numbers were made in order to obtain evidence about the time course of the development of the changes in structure and to make a detailed comparison between the normal mouse and the Lurcher mutant with respect to Purkinje cells, granule cells, olive neurons, and deep cerebellar nuclei neurons.

In the normal mouse the mean number of Purkinje cells between 10 and 730 days was 177000, s.d. $\pm$ 11600, $n = 12$. The number of granule cells probably reached a peak at about 17 days. At 26 days post-natal the number estimated was 27 million and at 730 days 28 million. The mean number of olive neurons between 14 and 730 days post-natal was 32700, s.d. $\pm$ 1900, $n = 9$; the mean number of deep cerebellar neurons counted at three adult ages was 17600, s.d. $\pm$ 1800. In the adult the ratio of Purkinje cells to olive cells is *ca.* 5.4:1, of granule cells to Purkinje cells is *ca.* 170:1, of Purkinje cells to deep cerebellar nuclei neurons is *ca.* 10:1, and of olive neurons to deep cerebellar nuclei neurons is *ca.* 1.85:1. This last would chiefly be of interest if there are olive neurons projecting solely to deep cerebellar neurons.

In the Lurcher mutant the number of Purkinje cells falls below normal from 8 days post-natally, reaches 10% of normal at 26 days and probably falls to zero at around 90 days. At this point such are the changes in the overall structure that confusion of Purkinje cells with Golgi cells may occur. At 4 days post-natal age the number of granule cells is smaller than normal by 25% and this difference increases with age to a reduction of *ca.* 90%. The number of olive cells is close to normal until 8 days of age, is only 60% of normal at 15 days when the highest number is reached, and is 25% of normal at 121 days. The deep cerebellar nuclei neuron numbers were the same as those in the normal.

Included in the discussion is a detailed critical comparison of these results from the normal mouse with all previous estimates of cell numbers in the cerebellum. The lesion in Lurcher is compared with that found in the other mouse cerebellar mutants and with experimentally evoked lesions of the cerebellum. For the Lurcher mutant the tentative conclusion is that the primary lesion may arise in the Purkinje cells.

I. Introduction

The Lurcher mutation arose spontaneously in the mouse colony of the Medical Research Council Radiobiological Research Unit at Harwell in 1954 and was described by Phillips (1960). The Lurcher mouse is recognized by its behavioural abnormality and with experience the mutant may be identified as early as 10 days post-natal. The behaviour was described by Phillips (1960) as a 'characteristic swaying of the hind quarters during which they fall to one side or the other as if their legs "gave way"'. The mutants also run backwards whereas a normal mouse never does this. In her paper on Lurcher, Phillips (1960) gave the position of the mutant gene on linkage group XI, chromosome 6 of the house mouse. She also showed that it was a semi-dominant gene lethal within the first few post-natal days in the homozygous condition. The heterozygote (*Lc*/+) lives to adult life, thrives, and breeds well although females tend to have smaller litters than normal. The colony in Bristol was obtained from Harwell as *Lc Mi*^{wh}/+ + on C3H background. When we obtained this mutant the nature of the neurological lesion was unknown, however, on removal of the cranium of an adult mutant animal it was immediately obvious that Lurcher had a very small cerebellum. Since then a number of studies have appeared concerned with the heterozygote (*Lc*/+) (Caddy & Biscoe 1975, 1976; Caddy, Martin & Biscoe 1977; Martin & Caddy 1977; Swisher & Wilson 1975, 1977; Vijayan & Wilson 1975; Wilson 1975, 1976).

Since our ultimate objective is to define the primary lesion it is clear that one necessary part of the definition of the lesion involves examination of the development. In order to attempt to do this the numbers of different cell types have been estimated at various ages. It follows that the numbers must be obtained for the normal as well as the affected animals.

This paper deals exclusively with the lesion in the heterozygote and provides an account of our findings on the normal and mutant mouse. The paper includes both qualitative and quantitative information.

II. Methods

1. *Breeding*

The animals used in this study were bred from three pairs given to us by Dr A. G. Searle of the M.R.C. Radiobiological Research Unit at Harwell. Normal animals were of the C3H strain of inbred mice. The Lurcher, *Lc*, gene is closely linked to *Mi*^{wh} which therefore made recognition of Lurcher heterozygotes reasonably easy. By mating + +/+ + females with *Lc Mi*^{wh}/+ + males offspring would be *Lc Mi*^{wh} (light brown heterozygotes); *Lc*+ (dark brown Lurcher heterozygotes); +*Mi*^{wh} (light brown normals); and + + (dark brown normals). The ratio of *Lc Mi*^{wh}:*Lc*+ would be about 10:1 and the ratio of + + :+*Mi*^{wh} would also be about 10:1. The Lurcher heterozygotes are fertile and are as healthy as normal mice. To recognize Lurcher mice younger than 10 or 11 days post-natal age homozygous *Mi*^{wh} females were bred

with *Lc* Mi^{wh}/+ + males. Since some cross-over occurs this meant that not all but some 90 % of the foetuses without eye pigmentation were Lurcher mutants.

Normal littermate controls have been used where possible otherwise normals were obtained by crossing + +/+ + females with + +/+ + males.

2. *Light microscopy*

Animals of less than 6 days post-natal age were killed with an overdose of pentobarbitone sodium (Nembutal) and the whole brain dissected out. The brains were then placed in Bouin's fixative for approximately 18 h. Animals older than 6 days were deeply anaesthetized with pentobarbitone sodium administered intraperitoneally (0.01 ml/g body mass of a 6 mg/ml solution, that is 60 μg/g) and perfused through the left ventricle, firstly with physiological saline and then with Bouin's fixative. These brains were then treated in the same way as those from the younger animals. The tissue was embedded in paraffin wax and 10 μm sections stained with luxol fast blue and cresyl violet. Most of the tissue was sectioned in the coronal (frontal) plane although some brains were cut sagittally. All the brains (except those from mice 730 days after birth) were sequentially sectioned; that is 2×10 μm sections cut and then five sections discarded. The animals 730 days old were sectioned serially at 10 μm. Photomicrographs were taken with a Zeiss Photomicroscope on Kodak Panatomic X film.

3. *Quantification*

(*a*) *General comments on the counting method*

In this study we were interested in estimating the total numbers of cells in particular populations, in seeing how these numbers changed during development, and in comparing the estimated totals from normal and Lurcher mice. Since we are not presenting our results in terms of cell densities we have not found it necessary to make allowances for the shrinkage that may occur during fixation and processing, (Palkovits *et al.* 1971 *a*, *b*, *c*; Hall *et al.* 1975).

The number of neurons in a particular population may be estimated by counting the number of cell bodies, or of nuclei, or of nucleoli. It is clear that the larger the size of the unit counted and the thinner the section in which it lies then the greater will be the probability that any particular unit may be cut so that parts of it will lie in more than one section. Thus the probability of counting that particular unit will be increased and the counts will be spuriously high.

In the present work the unit we have used for the counts was the nucleus in the case of the granule cells and the nucleolus in all other cases. The nucleus was chosen for the granule cells because the nucleolus is not resolved very easily in the light microscope and too much uncertainty was introduced by attempting to count it. The nucleolus was chosen in the other cases because it was the smallest object that was well within the resolving power of the light microscope, that could be recognized with ease, and that usually only occurred once in every nerve cell. So, for the present work the most important questions are concerned with the problem of split nuclei and split nucleoli.

For the granule cells the Abercrombie correction (Abercrombie 1946) was applied since the nucleus is *ca.* 4 μm in diameter, the section thickness was 10 μm throughout, and the nucleus was cut by the microtome knife. The case for the application of the correction is clear enough.

However, where nucleoli were counted the case for the application of a correction was less clear in our material and is discussed below.

The correction factors in common usage (see, for example, Abercrombie 1946; Floderus 1944) depend for their application on the premise that the nucleolus is cut or shattered by the microtome knife. That this might not always be the case was suggested by Jones (1937) on the grounds that the nucleolus may be harder than the surrounding tissue and hence be displaced. This suggestion was supported by the work of Cammermeyer (1967) on the rabbit, cat, chinchilla and mouse brain. He found that up to 2.8 % of nucleoli were either dislodged or displaced from the region of the surface of the section. Examination of our material from different ages and in the normal and Lurcher mutant shows that this is indeed so and we have seen examples of the displacements shown by Cammermeyer (1967) where the nucleolus may be found on the edge of the nucleus, apparently within the cytoplasm of the cell, immediately outside the cell, or some distance from the cell. This displacement is commonly in the direction of the cutting stroke and the nucleolus appears to be intact. As a corollary of these observations we have found that 2 % of cells cannot be shown to have nucleoli in any section. This would follow if the nucleolus were in fact displaced in some cells and so not recognized.

Further evidence for the displacement of nucleoli rather than for their being split comes from measurements on nucleolar size. If the true nucleolar diameters are distributed normally it follows that in the event that the nucleolus were split the measured diameter histogram should show a distribution skewed to the left. The problem of measurement here concerns the size of the nucleolus which in the cells of interest to us is about 2 μm in diameter. Our measurements show that the nucleolar diameters for Purkinje cells and olive cells are indeed normally distributed, though we do not place great reliance on measurements which necessarily are at the limits of resolution. Nevertheless they do not support the view that the nucleolus is split.

Consideration of the consequences of splitting the nucleoli also suggests that in the majority of cases the split fragments would in general be very small, would be stained less densely than whole nucleoli, or nucleoli split exactly at the equator, and would therefore be much less likely to be recognized and counted. Thus since one of the criteria used by the observer for recognizing a nucleolus is the relatively constant size in one cell population a judgement is continually made by the observer about what is acceptable as a nucleolus and what is not, a judgement which will make fragments less likely to be counted.

None of these points is germane to the problem that arises from the presence of two or more nucleoli. In our material some 2 % of cells appear to have two nucleoli though the number is sometimes greater in counts made on tissue from animals at about 10 days of age. We have accepted the principle that when two nucleoli can be seen in one cell, then only one is added to the total. However, this does not resolve the difficulty. Clearly, an accurate estimate of the true number of paired nucleoli is difficult to make because cells at the surfaces of the sections may be cut in such a way that one nucleolus will be in each half of a cell. Thus in the simplest case if the nucleoli are randomly distributed in a spherical nucleus the actual number of cells with paired nucleoli will be greater than 2 %. In practice examination of serial sections with the use of *camera lucida* drawings to make the comparison shows that the same cell may have a nucleolus in each of two sections in 2 % of cases. This error neatly cancels against the equal and opposite error produced by the presence of cells having no nucleoli, probably due to displacement.

It is acknowledged that measurements of nucleolar size are difficult to make with accuracy,

and comparison of serial sections by *camera lucida* drawings is often inaccurate. However, the fact that the errors described do count one against the other even if their magnitude is in dispute leads us to the conclusion that the best course is to not correct our original counts.

It is clear that without verification by alternative methods the results of the counting procedures must be treated with caution. In experiments quite separate from these we have been able to use two independent methods, namely to count the number of cells and the number of axons in the facial nucleus and facial nerve of the rat (Martin, Caddy & Biscoe 1977). In these experiments the number of myelinated axons in the nerve corresponded very well with the number of nerve cells uncorrected for split nucleoli. If a split nucleolus correction was applied given the size of the nucleolus and the section thickness then the estimate introduced a disparity of up to 34 %. Since the material was prepared in exactly the same way as in the experiments described here those results re-inforce our view that the correction should not be used.

Lastly, it is clear that it is unsafe to generalize about the application of correction factors because much will depend upon the exact nature of the material. When epon embedding is used, the nucleolus is certainly cut. However, in our paraffin wax procedures, we have no evidence that it is cut, quite the reverse. In other laboratories using other procedures, and in other parts of the central nervous system, then other conditions may apply. We conclude that each observer must reach his own conclusions about his material based on careful observation of the fate of the object that is to be enumerated.

(*b*) *The number of Purkinje cells*

The number of Purkinje cells was estimated for cerebella from animals aged between 4 and 730 days. In all the quantitative work undertaken only those neurones with nucleoli were counted. In coronal sections the Purkinje cells appear as a line of cells and the Purkinje cell line was defined as the length of line connecting adjacent cells. In the Lurcher mouse where the number of Purkinje cells is reduced the boundary between the granule cell and molecular layers was measured instead. In principle the number of Purkinje cells was estimated by multiplying the total length of this line by the number of Purkinje cells per millimetre of line. The Purkinje cell densities were found by counting the number of Purkinje cells along specific lengths of Purkinje cell line and dividing this by the length on which they lay. (The Purkinje cells were counted at a magnification of 500 times on a Reichert Biopan microscope.) These lengths as well as the total length of Purkinje cell line were measured by drawing the complete Purkinje cell lines from every 20th section at 40 times magnification by using a drawing apparatus on a Reichert Biopan microscope and then by using a D-MAC graphic table linked to a PDP 8 (DEC Corporation) computer to measure the lengths of line drawn. Once this information was obtained the following formula was used to calculate the total length of Purkinje cell line:

$$L = \tfrac{1}{2} \sum_{i=1}^{n-1} (l_i + l_{i+1})\, S_{i,\, i+1},$$

where l is length of Purkinje cell line per section, S is number of sections missed between counted sections (usually 20), and n is total number of sections measured. If D is the density of Purkinje cells per unit length, then the total number of Purkinje cells $N = LD$.

(*c*) *The number of granule cells*

The method used for estimating the total number of granule cells is very similar to that of Palkovits *et al.* (1971 *b*), the number of cells in a unit area of section is multiplied by the total area occupied by the granule cells. A grid drawn in white on a black background was superimposed on the image of the cerebellum with the *camera lucida*. This grid appeared as 36 10×10 μm squares and the section was observed at a magnification of 500 times. Counts of granule cells were made in all lobules in every 20th section. The sections were 10 μm thick and therefore there were usually an average of only two layers of granule cells per section which made counting, while focusing through the section, relatively easy. The granule cell number was calculated in granule cells per micrometre squared. The total area of the granule cell layer was obtained by measuring the granule cell layer width and multiplying the mean value of width by the total length of Purkinje cell line which had been obtained for calculating the number of Purkinje cells. Such a calculation treats the granule cell layer as a rectangle, which clearly it is not, but the errors introduced would be small enough to be negligible. The largest errors, in fact, would be at the deepest and most superficial parts of the folium where the folium curves most sharply and so the Purkinje cell line is concave in the deep parts and convex in the superficial parts. Thus the granule cell layer resembles a series of half annuli of circles connected by rectangles. The error introduced by calculating the granule cell layer area as if it were a rectangle is less than 0.001 %. The figure for the area of granule cell layer was a total for all the sections which contained any granule cells, therefore from the product of this area and the granule cell density we obtained a total for the number of granule cells per cerebellum. This number was then corrected for split nucleus using the Abercrombie (1946) correction for which our variables were 10 μm thick sections and 4 μm diameter nucleus.

(*d*) *The number of inferior olivary neurons*

The number of olive neurons was found by counting all the neurons in every seventh section and multiplying by seven. This number was then doubled to obtain the number of olive neurons per animal as only the right olive was counted in each case. To enable all the olive neurons to be counted, firstly the sections were projected at 260 times magnification onto drawing paper. The right olive was then drawn around and a few details in a small area filled in to enable orientation of the drawing when only looking at a small portion on the *camera lucida*. The drawings were then placed under the camera lucida drawing apparatus and the magnification was adjusted so that through the drawing apparatus it was 260 times and through the binocular eyepiece of the microscope it was 500 times. A cross was drawn over the olive neurons as they were identified and when one part of the olive had been scanned the paper was moved to a new field. The cells identified as olive neurons were those with a dark staining nucleolus in a pale staining, eccentrically placed nucleus and had cytoplasm containing heavily stained Nissl substance. The number of crosses on these drawings of olivary sections were counted and these numbers were then multiplied by 14 to obtain the total number of olivary neurons per animal.

(*e*) *The number of neurons in the deep cerebellar nuclei*

Neurons in *nuclei medialis*, *interpositus* and *lateralis* have been counted as a whole. Courville & Cooper (1970) for the monkey have concluded that it is possible to distinguish between nuclear

groups on the basis of (1) course of fibre bundles, (2) differential density of the neuropil and (3) orientation of component fibres. To these criteria Chan-Palay (1977) has added cytological characteristics of individual cells, their size, shape and organization for the dentate nucleus in rat and monkey. In this study on the mouse the distinctions between nuclear groups were less clear because the nuclei are smaller and in the mutant animal the nuclei were flattened in the dorso-ventral plane. The counts were made in a similar manner to that used for the inferior olivary nucleus.

(*f*) *Electron microscopy*

Animals were anaesthetized and those older than 5–6 days were fixed by intracardiac perfusion. In younger animals parts of the c.n.s. were dissected out and placed in the fixative. The fixative in all experiments was a 1 % glutaraldehyde and 1 % paraformaldehyde mixture in 0.1 M sodium cacodylate buffered to pH 7.3–7.4 with 0.1 M HCl. If the cerebellum of the animal was to be studied the tissue was bisected mid-sagittally and cut into approximately 1 mm thick sagittal slices. These cerebellar slices were then cut into triangular wedges to enable orientation during the embedding process. When the tissue was to be used to study the olive and the deep cerebellar nuclei the tissue was cut into 1 mm thick coronal slices and then with the aid of a dissecting microscope and a scalpel blade it was possible to dissect out these nuclei. When the tissue had been reduced to a block no larger than $2 \times 2 \times 1$ mm it was washed in buffer, placed in the secondary fixative, 1 % OsO_4 in 0.1 M sodium cacodylate buffer, for $1\frac{1}{4}$–$1\frac{1}{2}$ h, stained *en bloc* with 2 % uranyl acetate maleic acid (pH 5.2), dehydrated and embedded in Epon 812. Sections 1–2 μm thick were stained with methylene blue to allow further orientation of the block. Thin sections were examined by using a Philips EM300 electron microscope.

(*g*) *Golgi–Cox technique*

Out of all the modifications of Golgi techniques available we used the method of Hollingworth & Berry (1975) the details of which were given to us by Dr Berry. This technique has been changed very slightly by them from a technique used by Sholl (1953).

The fixative contains mercuric chloride and the tissue is left in the fixing solution for 6 weeks in the dark. Subsequent processing was conventional and after embedding in celloidin, sections were cut alternately 100 and 60 μm thick. The 60 μm thick sections were counterstained with cresyl violet.

Photomicrographs of these slides were made by using a Zeiss Photomicroscope and Kodak Panatomic X film.

This method was found to be extremely reliable and seems to impregnate cells randomly (Pasternak & Woolsey 1975).

III. Results

1. *Qualitative*

(*a*) *The structure of the cerebellum of the normal mouse*

The cerebellum of the normal mouse is similar to that of many other species. However the mouse does confer one advantage, it is large enough to allow physiological experiments to be performed and yet small enough to allow sampling of a substantial amount of the structure so that quantitative data can be obtained. The cerebellum is a laminated structure (see figure 1)†

† Figures 1–44 are on plates 1–15.

consisting of five layers in mice less than 15 days old and four layers thereafter (Larsell 1970; Larsell & Jansen 1972).

(i) *The Purkinje cell.* The Purkinje cells are the largest neurons in the cerebellum (*ca.* 20 μm diam.) and have one of the most elaborate dendritic trees to be found in the central nervous system. A Purkinje cell from a mouse 15 days old is shown in figure 3. The Golgi–Cox impregnation allows the spines on the dendrites to be seen. This cell has attained its adult configuration as Golgi–Cox impregnated tissue from animals over 1 year old has shown.

In the electron microscope the large nucleus of the Purkinje cell appears pale and the nucleolus is very electron dense. The nuclear membrane is consistently smooth in the mouse Purkinje cell which contrasts with the wrinkled membrane found by Palay & Chan-Palay (1974) in the rat. The nucleus is surrounded by rough endoplasmic reticulum (e.r.) and the cytoplasm has free ribosomes scattered throughout. Golgi apparatus is abundant and there are many mitochondria in the cytoplasm. Microtubules and neurofilaments fill up the interstices between the other organelles. Fortuitous sections include the primary dendrite of the Purkinje cell. In the primary dendrite the organelles align themselves parallel with the major axis of the dendrite; this alignment is especially well shown by the mitochondria, neurotubules and neurofilaments. This longitudinal arrangement continues throughout the major portion of the dendritic tree. Several cell types make synaptic contact with the dendrites and dendritic spines of Purkinje cells. Figure 7 shows a Purkinje cell dendrite with a spine, at arrow, making synaptic contact with a parallel fibre. Figure 8 shows a dendrite with several spines of different types. One of the spines has a single stalk but two heads (arrow), both heads are closely apposed to many parallel fibres. None of these parallel fibres appears to be in synaptic contact with the spines (i.e. no synaptic thickening is apparent). The spine indicated by a crossed arrow has two parallel fibre enlargements in close proximity but again there are no thickenings or other obvious synaptic elements. The spine shown in figure 8 marked by an arrowhead, is much smaller than the other two but it too has no synaptic contact.

(*b*) *The structure of the cerebellum of the heterozygote Lurcher mouse* (*Lc*/+)

Macroscopically the cerebellum in the adult heterozygous Lurcher mutant mouse is very small and may be easily distinguished from normal at about 20 days post-natal. In younger animals the reduction in size is not so obvious but with experience an affected brain can be recognized as early as 11 or 12 days after birth by the differing amounts of posterior colliculus and obex visible.

A sagittal section through the cerebellum of an adult Lurcher mouse stained with luxol fast blue and cresyl violet is shown in figure 2. It is the same magnification as the cerebellum of the adult mouse in figure 1 and is therefore directly comparable. The inserts (also identical magnification) show that although all the lobules are present the cerebellum is much smaller than the normal. Referring to the light micrograph in figure 2 one sees at once the apparent reduction in staining intensity of the internal granule cell layer and upon close inspection it is possible to note the absence of Purkinje cells at the boundary between the internal granule cell and molecular layers (Caddy & Biscoe 1975; Swisher & Wilson 1975, 1977).

(i) *The Purkinje cell.* Three Golgi–Cox stained Purkinje cells from a mouse 14 days old are shown in figures 4–6. The sections containing these cells have also been counterstained with cresyl violet and therefore the granule cells in the internal granule cell layer (i.g.l.) can be seen. The sections are 60 μm thick and therefore all the dendrites are not in focus. In contrast to the normal Purkinje cell which usually has a single primary dendrite all three of these Purkinje

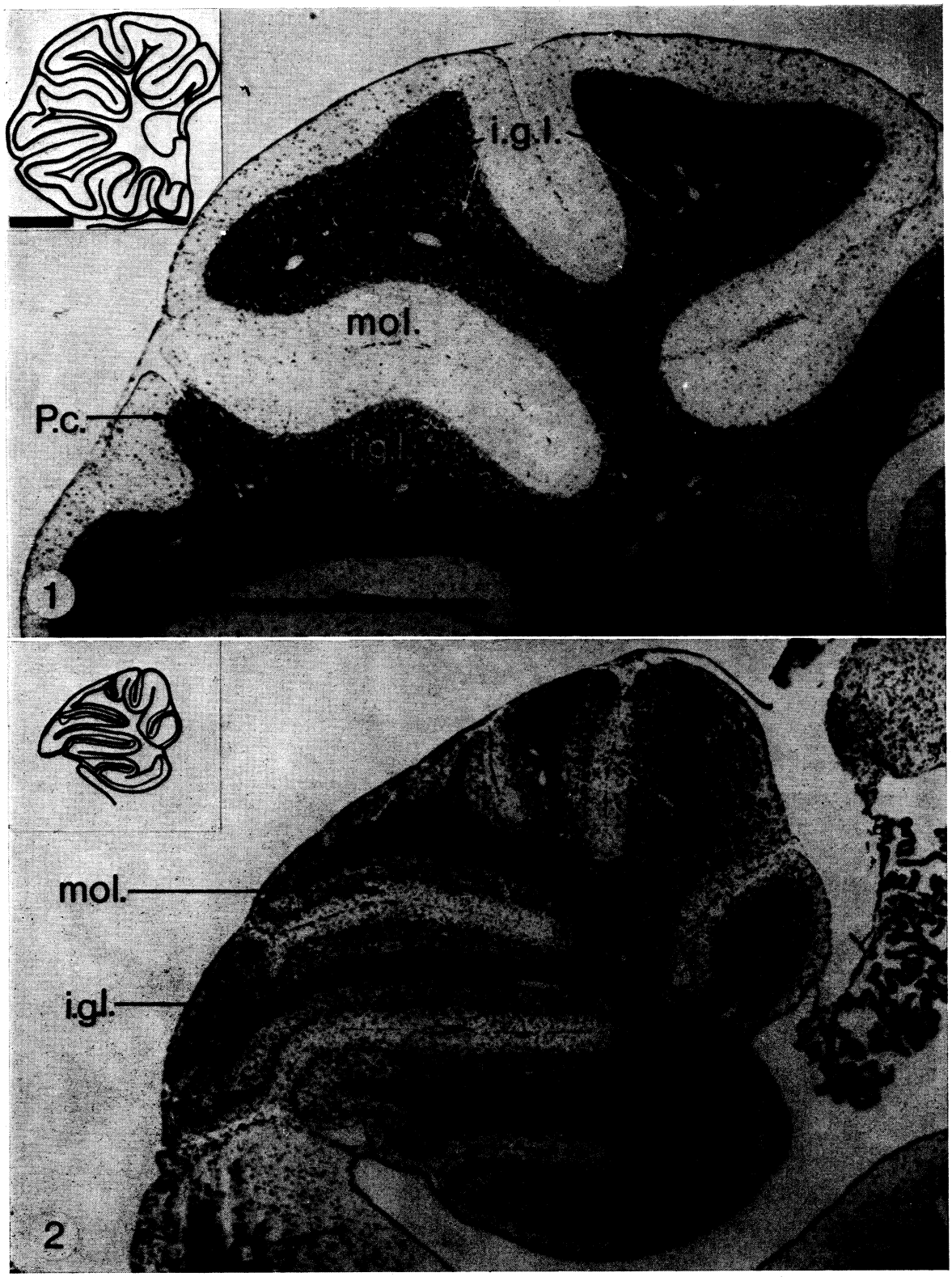

Light micrographs of sagittal sections of cerebellum from adult mice. Inserts show drawings of whole sections to compare size of normal cerebellum with that of the Lurcher mutant mouse. Sections stained with luxol fast blue and cresyl violet. Figures 1 and 2 are the same magnification as are the inserts; calibration bars for all photographs = 1 mm. Abbreviations: mol., molecular layer; i.g.l., internal granule cell layer; P.c., Purkinje cell layer; w.m., white matter.

FIGURE 1. The different layers of the cerebellum in the normal mouse are easily seen in this figure. Section taken from an animal 77 days old.

FIGURE 2. The loss of Purkinje and granule cells in this section of a Lurcher mouse cerebellum is obvious but the overall laminated structure is still maintained. Section from an animal 50 days old.

(*Facing p.* 176)

Light micrographs of Golgi–Cox impregnated tissue showing Purkinje cells from normal and Lurcher mice. Calibration bar = 10 μm for all micrographs.

FIGURE 3. Cell from a 15 day post-natal normal cerebellum showing the pial surface (pia) in the top left-hand corner. The smooth primary and secondary dendrites and spines on the more distal dendrites are easily seen. The section is 100 μm thick and fortunately the majority of this dendritic tree is in the plane of focus.

FIGURES 4–6. Examples of Purkinje cells seen in a 14 day post-natal Lurcher mouse. Spines can be seen on the dendrites and also on the soma of the Purkinje cell in 6. Axons are arrowed in 4 and 5. These sections are counterstained with cresyl violet and therefore the internal granule cell layer is visible (i.g.l.).

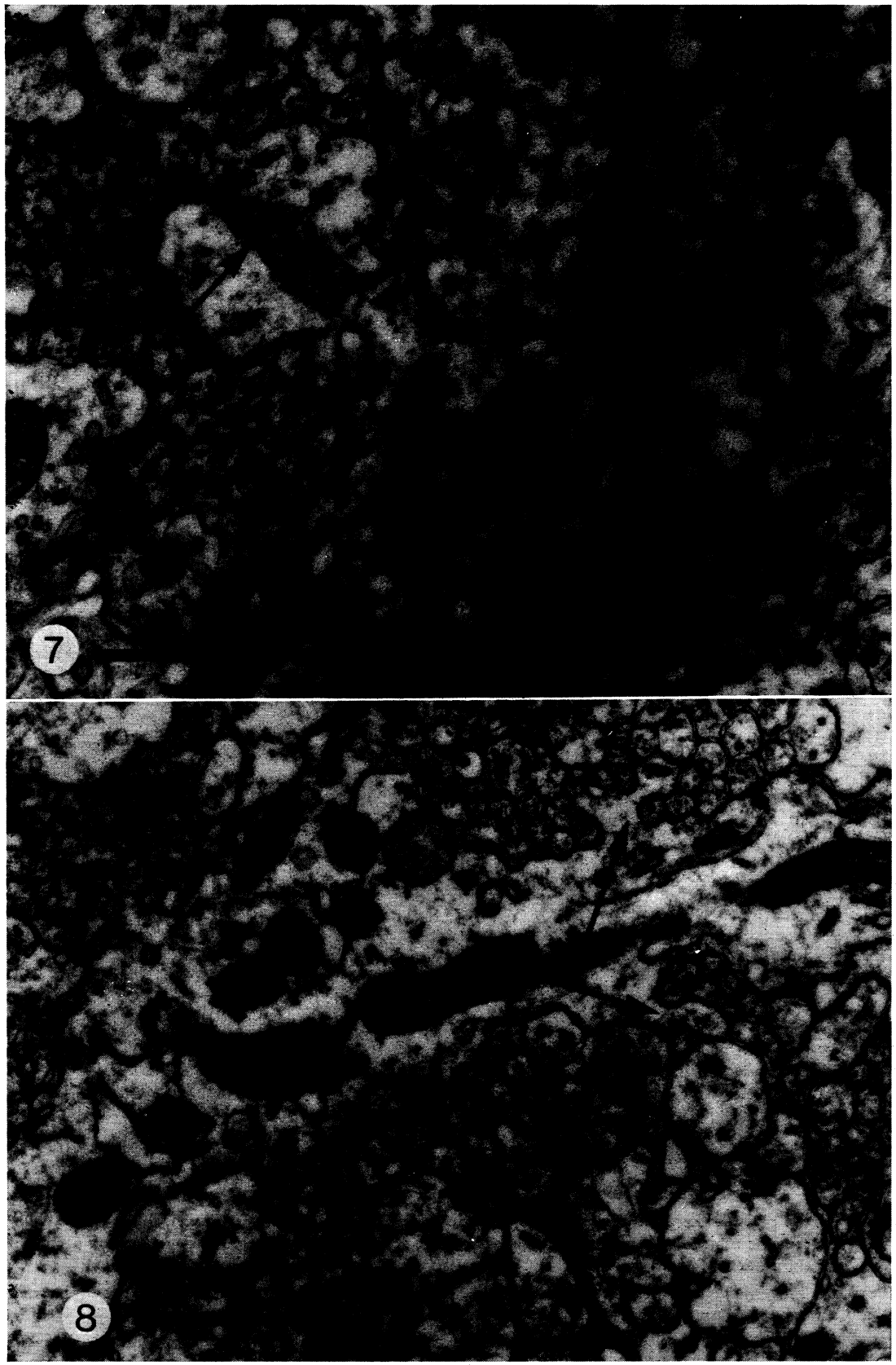

Electron micrographs of Purkinje cell dendrites from normal mice. Calibration bar = 1 μm for both micrographs.

FIGURE 7. Dendrite from a mouse 14 days old, surrounded by parallel fibres (stars) cut in cross section. A parallel fibre is seen synapsing with a dendritic spine (arrow).

FIGURE 8. Dendrite from a mouse 13 days old with three different spines. None of these spines is in synaptic contact with a parallel fibre although fibres surround them.

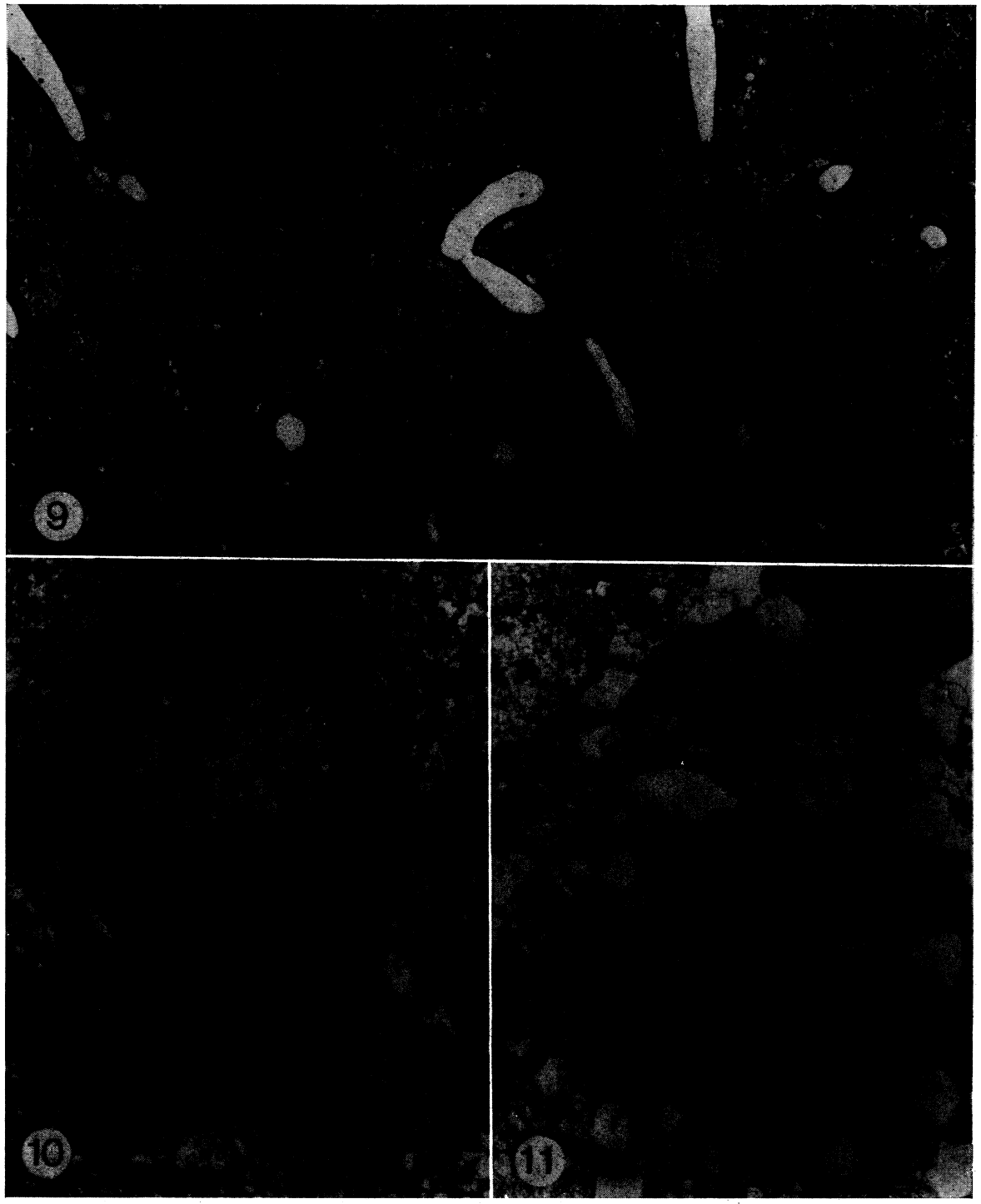

Electron micrographs from Lurcher mutant mice 15 days old.

FIGURE 9. Low power electron micrograph showing the internal granule cell layer (i.g.l.), the Purkinje cell layer (P.c.), and the molecular layer (mol.). Three Purkinje cells in different stages of degeneration are arrowed. Calibration bar = 10 μm.

FIGURE 10. Purkinje cell arrowed far left in figure 9. This higher power electron micrograph shows the rounded up mitochondria and the disrupted endoplasmic reticulum. Calibration bar = 1 μm.

FIGURE 11. Purkinje cell in an advanced stage of degeneration. The rounded profiles of mitochondria are visible. Calibration bar = 1 μm.

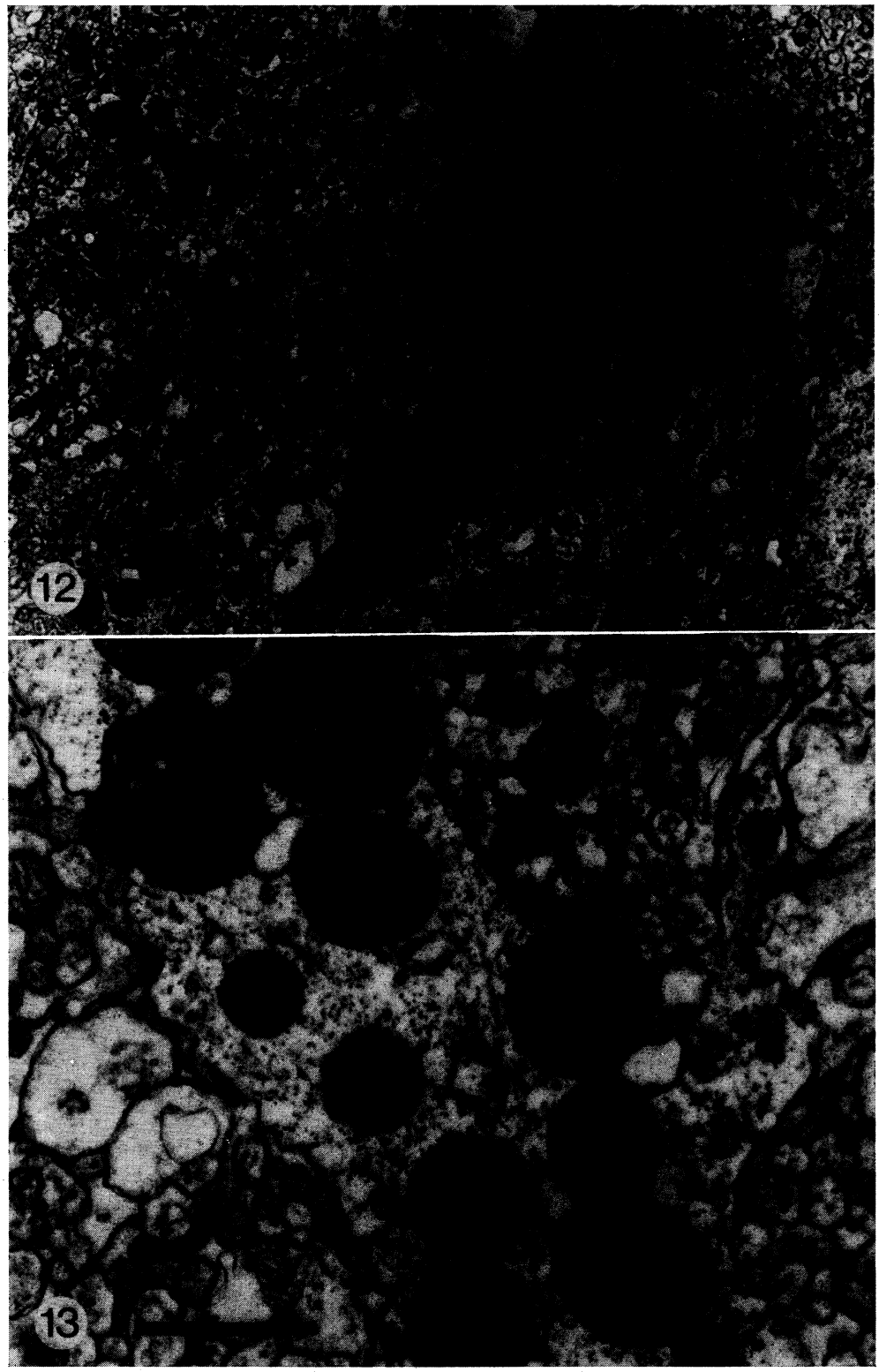

Electron micrographs of Purkinje cell dendrites from a Lurcher mouse 17 days old. Calibration bars =

FIGURE 12. Two portions of a dendrite can be seen. They are almost full of spherical mitochondria.

FIGURE 13. Higher magnification micrograph of figure 12 to show the unusual pattern of cristae in the spherical mitochondria.

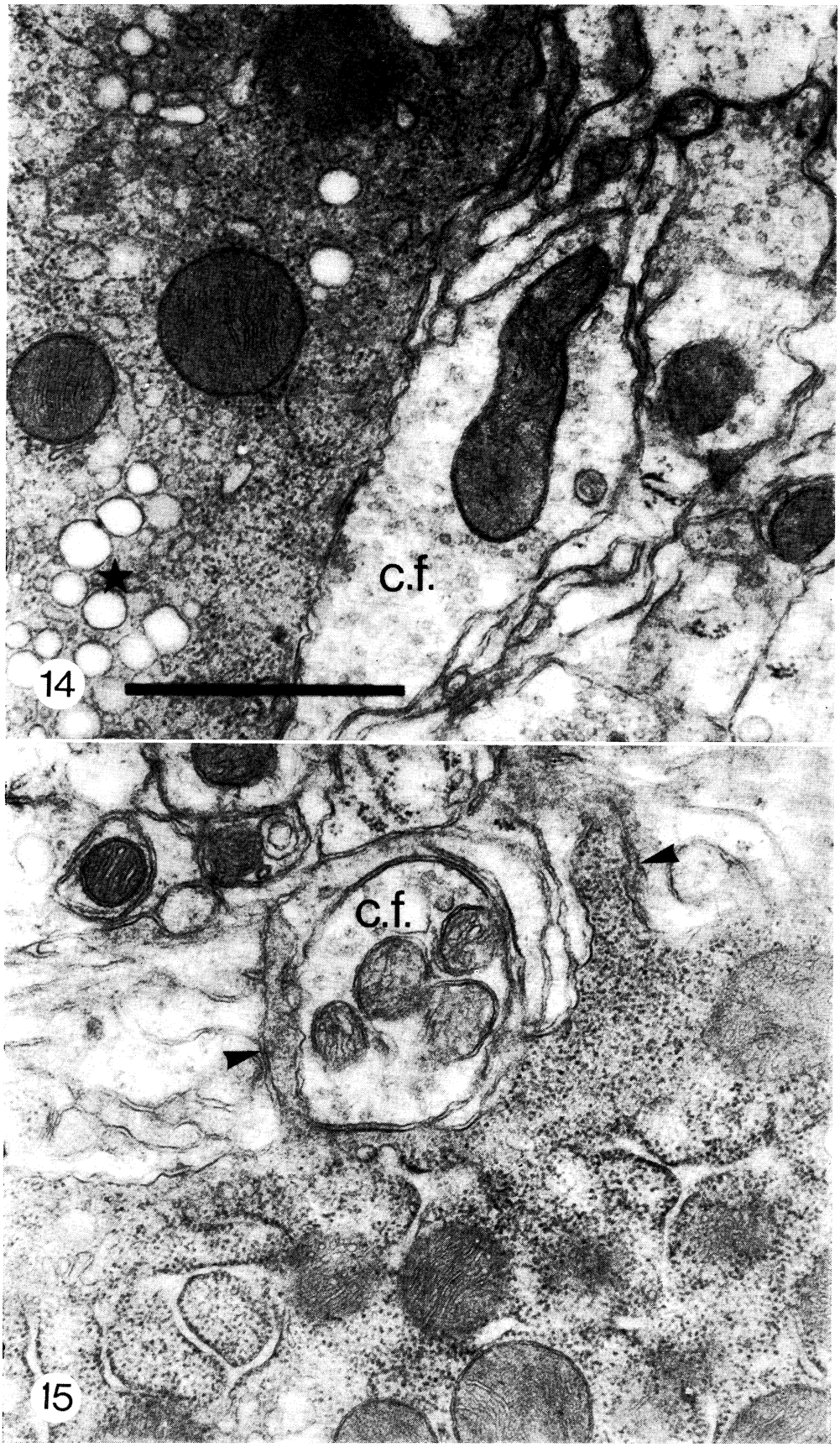

Electron micrographs of Purkinje cell dendrites from a Lurcher mouse 15 days old.
Calibration bar = 1 μm for both micrographs.

FIGURE 14. Dendrite on left in an advanced state of degeneration. Vacuoles (star) are present in the cytoplasm and a climbing fibre (c.f.) is in close apposition to the dendrite.

FIGURE 15. Two slender spines (arrowheads) emerge from the dendrite at the bottom of the field. A climbing fibre (c.f.) is closely apposed to one of these spines.

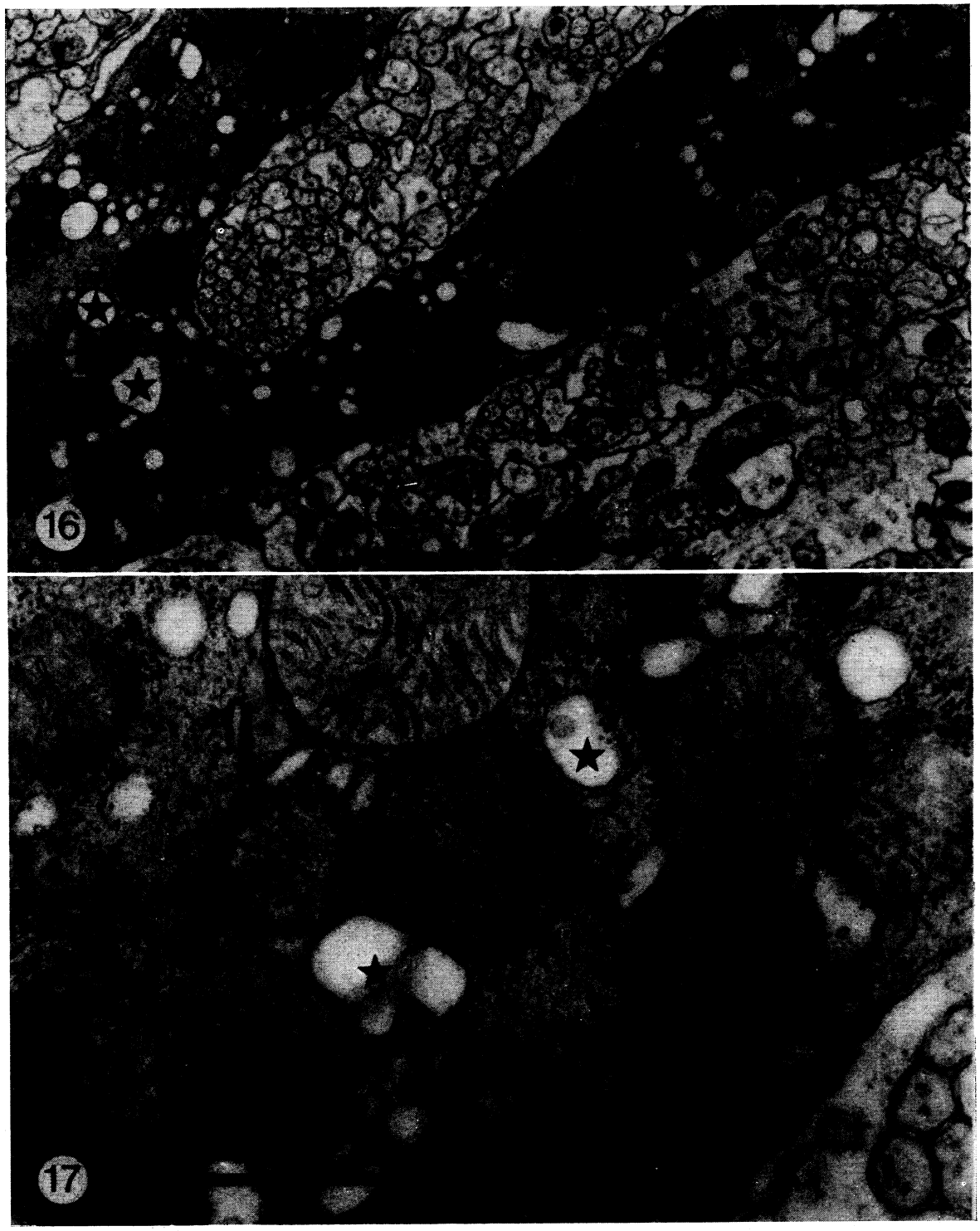

Electron micrographs of the Purkinie cell dendrites from a Lurcher mouse 17 days old. Calibration bars = 1 μm.

FIGURE 16. A dendrite in a very advanced state of degeneration. Neurofilaments and vacuoles (stars) can be seen in an electron-dense matrix which fills the dendrite.

FIGURE 17. Higher power micrograph of figure 16 showing the cristae patterns in the mitochondria, the vacuoles (stars) and the increased density of ribosomes.

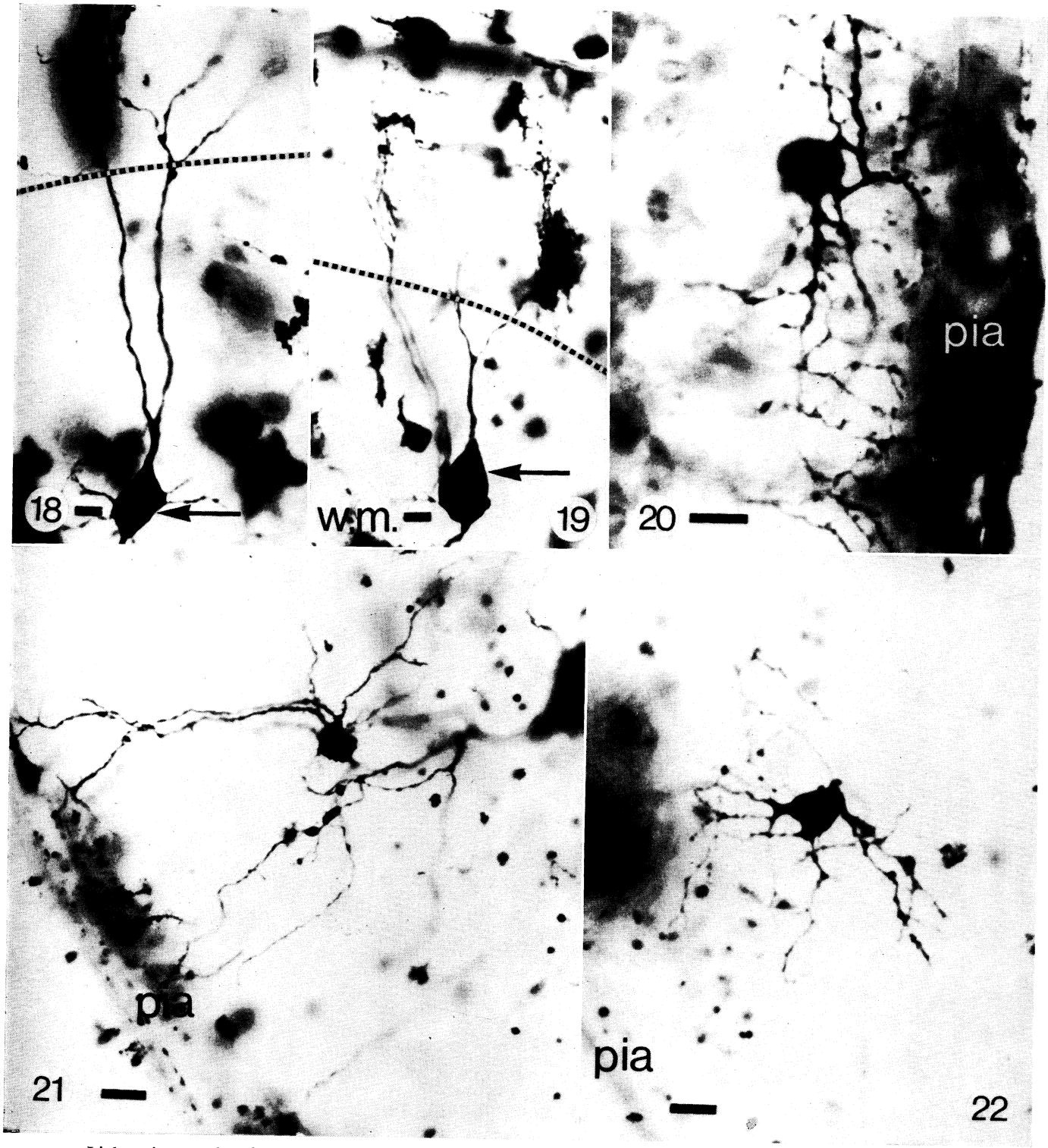

Light micrographs of Golgi–Cox impregnated tissue showing stellate cells, Golgi cells and a basket cell from normal and Lurcher mice. Sections are 100 μm thick except figure 22 which is 60 μm thick and counterstained with cresyl violet. Calibration bars = 10 μm.

FIGURE 18. Golgi cell from a normal mouse 429 days old showing two long main dendrites stretching towards the molecular layer where they branch profusely. Dashed line represents the level of the Purkinje cells.

FIGURE 19. Golgi cell from a Lurcher mouse 380 days old cerebellum showing essentially the same features as in figure 18.

FIGURE 20. A basket cell from a Lurcher mouse 14 days old is seen in the molecular layer close to the pial surface (pia). Most of the branching axons are rising towards the pial surface rather than descending towards the Purkinje cell layer. No Purkinje cells are in the area shown in this micrograph.

FIGURE 21. A stellate cell from a normal mouse 15 days old is shown with dendrites extending from pial surface to Purkinje cell layer.

FIGURE 22. A stellate cell from a Lurcher mouse 14 days old is shown. Its soma is closer to the Purkinje cell layer than in figure 18 and hence its dendritic tree extends in the direction of the pial surface.

cells have more than two primary dendrites, figure 4 shows at least three, figure 5 shows five and figure 6 shows three (compare our figure 4 with fig. 7*b* from Altman 1976*a*). The dendritic trees of these Lurcher cells are obviously smaller than that of the normal cell shown in figure 3. Dendritic spines can be seen and somatic spines are visible in figure 6. These somatic spines normally disappear about 7 days after birth and certainly before 15 days after birth. Axons can be seen emerging from the soma of the Purkinje cells in figures 4 and 5 (arrow).

The Purkinje cells from the Lurcher at 13 days after birth are quite different from the normal Purkinje cells. The nuclei in these 13 day Lurcher Purkinje cells are not circular in profile but have an irregular nuclear membrane. The Nissl bodies are disorganized although still positioned around the nucleus of the cell. The cytoplasm in the dendrites of these cells is disorganized and the organelles have a random orientation rather than lying parallel to the long axis of the dendrite as in the normal. At 15 days after birth in the Lurcher cerebellum normal as well as abnormal Purkinje cells are still found. Figure 9 shows a low power electron micrograph of several Purkinje cells. Three Purkinje cells abnormal in different ways are indicated by arrows. The Purkinje cell on the left looks normal except for the mitochondria which appear circular in this section. The Purkinje cell in the middle has a more electron dense cytoplasm than normal and also shows circular mitochondria. The arrowed Purkinje cell on the right in figure 9 shows a very electron dense cytoplasm and nucleus and at this magnification it is difficult to determine where the nucleus finishes and the cytoplasm begins. This cell also contains circular mitochondria. This mitochondrial change seems to take place in all the degenerating Purkinje cells studied in the Lurcher and we have never seen similar changes in the normal. Figure 10 shows, at higher magnification, the Purkinje cell to the left of figure 9. The majority of the mitochondria in this cell have circular profiles which would indicate that they are more uniform in shape and size, and are more commonly spherical than would be mitochondria from normal Purkinje cells. This change in shape has been seen in Purkinje cells and other neurons in one other mutant mouse called nervous (Landis 1973*a*, *b*). A Purkinje cell in the last stages of degeneration can be seen in figure 11. All the photomicrographs on plate 4 are from animals 15 days after birth and all stages of degenerating Purkinje cells can be seen at this age. Plates 5, 6 and 7 show Purkinje dendrites from mutant mice aged 17, 15 and 17 days respectively. The dendrites in figure 12 and the higher magnification in figure 13 show early degeneration. The mitochondria are rounded and the dendrite is full of free ribosomes which we have never seen in the normal (compare with figures 7 and 8). Dispersed single ribosomes have been seen in the visual cortex of *Macaca mulatta* but it was thought that this was a temporary inactive state (Palay, Billings-Gagliardi & Chan-Palay 1974). The dendrites in figures 14 and 15 are similar to those in figures 12 and 13 except that they are more electron dense and show vacuoles (stars). Figure 14 shows a normal looking climbing fibre abutting the dendrite but not actually synapsing with it and figure 15 shows a climbing fibre between two spines which is also not synapsing with the dendrite (criteria of Larramendi & Victor (1967) used for recognition of climbing fibre). Figures 16 and 17 show a dendrite at two magnifications. In figure 16, at low magnification, neurofilaments, vacuoles (stars), and spherical mitochondria can be seen filling a Purkinje cell dendrite which is in an advanced state of degeneration. At higher magnification, figure 17, the unusual patterns of the cristae in the mitochondria can be seen (Landis 1973*a*).

(c) The interneurons of the cerebellum in the normal and Lurcher mouse

(i) *The Golgi cell.* Golgi cell somata are about 12 μm in diameter and they lie at all depths in the granule cell layer. Their dendrites make synaptic contact with the parallel fibres in the molecular layer and thus for Golgi cells lying deep in the internal granule cell layer the dendrites course up to 100 μm through granule cells before reaching the molecular layer. This can be seen in figure 18 where the Golgi cell (arrow) lies deep among the granule cells. The large primary dendrite emerges from the soma, bifurcates after 20 μm and these two dendrites traverse the Purkinje cell layer (dashed line) to branch in the molecular layer.

Golgi cells seem to be as numerous in the Lurcher mutant as in the normal. A Golgi–Cox impregnated Golgi cell can be seen in figure 19. This cell lies in a similar position in the granule cell layer to the Golgi cell in figure 18, at least with respect to distance from the molecular layer – internal granule layer interface. The Golgi cell soma in figure 18 however is in the middle part of the thickness of the granule cell layer whereas the soma of the cell in figure 19 is close to the white matter (w.m.).

(ii) *The basket cell.* One cell type found in the molecular layer is the basket cell. The characteristics of the basket cell axon are due entirely to the fact that it wraps itself around the Purkinje cell soma and therefore when the Purkinje cells are absent, as in the adult Lurcher, the basket cell axon is more difficult to recognize because it is not obvious. The criteria we have used to identify basket cells in the Lurcher mouse are: (i) position, that is in the molecular layer (ii) characteristic long trailing axon. The basket cell in figure 20 is from a Lurcher mouse 14 days after birth and although it appears fairly normal it is lying in a more superficial position than normal and is also upside down. The axons of this basket cell are ascending towards the pia rather than descending towards the Purkinje cell layer.

(iii) *The stellate cell.* A stellate cell impregnated with the Golgi–Cox technique is shown in figure 21. This shows a typical cell from the middle of the molecular layer in the normal mouse with dendrites radiating out from the cell body in all directions.

The stellate cells of the normal molecular layer can also be found in the Lurcher molecular layer. In the Lurcher however the stellate cell dendritic tree covers a smaller volume and the dendrites seem to follow a more tortuous route (figure 22). They may in fact not be any shorter than those in the normal, but because of the reduced width of the molecular layer in the Lurcher there are restrictions on the growth of the dendritic trees of the stellate cells.

(iv) *The granule cell.* Two Golgi–Cox impregnated granule cells from an adult normal mouse can be seen in figure 23. Arrows point to the claw-like endings of the granule cell dendrites which wrap themselves around and synapse with the mossy fibre glomeruli one of which can be seen in the top left of figure 23 (crossed arrow).

Granule cells in the adult Lurcher mutant mouse appear normal although there are fewer of them. In Golgi–Cox impregnated sections (see figure 24) the granule cells in the mutant show the same claw-like endings of the dendrites as do the normal. In this section the dendritic claw is wrapped around a mossy fibre glomerulus (arrow).

Electron micrographs of granule cells in a normal mouse 20 days old are shown in figure 25. They are easily recognized because of their small size (about 5 μm diameter), dense chromatin patterns in the nuclei, very thin cytoplasm surrounding the nucleus, and their position relative to the Purkinje cells and white matter.

Examples of the granule cells in a Lurcher mouse are shown in figure 26. Some of the nuclei

do not show the dark chromatin patterns found by us in normal granule cells. Presumably these granule cells in this animal 20 days after birth are destined to degenerate; an hypothesis substantiated by electron microscopy in adult Lurcher mutant mice which do not show this abnormal type of granule cell and where the total number of granule cells is reduced (see below).

(*d*) *The structure of the inferior olivary nucleus from the normal and Lurcher mouse*

In coronal sections of the brain stem from the normal mouse stained with luxol fast blue and cresyl violet the olive appears as a pale stained area lying just dorsal to the medullary pyramid. In figure 27 the nucleus is outlined with arrow heads in a micrograph of a section taken from a mouse 730 days old. The intramedullary course of the hypoglossal nerve, arrow, can also be seen in this section. A higher power light micrograph of olive neurons can be seen in figure 28 which shows the dark staining Nissl bodies of the cytoplasm, the pale nucleus and the very dark staining nucleolus. The dendritic trees of the olive neurons impregnated with the Golgi–Cox technique can be seen in figure 31. Some of the cells, such as the one indicated by a long arrow show the highly ramified spherical dendrites referred to by Scheibel & Scheibel (1955) and some have a relatively simple dendrite pattern marked by a short arrow in figure 31.

Figure 33 is an electron micrograph of an olive neuron, it confirms the view found in the light micrograph of figure 28 that the cytoplasm contains abundant Nissl bodies. The nucleus of the cell is placed fairly centrally in a slightly elliptical shaped soma with the Nissl bodies lying at the poles. The cytoplasm also contains Golgi apparatus, mitochondria and microtubules which cannot be seen in this low magnification photomicrograph.

The inferior olivary nucleus from the Lurcher mutant mouse, although smaller than normal, is still found with ease in coronal sections of the brain stem stained with luxol fast blue and cresyl violet. It occupies the same rostral–caudal extent of the brain stem as in the normal and is found dorsal to the medullary pyramid. Figure 29 shows the olive outlined with arrowheads in an animal 730 days after birth. The intra-medullary course of the hypoglossal nerve can be seen at the arrow. At higher magnification, figure 30, several cells which were not included in the olivary neurone count (arrows) are shown. The Golgi–Cox impregnated cells of figure 32 are ones with highly ramified spherical dendrites (Scheibel & Scheibel 1955; Scheibel *et al.* 1956). In the many sections at four different ages (10, 11, 14 and 380 days post-natal) which were cut in the sagittal and coronal planes only cells with highly ramified spherical dendrites were impregnated with the Golgi technique. It is possible that in these four Lurcher mice the cells with complex dendritic patterns are the only ones impregnated though we have no reason to suppose this is so. Comparing the cells in figure 32 with those in figure 31 it would seem that the neurons remaining in the Lurcher olive were of one type only (see § IV for further comment).

Electron microscopy shows that the inferior olivary neurons in the Lurcher mouse are similar to the smaller type of cell found in the normal. This similarity is exemplified in the micrographs of figures 33 and 34 where the cytoplasm contains the same organelles in similar positions. This would indicate that the olivary neurons remaining in the Lurcher mouse are normal at least as far as structure is concerned.

(*e*) *The mossy and climbing fibres of the normal and Lurcher mouse*

These fibres have complicated terminals in the cerebellum called glomeruli. Electron micrographs of a mossy fibre glomerulus and a climbing fibre glomerulus are shown in figures

35 and 36, respectively. The basic structural difference between the two types lies in the density of synaptic vesicles, the climbing fibre glomerulus is very densely packed while the mossy fibre terminal has more loosely dispersed vesicles. According to Palay & Chan-Palay (1974) the glomeruli in the rat are distinguishable because the climbing fibre has a central cluster of mitochondria. This was not a distinguishing feature in the mouse cerebellum.

Two glomeruli from the Lurcher mouse can be seen in figures 37 and 38; figure 37 shows a mossy fibre glomerulus from a 63-day-old Lurcher, and figure 38 shows a climbing fibre terminal from a 19-day-old Lurcher. The difference in synaptic vesicle density between these glomeruli can be seen. The climbing fibre glomerulus in figure 38 is the only one found in our material, both normal and Lurcher, that showed the very high density of synaptic vesicles reported by Palay & Chan-Palay (1974) in the rat. Both these glomeruli are making synaptic contact with profiles of granule cell dendrites. Mossy fibre glomeruli stain well with Golgi–Cox impregnation and two are shown in figure 39 indicated with arrows. These are of the complex type as described in the rat by Palay & Chan-Palay (1974) but the simple type are also present.

The mossy fibre glomeruli in the Lurcher mutant mouse are the same as those described in the normal mouse. The glomeruli in figure 40 are of the complex variety but simple glomeruli may also be seen.

(f) The structure of the deep cerebellar nuclei from the normal and Lurcher mouse

In coronal sections of the cerebellum and brain stem stained with luxol fast blue and cresyl violet the deep cerebellar nuclei can be seen grouped in a pale stained area situated in the white matter on the ventral surface of the cerebellum. Figure 41 is a light micrograph of the deep cerebellar nuclei in a normal mouse 730 days old and shows the difficulty of distinguishing three subdivisions of the nuclei, lateral, interpositus and medial. The cells range in size from 12 to 22 μm in diameter (figure 42) and show a striking contrast of the Nissl bodies with the pale stained nucleus. As with most neurons, the nucleoli are prominent because they stain dark purple with the cresyl violet.

The Lurcher deep cerebellar nuclei appear to be of similar size to those in the normal when viewed in coronal sections (compare figures 41 and 43). However the nuclei are flattened dorso-ventrally and are shorter in the rostro-caudal direction. The neurons in Lurcher are of similar size to normal ranging from 12 to 22 μm in diameter (figure 44). The major difference under the light microscope is the increase in cell proximity in Lurcher (compare figures 42 and 44), which would account for the reduction in overall size of these cell groups.

Description of plate 9

Light micrographs of Golgi–Cox impregnated tissue showing granule cells from normal and Lurcher mice. Sections are 100 μm thick. Electron micrographs of granule cells from 20 day post-natal normal and Lurcher mice. Calibration bar = 10 μm for figures 23 and 24; 1 μm for figures 25 and 26.

Figure 23. Granule cells from a normal mouse 429 days old showing claw like endings (arrows) and a mossy fibre glomerulus (crossed arrow).

Figure 24. Granule cell from a Lurcher mouse 380 days old showing a dendrite contacting a mossy fibre glomerulus (arrow).

Figure 25. Granule cells from a normal mouse; nuclei (n) show dark chromatin patterns.

Figure 26. Granule cells from a Lurcher mutant mouse which shows one normal looking cell and four cells which have very pale staining nuclei (n) with sparse clumps of chromatin.

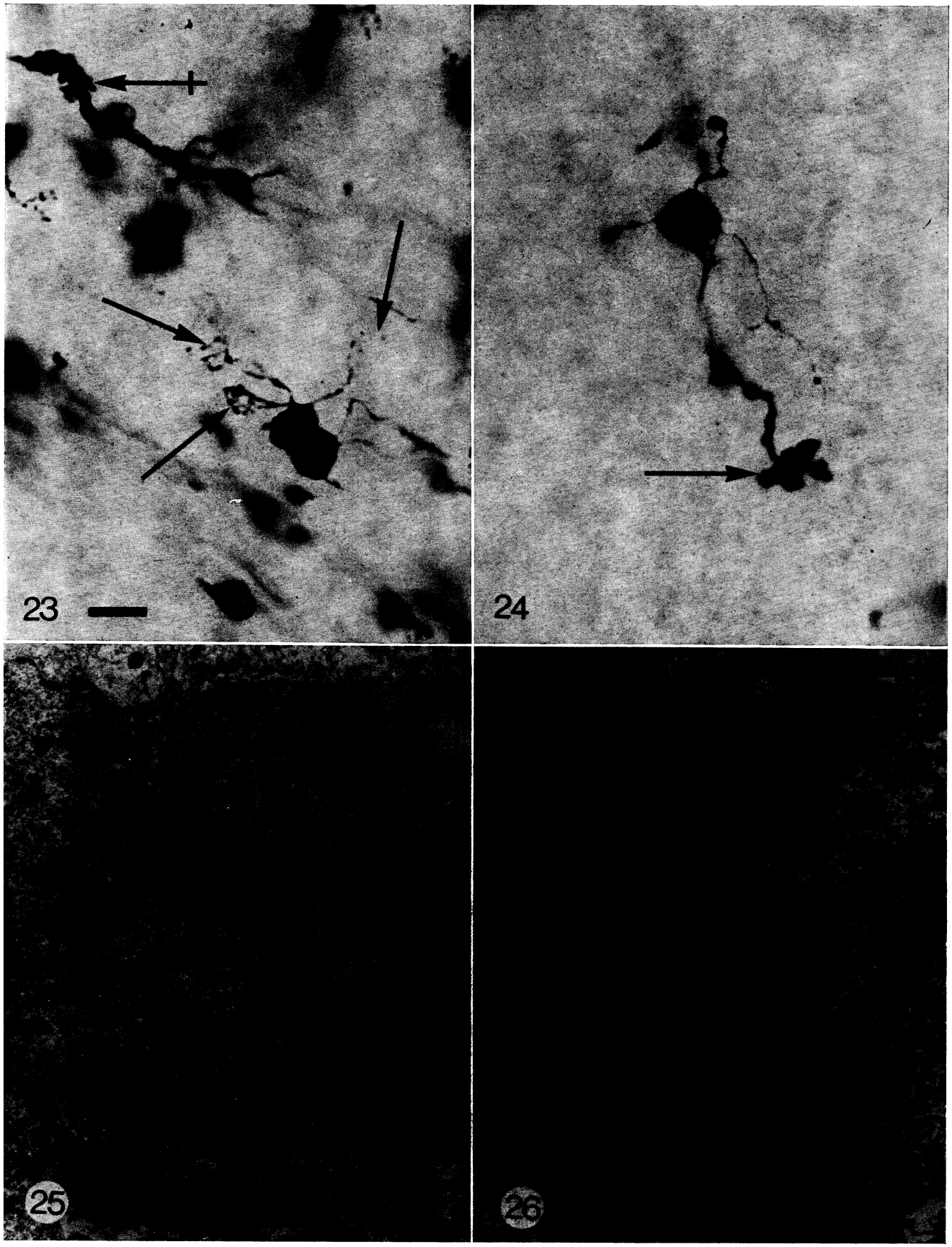

FIGURES 23–26. For description see opposite.

(*Facing p.* 180)

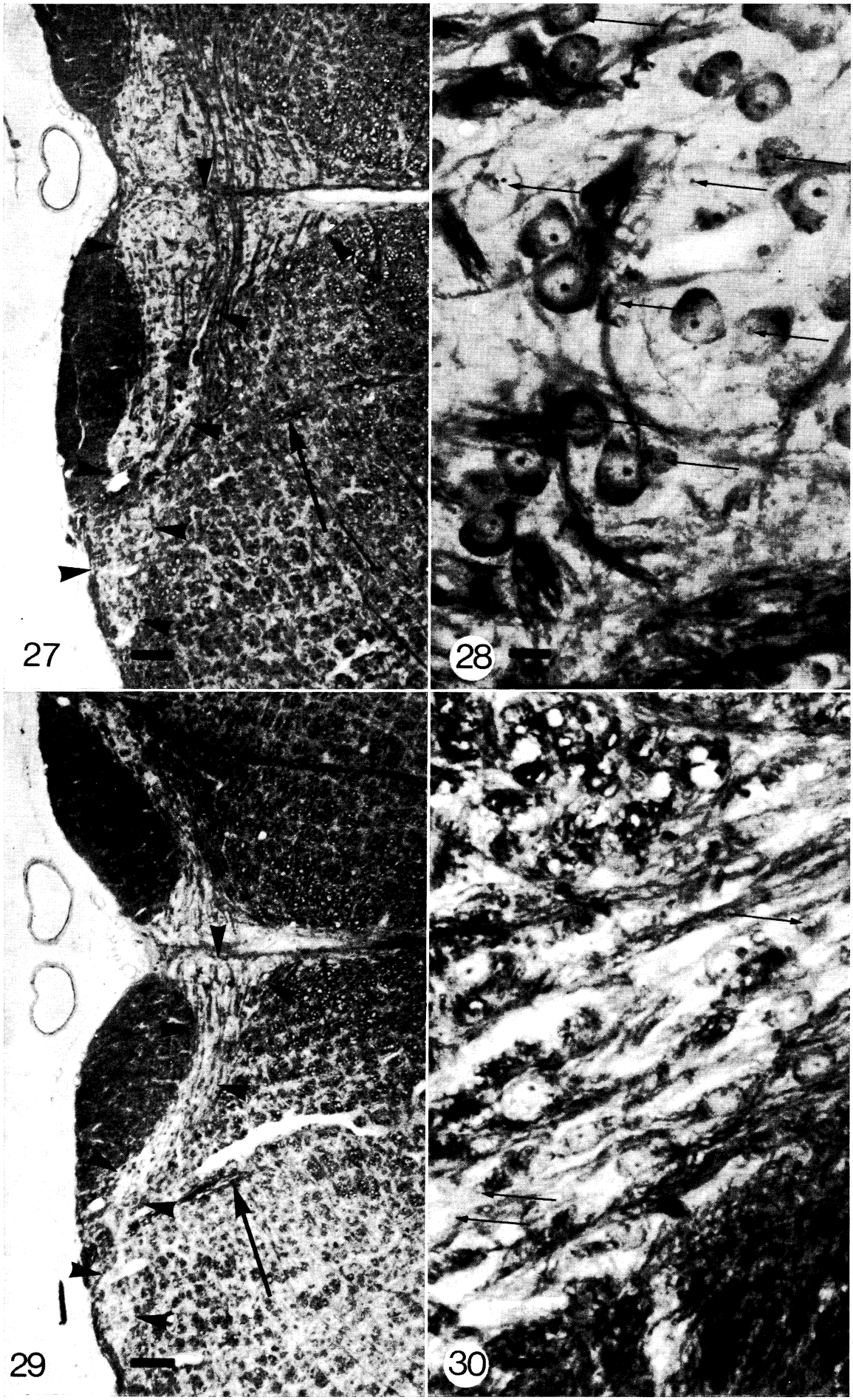

FIGURES 27–30. For description see opposite.

Description of plate 10

Light micrographs of inferior olivary nucleus from normal and Lurcher mice 730 days old. Figures 27 and 29 show the position occupied by the olive (outlined by arrowheads) in coronal sections of the brain stem. Figures 28 and 30 show higher magnification micrographs to enable the olive neurons to be identified. Section stained with luxol fast blue and cresyl violet.

Figure 27. Olive from normal mouse showing the intermedullary course of the hypoglossal nerve (arrow). Calibration bar = 100 μm.

Figure 28. The olive neurons of the normal mouse. The cells arrowed are the ones that would not be counted in this section. Calibration bar = 10 μm.

Figure 29. Olive from a Lurcher mouse also showing the intermedullary course of the hypoglossal nerve (arrow). Calibration bar = 100 μm.

Figure 30. In this higher magnification micrograph the cells arrowed are the ones that would not be counted in this section. Calibration bar = 10 μm.

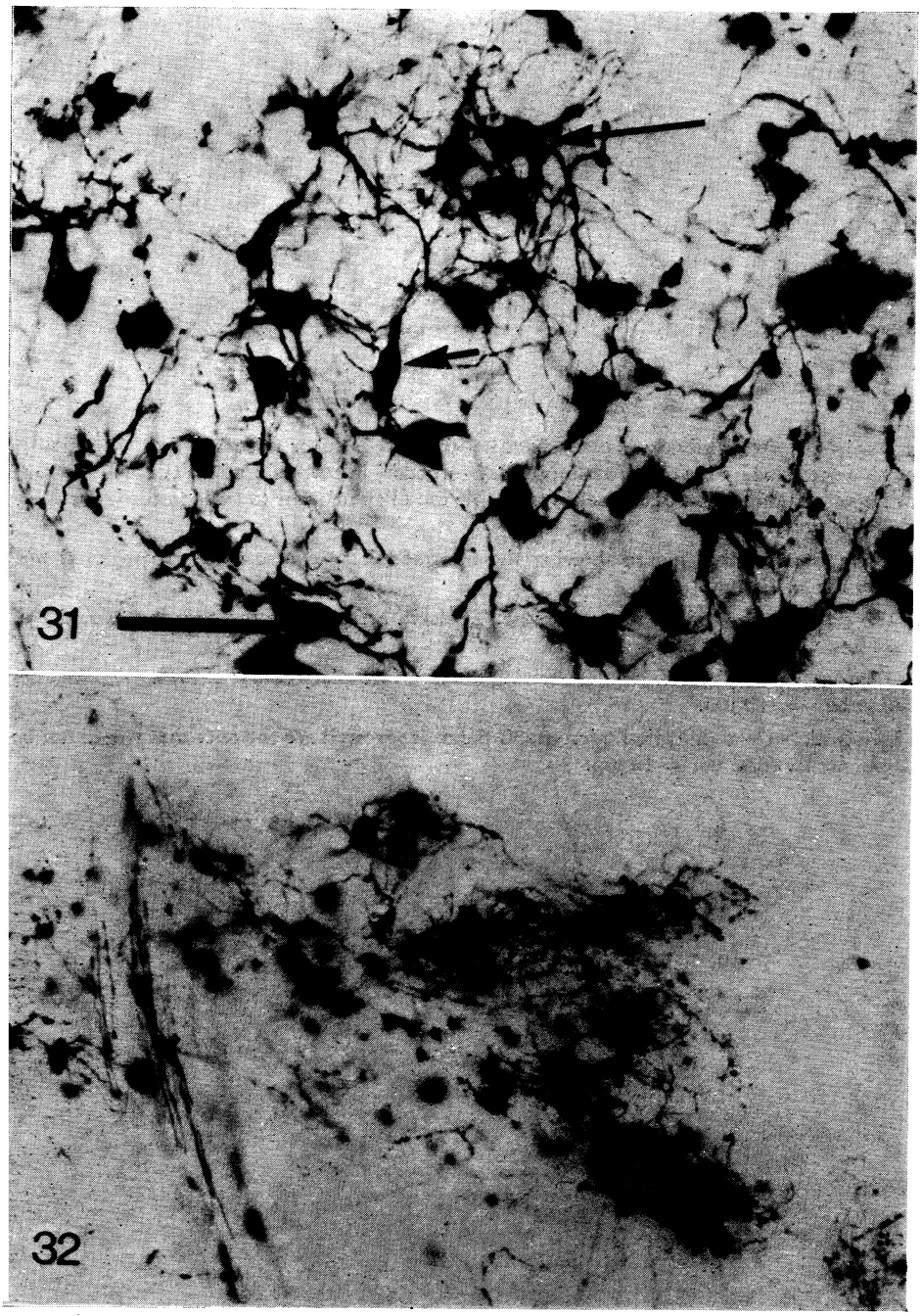

Light micrographs of Golgi–Cox impregnated inferior olivary nucleus from normal and Lurcher mice. Sections are 100 μm thick. Calibration bar = 100 μm for both micrographs.

FIGURE 31. Neurons from a mouse 429 days old showing some cells with simple dendritic patterns (short arrows) and one with highly ramified spherical dendrites (long arrow).

FIGURE 32. Neurons from a Lurcher mouse 14 days old showing only cells with highly ramified spherical dendrites.

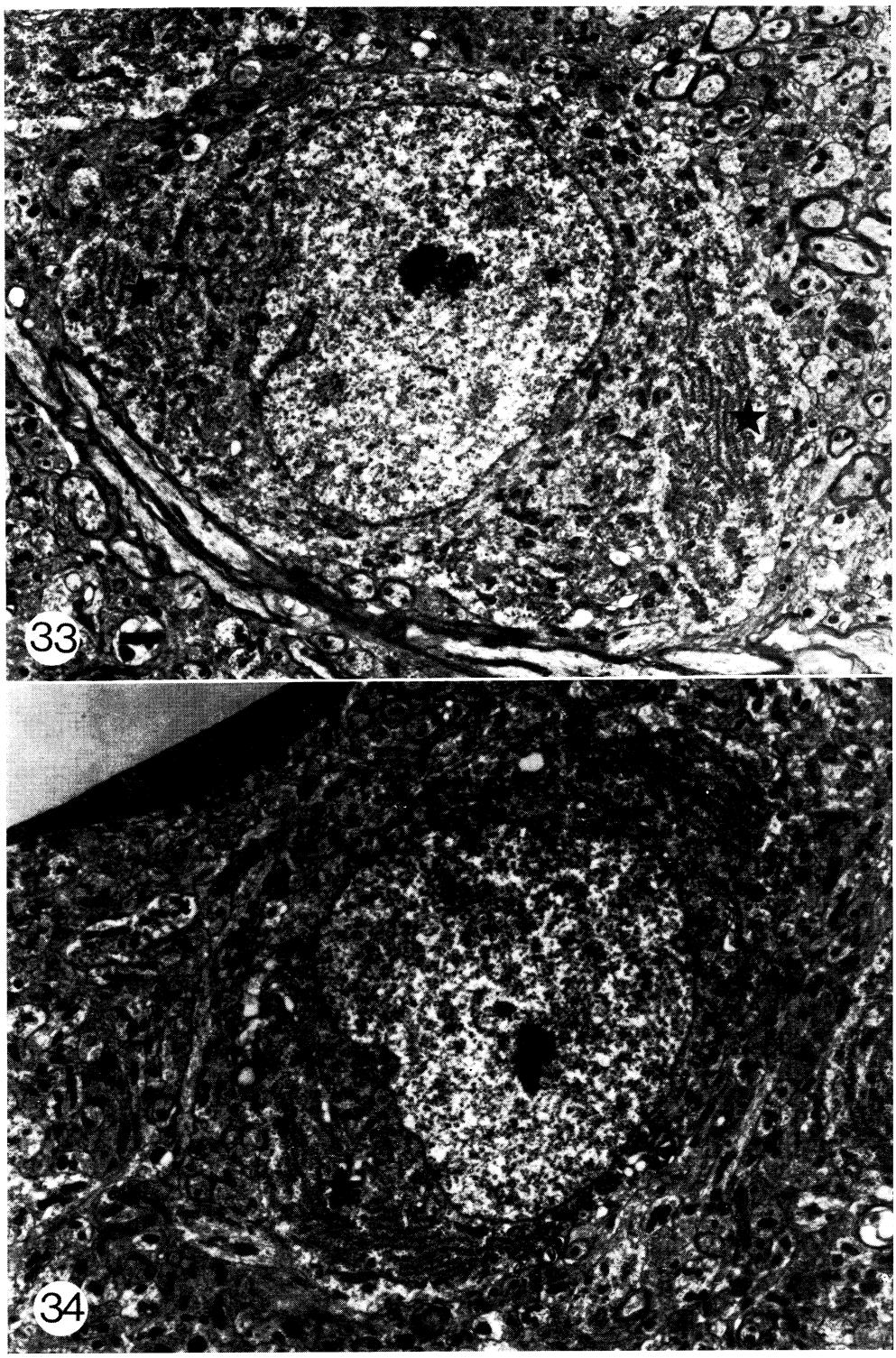

Electron micrographs from normal and Lurcher mice 17 days old showing olive neurons. Nissl bodies are indicated by stars. Calibration bar = 1 μm for both micrographs.

FIGURE 33. Normal mouse olive neuron.

FIGURE 34. Lurcher mutant mouse olive neuron.

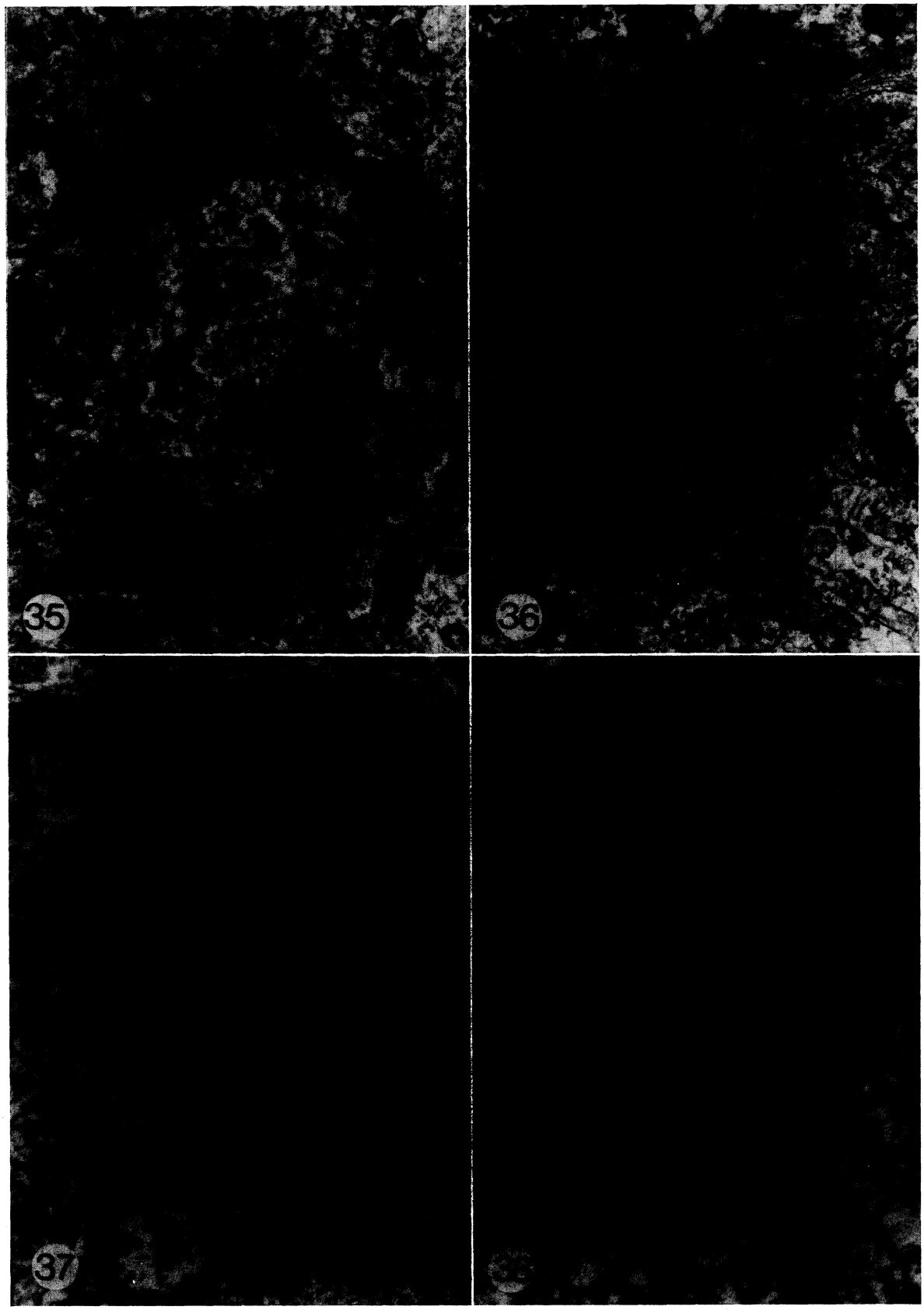

Electron micrographs of mossy and climbing fibre glomeruli from normal and Lurcher mutant mice. Arrowheads show synapses with granule cell dendrites and Golgi cell axons. Calibration bar = 1 μm for all micrographs.

FIGURE 35. A mossy fibre glomerulus from a normal mouse 15 days old. Note the fairly low density of synaptic vesicles.

FIGURE 36. A climbing fibre glomerulus from a normal mouse 15 days old. Note the higher density of synaptic vesicles when compared with figure 35.

FIGURE 37. A mossy fibre glomerulus from a Lurcher mouse 63 days old. The low packing density of synaptic vesicles is shown and a granule cell in close apposition to the glomerulus can be seen (arrows).

FIGURE 38. A climbing fibre glomerulus from a Lurcher mouse 19 days old. The packing density should be compared to that in figure 37.

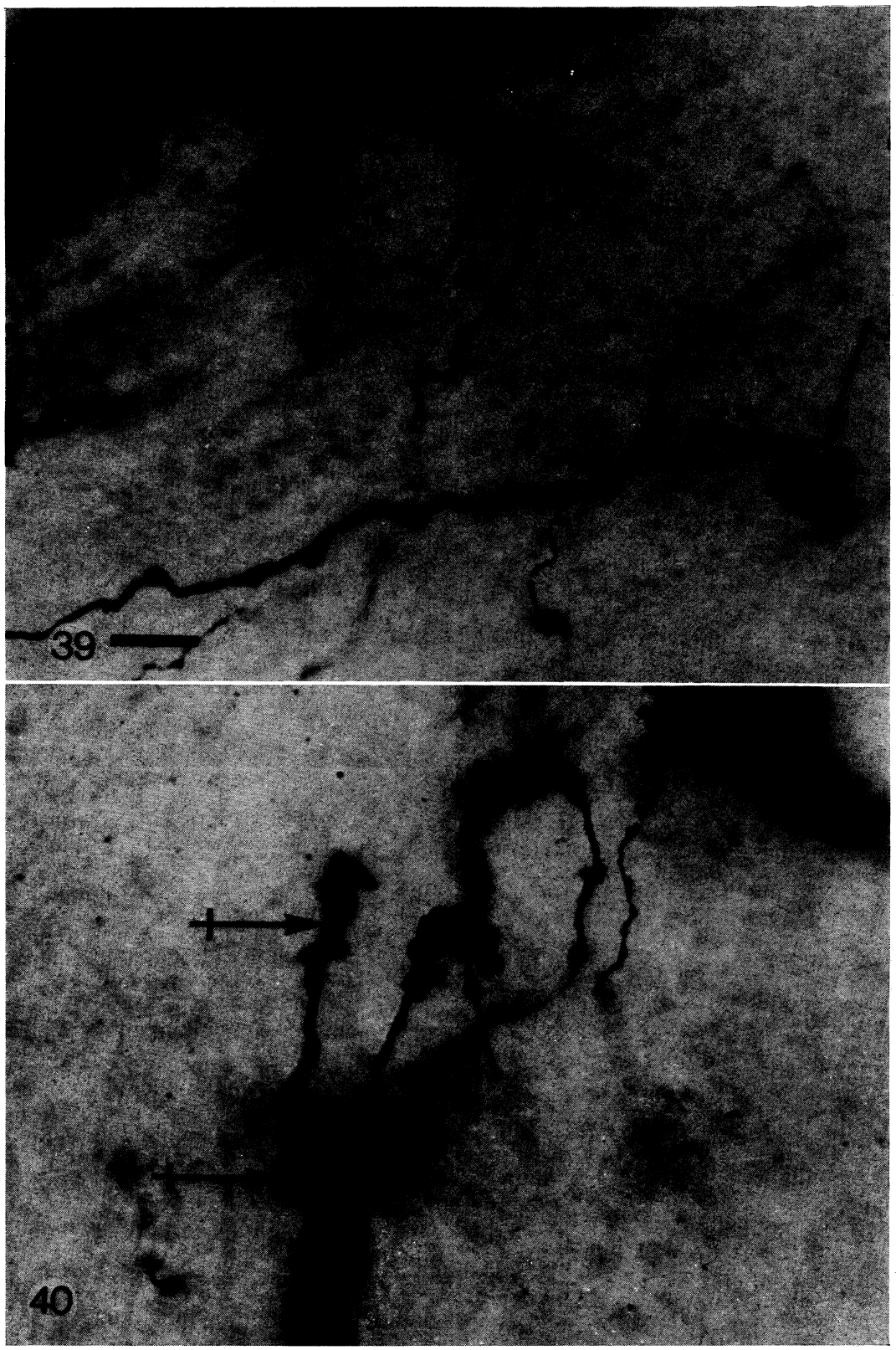

Light micrographs of Golgi–Cox impregnated mossy fibre glomeruli from adult normal and Lurcher mice. The glomeruli are arrowed. The photographs were taken in the internal granule cell layer. Sections are 100 μm thick. Calibration bar = 10 μm for both micrographs.

FIGURE 39. This is a photomontage to show two mossy fibre glomeruli of the complex type in a normal mouse 429 days old.

FIGURE 40. Three mossy fibre glomeruli in a Lurcher mouse 380 days old. These are also of the complex type although it is difficult to see those at the crossed arrows because they are out of the plane of focus.

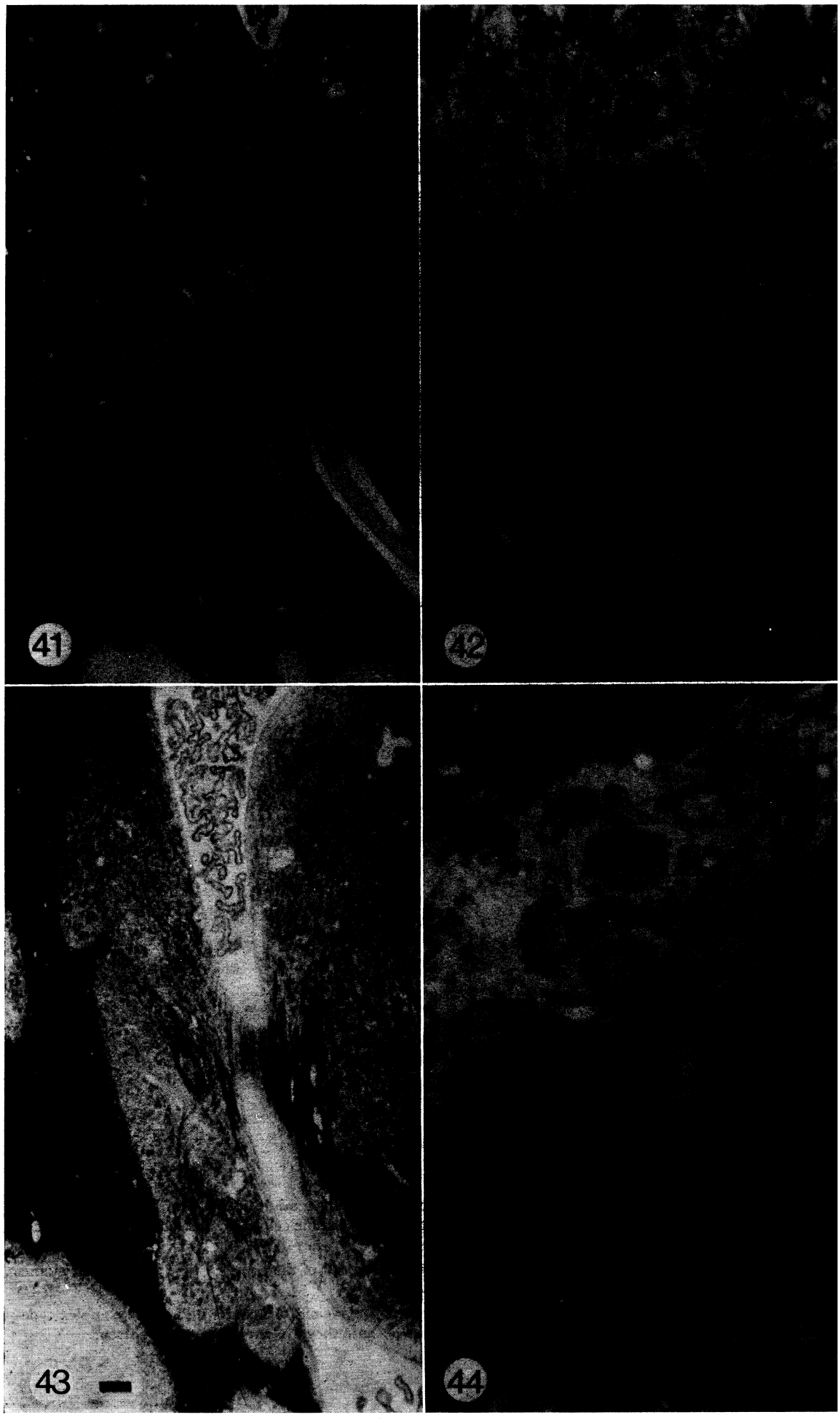

FIGURES 41–44. For description see opposite.

2. *Quantitative results in the normal mouse*

(*a*) *Purkinje cells*

The numbers of Purkinje cells were estimated in animals between 4 and 730 days post-natal age. Between 2600 and 4100 cells were counted in each animal. Figure 45 is a graph showing the variation in total Purkinje cell number with age; the black circles represent the normal mouse.

The total number of Purkinje cells between 4 and 10 days after birth appears to be increasing, this is believed to be an artefact arising from the method of counting used. The number of Purkinje cells cannot be increasing at this stage since they undergo their last cell division at least 11 days prior to this time at 13 days embryonic age (Miale & Sidman 1961; C. Rickets, personal communication). As mentioned in the qualitative results the Purkinje cells become

TABLE 1

age	Purkinje cells		olive neurons		ratio Purkinje cells:olive neurons	
days	normal	Lurcher	normal	Lurcher	normal	Lurcher
4	137000	149000	13700	16400	9.7	8.4
			14400	19000		
5	—	—	17400	—	—	—
6	—	—	19400	17200	—	—
8	132000	130000	15300	14400	8.9	7.9
	140000	—	—	18600	—	—
10	180000	120000	25000	16300	7.2	7.4
11	—	—	24600	12800	—	—
12	—	—	25300	16700	—	—
			25800	—	—	—
			30200	—	—	—
13	168000	86000	27000	17700	5.6	4.9
	168000	—	—	—	—	—
	186000	—	—	—	—	—
14	158000	73000	32900	19600	4.8	3.7
			33300			
15	180000	88000	35300	21800	5.1	4.0
17	195000	77000	35600	16500	5.4	4.7
26	184000	16000	32300	14800	5.7	1.1
63	194000	6000	30400	9700	6.4	0.62
91	170000	360	30900	10600	5.5	0.04
121	177000	918	33100	6100	5.4	0.15
730	165000	1384	30200	7100	5.5	0.2

DESCRIPTION OF PLATE 15

Light micrographs of the deep cerebellar nuclei from normal and Lurcher mice 730 days old. Sections stained with luxol fast blue and cresyl violet.

FIGURE 41. Section in an approximately mid rostral–caudal region of the nuclei in a normal mouse. Calibration bar = 100 μm.

FIGURE 42. Higher magnification micrograph of figure 41 showing the variation in neuron sizes. Calibration bar = 10 μm.

FIGURE 43. Section in an approximately mid rostral–caudal region of the nuclei in a Lurcher mouse. Calibration bar = 100 μm.

FIGURE 44. Higher magnification micrograph of figure 43 to show a variation in neuron sizes and also the increase in packing density when compared to the normal in figure 42. Calibration bar = 10 μm.

a monolayer between 6 and 8 days after birth, therefore counting Purkinje cells before this age is made difficult by the fact that the layer is sometimes two or more cells thick. At 4 days the layer was assumed to be two cells thick for counting purposes but in places it is more than this and therefore a low count would have resulted. At 8 days post-natal the Purkinje cells form a monolayer but this estimate was also low probably due to a problem with recognition of this cell type. If the cells did not satisfy our criteria for counting then they were left out. Some of the cells not counted then could have been less mature than others and were disregarded for this reason. After 10 days the estimates of Purkinje cell numbers remains fairly constant up to

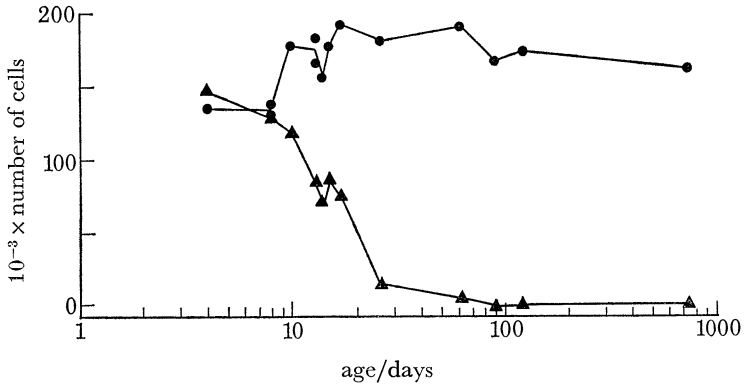

FIGURE 45. Graph showing variation in total number of Purkinje cells with age in the normal and Lurcher mutant mouse. Cirlces indicate the normal mouse results and the triangles the Lurcher mutant mouse.

730 days after birth. Some authors have described degeneration of nerve cells with age (see Hanley 1974 for review of literature). Johnson & Erner (1972) calculated that neurons per whole brain in mice fall from approximately 4.6 millions at 1 month of age to 3.2 millions at 24 months (cells counted were 15 μm or larger in diameter). This represents a loss of 20 % of the large neurons in 24 months whereas the fall in Purkinje cells over a similar period was 9 % in our estimates. As can be seen from the graph (figure 45) this variation could be accounted for by experimental errors inherent in all counting techniques. The actual numbers of cells at each age are given in table 1.

(*b*) *Granule cells*

The estimates of numbers of this, the smallest and most plentiful neuron in the cerebellum, are shown in table 2 and the graph of numbers against age is shown in figure 46.

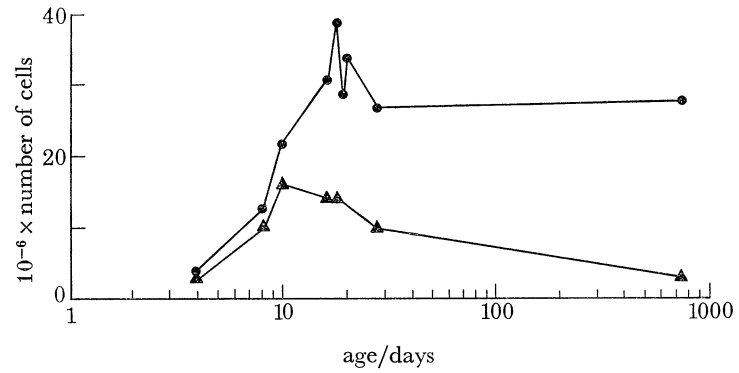

FIGURE 46. Graph showing the variation in total number of granule cells with age in the normal and Lurcher mutant mouse. Circles indicate the normal mouse results and the triangles the Lurcher mutant mouse.

Depending on age between 2000 and 6000 cells were counted in each animal. As with the Purkinje cells we are confronted with a steep increase in the numbers of granule cells between 4 and 17 days after birth. This increase was predictable, however, since these estimates were made on the internal granule cell layer which over this period of time is receiving cells from those proliferating in the external granule cell layer (Fujita 1967). What is more interesting is the decrease in granule cells between 17 and 26 days after birth. The factors controlling this process are not known at present but consideration is given to the problem in the Discussion. The near identity of the numbers at 26 and 730 days of age, coupled with present knowledge about the granule cell birthday makes fluctuation in numbers of granule cells in adult life improbable.

(*c*) *Olive neurons*

Estimates of numbers of olive neurons were made by using the same animals as those for the Purkinje cell counts (table 1). In each animal between 1000 and 2500 neurons were counted. A rigid set of criteria, described in the Methods, were used for counting these neurons and

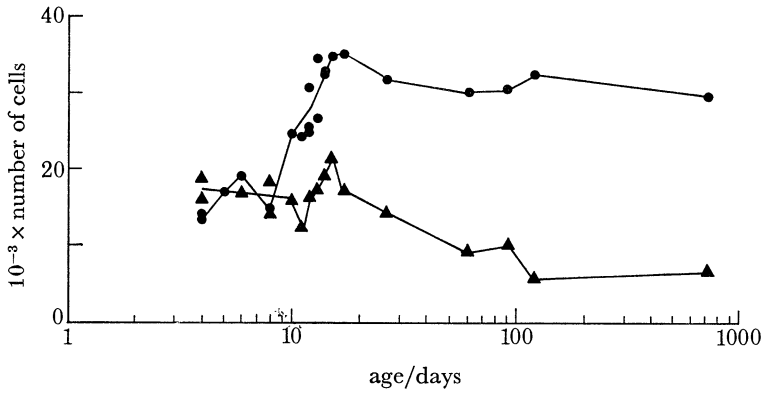

FIGURE 47. Graph showing the variation in total number of olive neurons with age in the normal and Lurcher mutant mouse. Circles indicate the normal mouse results and the triangles the Lurcher mutant mouse.

for this reason none of the cells arrowed in figures 28 and 30 were counted. The graph in figure 47 shows the variation in the total number of olive neurons with age (black circles represent estimates from the normal mouse) and the graph shows that the olive neuron number is increasing between 4 and 14 days after birth. This may reflect a continuing migration of cells into the olive but since these cells undergo their last cell division on day 11 of gestation (Taber Pierce 1973) and therefore 22 days before the adult number of neurons is present in the olive this seems unlikely. Therefore it is possible that the olive neurons are in fact in their adult location but are immature and so the increase in cell numbers would represent the maturation of neurons already present which then become recognizable. From 14 to 730 days after birth the olive neuron number remains fairly constant. As with the Purkinje cells there seems to be no obvious signs of neuron death with increasing age.

(*d*) *Deep cerebellar nuclei*

The estimates of numbers of deep cerebellar nuclei neurons were made at three ages: 63, 91 and 730 days after birth. The actual number of cells counted varied between 1100 and 1400 per animal. The results for these ages are listed in table 2. We have no unique explanation for

the 17% discrepancy between the estimate at 63 days and that at 91 days after birth; the estimate at 730 days is within 3% of that at 91 days.

(e) Ratio of neuron numbers

The fact that Purkinje cells are each contacted by one climbing fibre makes the ratio of Purkinje cells to olive neurons interesting. In the normal mouse this ratio is about 5.5:1 which gives a measure of the divergence in the olive–Purkinje cell system unless another source of climbing fibres exist. The inferior olive is the only source that has been established (Desclin 1974).

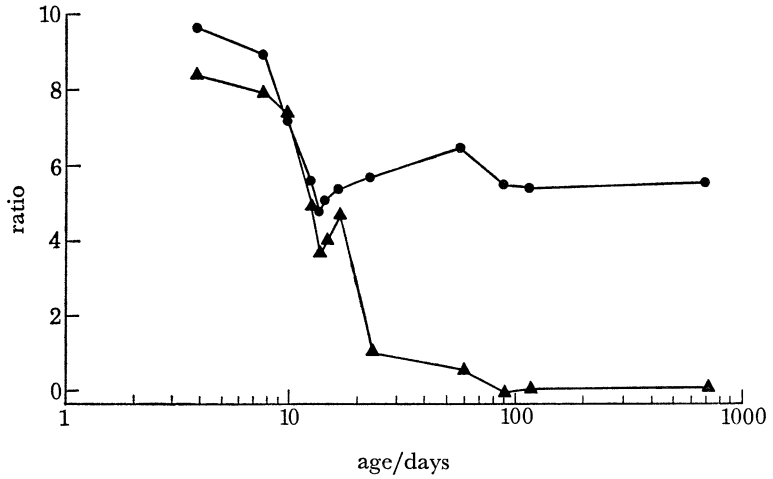

FIGURE 48. Graph showing the variation in the ratio Purkinje cells:olive neurons with age in the normal and Lurcher mutant mouse. Circles indicate the normal mouse results and the triangles the Lurcher mutant mouse.

The graph in figure 48 shows how, in the normal mouse (black circles), the ratio Purkinje cells:olive neurons falls between 4 and 14 days after birth and then remains fairly constant thereafter (table 1). This decrease is caused by the increase in the number of olive neurons over this period (see § III. 2*c*).

The ratio of granule cells to Purkinje cells is an indication of the convergence of parallel fibres onto the Purkinje cells. This ratio in the normal mouse increases to a maximum at 17 days post-natal and has fallen to about the adult level at 26 days post-natal (table 2).

The ratio of Purkinje cells to deep cerebellar nuclei neurons has only been calculated at 63, 91 and 730 days post-natal. These ratios are shown in table 2.

The ratios of olive neurons to deep cerebellar nuclei neurons are shown in table 2. This ratio is important if there are olive neurons projecting climbing fibres solely to the deep cerebellar nuclei (see § III. 1*d*). These ratios in table 2 have been calculated from the total number of olive neurons.

If there is a specific olive cell type that gives axons to the deep cerebellar cells and not also to Purkinje cells then the number of such olive cells would modify the functional Purkinje cell:olive cell ratio and also allow subdividion of the supply to the deep cerebellar nuclei.

3. *Quantitative results in the Lurcher mouse*

(*a*) *Purkinje cells*

Littermates were used for the estimates made on Lurcher and normal animals at each age with the exception of the oldest animals. The number of Purkinje cells counted in each animal varied between 19 and 3100. The actual numbers of Purkinje cells estimated are listed in table 1. The graph in figure 45 shows the variation in total number of Purkinje cells with age for both the Lurcher (triangles) and the normal mouse. At 4 and 8 days after birth the estimates are very nearly the same for both the Lurcher and the normal mouse. After this time the number of Purkinje cells in the Lurcher mouse falls sharply until at 26 days there are less than 10 % of the Purkinje cells remaining. Between 26 and 91 days after birth the estimated total number of Purkinje cells falls to 360. The actual number of Purkinje cells we counted in this animal at this age was 19 compared with 3760 in the normal. At this age, and older, the cerebellum is disorganized in the Lurcher, especially the boundary between the molecular and internal granule cell layers and it is possible that some, if not all, the cells counted as Purkinje cells were in fact Golgi cells. We found considerable difficulty in distinguishing between Purkinje and Golgi cells stained with luxol fast blue and cresyl violet at these ages. After 91 days of age the actual number of Purkinje cells counted was slightly higher but we are sure that this is because of the problem of identification of cell types and therefore we do not attach any significance to this apparent change.

(*b*) *Granule cells*

The estimates of the numbers of granule cells (table 2) were made by using the same material as that used for Purkinje cell and olive cell counts. The number of granule cells actually counted was between 2000 and 6000 per animal. At 4 days after birth the number of granule cells in the Lurcher (figure 46, triangles) is smaller than the normal by 25 % and this difference increases with age. It may be deduced from the graph that external granule cells are migrating in from the external granule layer at least until 17 days after birth when the external granule cell layer ceases to exist. Between 26 and 730 days after birth we have not made any estimates of granule cell numbers and therefore the decline in cell numbers shown by the graph in figure 46 may or may not be constant over this period. The most likely sequence is that in the adult animal (about 100 days after birth) the number of granule cells would be reduced to the number estimated at 730 days after birth and between 100 and 730 days the number remains constant. No obvious sign of continuous degeneration of granule cells had been seen in Lurcher mice at this age.

(*c*) *Olive neurons*

These estimates of numbers of olive neurons (table 1) were made by using the same animals as those used for the Purkinje cell estimates. Between 450 and 1400 neurons were counted in each animal. The graph in figure 47 (triangles) shows the way in which the number of olive neurons varies with respect to age. From 4 to 8 days after birth the olive neuron number remains close to that of the normal, but at 10, 11 and 12 days while the normal numbers are increasing the Lurcher numbers remain static. Between 12 and 15 days after birth the estimate of numbers of neurons in the Lurcher rises, probably for the same reason as the rise in the normal (see § III. 2*c*). However, in the Lurcher mutant mouse the increase in number of olive

neurons is never such that it equals that of the normal. At 15 days after birth in the inferior olive of the Lurcher only 60% of the normal number of olive neurons are remaining. The highest number is reached at this age and after this the numbers decline until at 121 days after birth less than 25% of the olive neurons remain. This number then probably remains constant as is shown by the estimate at 730 days after birth.

(d) Deep cerebellar nuclei

As in the normal the estimates of deep cerebellar nuclei neurons were made at three ages (63, 91 and 730 days) and the actual number of cells counted in each animal varied between 1100 and 1400. The results are listed in table 2. The estimates for Lurcher and normal are remarkably similar for the three ages. Thus although one of the largest inputs and the only inhibitory input to the deep cerebellar nuclei (from the Purkinje cell axons) is missing in the Lurcher, the deep cerebellar nuclei themselves are unaffected as far as cell number is concerned.

TABLE 2

age	10^{-3} × granule cells		ratio granule cells: Purkinje cells		deep cerebellar nuclei neurons		ratio Purkinje cells: deep cerebellar nuclei neurons		ratio olive neurons: deep cerebellar nuclei neurons	
days	normal	Lurcher	normal	Lurcher	normal	Lurcher	normal	Lurcher	normal	Lurcher
4	3800	2800	28	19	—	—	—	—	—	—
8	13000	10000	96	77	—	—	—	—	—	—
10	22000	16000	122	133	—	—	—	—	—	—
15	31000	14000	172	159	—	—	—	—	—	—
17	39000	14000	200	182	—	—	—	—	—	—
19	29000	—	—	—	—	—	—	—	—	—
20	34000	—	—	—	—	—	—	—	—	—
26	27000	10000	147	625	—	—	—	—	—	—
63	—	—	—	—	15500	15500	12.6	0.39	1.96	0.62
91	—	—	—	—	18900	18400	11.1	0.02	1.63	0.57
730	28000	2900	170	2100	18400	18700	11.1	0.07	1.64	0.37

(e) Ratio of neuron numbers

The graph in figure 48 shows how, in the Lurcher mouse (triangles), the relation of Purkinje cells to olive neurons follows closely that of the normal until after 17 days of age when the number of Purkinje cells falls dramatically and hence the ratio decreases until at 91 days after birth the ratio is close to zero (table 1).

Similarly, the relationship of granule cells to Purkinje cells for the Lurcher mouse conforms with the normal until after 17 days of age when the Purkinje cell number falls and therefore the ratio rises (table 2).

The ratios of Purkinje cells to deep cerebellar nuclei neurons in the Lurcher mutant mouse shown in table 2 are almost zero because there are few if any Purkinje cells left at this age.

The ratios of olive neurons to deep cerebellar nuclei neurons are shown in table 2. These numbers should be considered in the light of the presumption that in the Lurcher mouse the climbing fibre connections with granule and Golgi cells are still present. It may also be assumed that in this animal there are olive neurons projecting directly to the deep cerebellar nuclei.

IV. Discussion

These results will be discussed in the following sequence. First the qualitative results and the quantitative results for the normal and Lurcher mouse, then a comparison with experimentally produced lesions, and lastly a comment on the ratios of cell types in the normal.

1. *Qualitative results in the normal mouse*

The cerebellum of the normal mouse is similar in many details to that of the rat which has been described in great detail by Palay & Chan-Palay (1974), while Larramendi (1969, 1970) and Larramendi & Lemkey-Johnston (1970) have described the various cell types found in the mouse cerebellum. The results in this paper agree with these authors except for the differences described by Palay & Chan-Palay (1974) between climbing and mossy fibre glomeruli. In our mice the climbing fibre glomeruli have a higher density of synaptic vesicles when compared with the mossy fibre glomeruli but they are not so easily recognized as they are reported to be in the rat (see Caddy *et al.* 1977).

The inferior olive in the normal mouse is very similar to that found in the rat and the subdivisions given to the rat olive apply equally for the normal mouse. The two different types of neurons in the olive as described by Scheibel & Scheibel (1955) were found in our mice by using the Golgi–Cox technique.

The deep cerebellar nuclei in the normal mouse can be divided into the three subdivisions used to define the rat nuclei: medial, interpositus, and lateral.

2. *Quantitative results in the normal mouse*

The quantitative work in this paper has involved counting cells of the cerebellum and the inferior olive in normal and mutant mice at post-natal ages from 4 to 730 days. This, of necessity, has only been possible by restricting the numbers of the cells counted to a small percentage of the total number.

The number of Purkinje cells, granule cells, olive neurons and deep cerebellar nuclei neurons has been estimated in many species by different authors (see table 3). Table 3 contains most of the estimates of neuron numbers made on mammals in this century. Many of the authors had left their estimates as cell densities but to enable direct comparison to be made to our figures we have calculated total numbers from these densities using information obtained from our own work and that of Smolyaninov (1971) and Lange (1975).

(*a*) *Purkinje cells*

Apart from the results described here other authors have made measurements of the number of Purkinje cells in the mouse. Blinkov & Glezer (1968) have said 'For each Purkinje cell there are in the mouse 140 cells of the granular layer' but provide little further information. Johnson & Erner (1972) described neuron death in very old mice (24–29 months) and Lange (1975) calculated Purkinje cell densities in normal mice. The results obtained for normal mice by different authors (table 3) are remarkably similar which indicates the reliability of some of the counting techniques. Purkinje cells have been counted in many other species, including man, as shown in table 3. Lange (1975) calculated Purkinje cell densities in a large variety of animals (man, elephant, pilot whale, bottle nose dolphin, common porpoise, horse, bull, pig, sheep, rhesus monkey, vervet monkey, fox, squirrel monkey, cat, rabbit, opossum, guinea pig, hedgehog,

TABLE 3. ESTIMATED NEURON NUMBERS OBSERVED

(Some of the estimates of neuron numbers are quoted in the literature as densities. In this table we have adjusted all the values to give totals. Fox & Barnard, Hall *et al.*, Lange and Smolyaninov all calculated Purkinje cell density, in Purkinje cells/mm^2 of Purkinje cell layer. By using Smolyaninov's area of the cortex of the cerebellum the total number of Purkinje cells was calculated for each species except the mouse. Since we have calculated the actual area of the Purkinje cell layer for the mouse we have used our figures to calculate total number of Purkinje cells in this animal. Fox & Barnard, for the monkey, obtained a value for granule cell density which we have multiplied by the volume of the granule cell layer obtained from Smolyaninov's figures to obtain the total number. Blinkov & Glezer and Smolyaninov have calculated granule cell densities for the mouse. We have multiplied these figures by the volume of the granule cell layer calculated from our work to obtain total cell numbers. From Lange's mouse granule cell density and our volume of the granule cell layer we have calculated the total number of granule cells in the mouse and using our ratio of granule cells to Purkinje cells the number of Purkinje cells was calculated.)

species	Purkinje	granule	olive	d.c.n.	author(s)
man	15.0×10^6	10^{10}–10^{11}	—	—	Braitenberg & Atwood
man	—	—	0.909×10^6	—	Escobar *et al.*
man	—	—	1.06×10^6	—	Okamoto
man	12.6×10^6	—	—	—	Hall *et al.*
man	—	—	—	62.3×10^4	Heidary & Tomasch
man	17.9×10^6	5.35×10^{10}	—	—	Lange
man	—	—	1.03×10^6	—	Moatamed
man	21.6×10^6	3.46×10^{10}	—	—	Smolyaninov
monkey	—	—	—	11.4×10^4†	Chan-Palay
monkey	3.68×10^6	0.35×10^{10}	—	—	Fox & Barnard
monkey	2.05×10^6	0.39×10^{10}	—	—	Lange
monkey	3.6×10^6	0.34×10^{10}	—	—	Smolyaninov
cat	0.5×10^6	—	—	—	Bell & Dow
cat	—	—	0.141×10^6	—	Escobar *et al.*
cat	1.87×10^6	0.29×10^{10}	—	—	Lange
cat	1.5×10^6	—	0.13×10^6	—	Mlonyeni
cat	1.2 to 1.3×10^6	0.22×10^{10}	—	4.6×10^4‡	Palkovits *et al.*
cat	3.58×10^6	0.215×10^{10}	—	—	Smolyaninov
rat	0.35×10^6	—	—	—	Armstrong & Schild
rat	—	—	—	1.14×10^4§	Chan-Palay
rat ♂	0.54×10^6	—	—	—	Inukai
rat ♀	0.46×10^6	—	—	—	Inukai
rat	0.141×10^6	0.013×10^{10}	—	—	Lange
rat	—	—	0.05×10^6	7.8×10^4	Schild
rat	0.45×10^6	0.012×10^{10}	—	—	Smolyaninov
mouse	—	0.0044×10^{10}	—	—	Blinkov & Blezer
mouse	0.18×10^6	0.0028×10^{10}	0.03×10^6	1.8×10^4	this paper
mouse	0.175×10^6	0.0039×10^{10}	—	—	Lange
mouse	0.25×10^6	0.0044×10^{10}	—	—	Smolyaninov
vampire bat	—	—	0.03×10^6	—	Escobar *et al.*

† Dentate nucleus only counted.
‡ Deiters nucleus not counted.
§ Lateral nucleus only counted.

rat, mole, and mouse). Smolyaninov (1971) has also counted Purkinje cell densities in a number of species (man, macaque, cat, rat, and mouse) and from his results it is possible to calculate total numbers of cells (see table 3). In order to estimate cell numbers in a variety of species Smolyaninov (1971) calculated the density of Purkinje cells in sections tangential to the layer of Purkinje cells and also the surface area of the cerebellum by dividing the volume of the cerebellum by summation of the thickness of the molecular with that of the granule cell layer. Thus he gives the surface area of the cortex of the cerebellum of the mouse as 153 mm^2

whereas the area of Purkinje cell layer is 100 mm^2. These two numbers in fact agree remarkably well if the geometry of the cerebellum is taken into account and a simple calculation performed on the basis that the molecular layer is 150 μm thick. Our area is calculated from the total length of Purkinje cell line measured in our 10 μm thick sections multiplied by the thickness of the sections to give the area. As Smolyaninov does not give a full explanation of his calculations for estimating the number of Purkinje cells the discrepancy over the area of the Purkinje cell layer, the absence of information about shrinkage, and the lack of information about the percentage of cells counted may partly account for the differences between us.

The number of Purkinje cells in man has been estimated by Braitenberg & Atwood (1958) Hall *et al.* (1975), Lange (1975) and Smolyaninov (1971). Their estimates 15×10^6, 12.6×10^6, 17.9×10^6 and 21.6×10^6 respectively, vary considerably but in the study by Hall *et al.* (1975) more cells were counted and more brains were sampled than in the other experiments and therefore this count would be expected to be the most accurate.

Fox & Barnard (1957), Lange (1975) and Smolyaninov (1971) have all counted Purkinje cells in the monkey. The estimates of Fox & Barnard and Smolyaninov (3.68×10^6 and 3.6×10^6) are very close but that of Lange (2.05×10^6) is low especially as these authors all used the same species of monkey. This low count must be a result of either the counting procedure or variation between animals. In the cat estimates made by Bell & Dow (1967), Lange (1975), Mlonyeni (1973), Palkovits *et al.* (1971*a*) and Smolyaninov (1971) are 0.5×10^6, 1.87×10^6, 1.5×10^6, 1.2 to 1.3×10^6 and 3.58×10^6, respectively. This variation should occasion no surprise for some of the estimates are based on a very small percentage of the total volume of tissue. The estimate of Bell & Dow (1967) was made on the basis of weight ratio between human and cat taking the number of Purkinje cells in the human to be 15×10^6 (Braitenberg & Atwood 1958). The results for the rat by Armstrong & Schild (1970), Inukai (1928), Lange (1975) and Smolyaninov (1971) are 0.35×10^6, 0.50×10^6 (averaged between ♂ and ♀), 0.141×10^6 and 0.45×10^6, respectively. The Armstrong & Schild result may be explained, as they say in their discussion, by the fact that they did not incorporate a correction for shrinkage that was used by Inukai (1928) which if removed reduces the discrepancy dramatically. The estimates for the number of Purkinje cells in the mouse are quite similar. The total we give for Smolyaninov was obtained by multiplying his cell density by our area of Purkinje cell layer. The number ascribed to Lange was found by dividing his granule cell number by our ratio of number of granule cells to number of Purkinje cells. In Lange's (1975) table (his p. 119) he has a column labelled P.C.L. which is not clearly explained and it may be that this column represents cells/mm^2 of Purkinje cell layer. In our table 3 we have used the numbers in this column to calculate total Purkinje cell numbers for man, monkey, cat and rat. There are of course problems inherent in such different experiments in different laboratories. Particularly problems that could arise from different amounts of shrinkage with different procedures. However there is little guidance available in these papers so we have adopted the simplest approach in order to arrive at the the totals rather than applying corrections whose magnitude would be unpredictable.

The estimate of the total number of Purkinje cells in man made by Braitenberg & Atwood (1958) was calculated by finding the number of Purkinje cells per square millimetre of tissue and multiplying by the total area of the unfolded cerebellar cortical sheet. They say that this value is 50000 mm^2 (their p. 12) and was calculated from their fig. 3; however the value did not seem, according to the text, to be the value used to obtain the total number of granule cells.

We therefore measured the area of their fig. 3 by using a Graf–Pen graphic digitizer attached to a Tektronix 4051 desk top computer and found that this area represented about 100000 mm^2. This alters the number of Purkinje cells to 30×10^6 and the numbers of granule cells to 9×10^{10} to 21×10^{10}. Without access to Braitenberg's & Atwood's original data it is impossible to say whether it is their fig. 3 which is wrong or their calculation. This discrepancy leaves the ratio of granule cells to Purkinje cells the same as before (3000–7000 : 1). The values shown by these authors were obtained by counting a very small percentage of the total cells and many errors are likely to be accentuated here.

The present estimates of numbers of Purkinje cells in the normal mouse show that between 10 and 730 days no appreciable loss of Purkinje cells occurs. The work of Johnson & Erner (1972) suggests that between 1 and 24 months the number of large neurons in the whole brains of their mice falls by 30 % and by 29 months it decreases by 76 %. It would appear that the Purkinje cell is particularly insensitive to the ravages of time when compared with other large neurons in the brain or, as Johnson & Erner suggested, their estimates in old animals could have been low because of their technique. They homogenized whole brain by exposure to ultrasonication and suggest that in the older animals the neurones were more easily disintegrated and that this fragmentation could have led to a reduced neuron count. The reasons for the low counts at 4 and 8 days post-natal have been discussed in the Results and suffice to say here that our estimates may be low because of the experimental procedure.

(*b*) *Granule cells*

The numbers of granule cells are very large and therefore few people have attempted to estimate total populations. Blinkov & Glezer (1968) stated the ratio of Purkinje cells to cells of the granular layer in the mouse but did not give any idea of methods used. They also quote an estimate of the packing density in the granular layer of the mouse as 3.5×10^6 cells per cubic millimetre. They do not say what age or strain of mouse was used but calculations based on our present estimates of adult numbers give the same granule cell density. The estimates of total numbers of granule cells in the mouse show remarkable similarity especially when such large numbers of neurons are involved. Palkovits *et al.* (1971 *b*) have attempted to estimate numbers of granule cells in the cat where they have corrected for shrinkage due to fixation, dehydration and embedding. Lange (1975) has calculated cell densities of granule cells in the animals listed previously. Fox & Barnard (1957) have also calculated granule cell density in the monkey which is in good agreement with those obtained by Lange (1975) and Smolyaninov (1971). Braitenberg & Atwood (1958) estimated that there are between 10^{10} and 10^{11} granule cells in the cerebellum of man (see above). Total numbers of granule cells in man calculated from Smolyaninov's (1971) figures are 3.46×10^{10}. Our estimates of granule cell numbers have been confined to the internal granule cell layer and hence there is an enormous increase in the number of granule cells in this layer in the normal mouse cerebellum as cells migrate in from the external granule cell layer. This increase reaches its peak at about 17 days after birth which is the stage when the external granule cell layer disappears. This result was expected because it is well known that granule cells proliferate in the external granule cell layer before migrating through the molecular layer to the internal granule cell layer (Altman 1972; Fujita 1967; Fujita *et al.* 1966; Miale & Sidman 1961; Sidman & Miale 1959).

The result that was not expected was that between 15 and 26 days after birth an increase and decrease of granule cells appears to take place. Repeated estimates at 17 days after birth

were not done but from the other estimates at around this age it does appear that an over-production of this cell type is a feasible explanation of the results and that excess cell numbers subsequently degenerate. If this is so then it represents an example of programmed cell death in the cerebellum. It is interesting to note that Sidman & Rakic (1973) while discussing the granule cells in the staggerer mutant mouse say that 'Despite their normal form, more cells die than in control specimens at almost all times during the second and third post-natal weeks', indicating that normal cell death has indeed been seen.

(*c*) *Olive neurons*

Since the inferior olivary nucleus provides many, if not all, the climbing fibres which project to the cerebellum then the number of neurons in the olive is of great interest.

The literature contains no information on estimates of neuron numbers in the olive of the mouse but the estimate on the vampire bat is in very close agreement with our estimate in the mouse (Escobar *et al.* 1968). In that study their estimate of olivary neurons in man agrees very well with that of Futami & Okamoto as described by Okamoto (1968) and also with the excellent study of Moatamed (1966). In this work Moatamed counted cells with nucleoli in serial sections through the olive of a 42-year-old man and then calculated errors which would ensue if a different number of sections were left uncounted in a sequential count. The estimate in the cat by Escobar *et al.* (1968) is also in close agreement with the only other count of cat olivary neurons by Mlonyeni (1973). The number of olive neurons in the rat estimated by Schild (1970) lies between our estimate for the mouse and the estimates for the cat which is as one might expect. The fact that these estimates in different species are comparable to such a degree gives a measure of reliability.

(*d*) *Deep cerebellar nuclei neurons*

No quantitative information is available for the mouse deep cerebellar nuclei but Schild (1972) counted the neuron numbers in nuclei of the rat and Palkovits *et al.* (1977) estimated the numbers in the cat cerebellar nuclei. Chan-Palay (1977) has estimated the number of neurons in the dentate nucleus of the monkey and the lateral nucleus of the rat. Heidary & Tomasch (1969) counted the neurons in each of the nuclei dentatus, emboliformis, globosus and fastigius of three humans aged 3 months, 41 and 45 years. None of these estimates are comparable because of the use of different species or because not all nuclei were included in the counts.

The results of the estimates of neurons in the normal mouse deep cerebellar nuclei suggest that the total number of neurons has not been reached by 63 days after birth. It is possible that not all the neurons are mature by this age and they were not counted because they did not satisfy our criteria.

3. *Qualitative results in the Lurcher mouse*

(*a*) *Purkinje cell changes and other cerebellar mutants*

Abnormalities of the endoplasmic reticulum seen by us in Lurcher at about 13 days after birth have also been described in the nervous mouse where they have been called 'serpentine' by Landis & Mullen (1977). These workers have also shown early morphological changes in Purkinje cells in the Purkinje cell degeneration mutant mouse (pcd) where most of these cells die during the third and fourth week.

The rounding up of mitochondria described here for Lurcher and first seen at 15 days after birth has also been described in the mutant mouse nervous (Landis 1973 *a*, *b*). In Purkinje cells

in the nervous mutant rounded mitochondria appear in the soma of all the Purkinje cells by 15 days after birth. However some Purkinje cells survive the critical period and do not die; the mitochondria of these cells look normal and have presumably reverted to their original shape. Landis (1973*b*) also describes spherical mitochondria in neurons in other parts of the brains of nervous mice but those neurons have never been seen to degenerate. In the Lurcher mutant mouse the Purkinje cells are the only neurons seen with spherical mitochondria and unlike those in nervous they all eventually degenerate. Also, unlike the nervous mutant mouse, the spherical mitochondria are found in the Purkinje cell dendrites of the Lurcher. This suggests that the mitochondrial changes may be secondary and not primary events with the cytoplasm of both the soma and the dendrites becoming more electron dense and vacuolated until the cells are presumably removed by macrophages. In none of the other mutant mice with degenerating Purkinje cells is there a description of events leading to cell death.

The Purkinje cells in other mutants have been shown to be altered in a number of different ways. The mutant mouse reeler has its Purkinje cell arrangement severely disturbed (Hamburgh 1960, 1963) and Rakic (1975*b*) has shown that Purkinje cell dendritic spines having lost their presynaptic elements become enveloped with glia rather than make atypical synapses. Recently Mariani *et al.* (1977) have looked in detail at the reeler from 21 to 226 days of life. They used Golgi impregnation to examine the shapes of the Purkinje cells and electron microscopy to see the fine structure of the Purkinje cells and their synapses.

The staggerer mutant mouse abnormality was described by Sidman *et al.* (1962) as a reduction in the number of granule cells and unaligned Purkinje cells. Sidman & Rakic (1973) and Sotelo & Changeux (1974*b*) suggested that the primary site of gene action in staggerer was the Purkinje cell and that death of the granule cells is probably caused by a retrograde transsynaptic effect (Sotelo 1975*a*; Sotelo & Changeux 1974*a*). Hirano & Dembitzer (1975) described the fine structure of spines on dendrites of Purkinje cells in the staggerer mutant and Landis & Reese (1977) have looked at freeze fractured membranes of spines in the electron microscope. Yoon (1976) suggested that two changes occur in the staggerer mutation (1) external granule cell hypoplasia and (2) delay or arrest of development of Purkinje cells.

Yoon (1977*a*) found that the Purkinje cells in a double mutant of mouse affected by staggerer and reeler conditions were very similar to those in staggerer.

The Purkinje cell dendritic spines in weaver mouse cerebellum have also proved of great interest to many authors. Hanna *et al.* (1976) have studied the spines by using freeze fracture techniques in the electron microscope while Hirano & Dembitzer (1973, 1975), Rakic (1975*a*, *b*), Sotelo (1973, 1975*a*, *b*) and Sotelo & Changeux (1974*b*) have used conventional electron microscopy. All these authors are in agreement that the dendritic spines are not contacted but are intact. Sotelo (1975*a*) described three categories of spines in weaver: normal, hypertrophic and branching. Sotelo's (1975*a*) fig. 3 which shows branching spines should be compared to our figure 8 which shows branching spines in the normal mouse. The only difference between these two types is that the normal mouse spines are surrounded by parallel fibres and those from weaver are covered with glia. It seems that this type of spine is not abnormal at least in our strain of mouse (C3H).

Another mutant mouse in which clinical features suggested a cerebellar lesion (ataxia and a fine tremor during activity) is called agitans. It was first described by Martinez & Sirlin (1955) as having a considerable quantity of atrophied Purkinje cells but as Sidman *et al.* (1965) point out these changes in cells are commonly seen in normal specimens fixed by immersion.

In recent years the Lurcher mouse has received some attention. We (Caddy & Biscoe 1975) described the early light microscopical and fine structural changes in the cerebellum and in Caddy & Biscoe (1976) we described the time course of degeneration of the Purkinje cells over the first 91 days of life. Swisher & Wilson (1975) in their description of Purkinje cells state that at 15 days after birth the Purkinje cells begin to disappear although we have shown that even at 10 days after birth about 30 % of the cells have already degenerated. Wilson (1976) described ectopic Purkinje cells which were slightly smaller than normal Purkinje cells but as they were in the granular layer they could be confused with Golgi cells in the light microscope.

(*b*) *Granule cells*

Unlike other mutants in which the granule cells die (weaver, reeler and staggerer) the granule cells in Lurcher remain as a discrete internal granule cell layer. The basic difference between the Lurcher mutant and all the other cerebellar mutants is that either the granule cells or the Purkinje cells die in weaver, reeler, staggerer, nervous and Purkinje cell degeneration mutants whereas both cell types die in Lurcher. It appears that if one cell type dies then the other type assumes an abnormal position whereas if both cell types die then, as in Lurcher, the layers of cortex remain distinct and the remaining cells retain synaptic contact.

According to our quantitative results the granule cells in the Lurcher mutant mouse achieve normal cell numbers in the internal granule cell layer before degeneration begins. This degeneration takes place very rapidly and using light microscopy we have not seen obvious signs of cell death in the cerebellum. Swisher & Wilson (1977) have described pycnotic granule cells in the molecular layer and also granule cells which have apparently failed to reach the internal granule cell layer (Swisher & Wilson 1975). We have not seen pycnotic granule cells in our tissue but granule cells that are trapped in the molecular layer are often seen even in normal animals (Palay & Chan-Palay 1974). Swisher & Wilson (1977) suggest that the external cell layer in the Lurcher is thinner and disappears earlier than in the normal mouse. We have no evidence to support the latter claim but the thickness of the external granule cell layer is difficult to measure because sectioning in any plane reveals oblique sections through the layer which necessarily makes it look thicker.

On the other hand, in the electron microscope it is possible to see various stages of degeneration of the granule cells from slight changes in the chromatin in the nucleus to death of the cell resulting in an unidentifiable electron dense mass.

(*c*) *Olive neuron*

Scheibel & Scheibel (1955) studied the olivary neurons in many species using a Golgi technique. They found basically two types of neuron, one with large, simple and unramified dendrites and the other with smaller, highly ramified spherical dendrites. They looked at the olive from mice but most of the work is concerned with dogs, cats, macaques and humans. Scheibel *et al.* (1956) expanded this study in the cat and found three cell types, the above two plus a transitional type. In the Golgi–Cox impregnated tissue from Lurcher mice we have only seen neurons with the compact highly ramified spherical dendrites. In the normal controls which were impregnated at the same time as the Lurchers the larger neurons with simple unramified dendrities were also seen. If the cells with highly ramified spherical dendrites were the only type left in Lurcher then they must be projecting to the cells left in the cerebellum

(granule & Golgi cells) and the cells of the deep cerebellar nuclei. It is usually assumed on quite good evidence (see Armstrong 1974) that climbing fibres to Golgi, granule and deep cerebellar nuclei neurones are collaterals of climbing fibres to Purkinje cells. If the degeneration in the olive is secondary to the degeneration in the cerebellum then it seems probable from our results that the climbing fibres originating in neurons with long unramified dendrites could be projecting to the cerebellar cortex only and that the neurons with ramified dendrites could project to both the cerebellar cortex and deep nuclei. Alternatively it could be the case that the neurons with ramified dendrites project exclusively to the Golgi neurons in the cortex which would explain their survival. This is, of course, pure speculation but it would be very interesting to look at the olive in pcd and nervous to see if other mutants with Purkinje cell degeneration have a similar neuron loss. If we could differentiate between these two types of neurons in the electron microscope it might be possible to look in much greater detail at the neurons left in the Lurcher olive to see if they were in fact the ramified dendrite type. Unfortunately at present we are unable to discriminate the two types in the electron microscope except by serial reconstruction which we have not undertaken.

(*d*) *Deep cerebellar nuclei neurons*

It has been suggested by Sidman (1976) that in the lateral nucleus of the *pcd* mutant mouse, when all the Purkinje cells have degenerated, the positions on the soma previously occupied by Purkinje cell axon terminals have been replaced by a glial coating. This is certainly a good example of inviolable synaptic specificity at least for the soma of this cell type. In contrast in the Lurcher mouse there did not seem to be a significant reduction in the number of synapses in the deep cerebellar nuclei when compared with the normal. Certainly there was not the replacement of synaptic sites with glial processes. In young Lurcher mice it is possible to find early degeneration of Purkinje cell axons and terminals in the deep cerebellar nuclei. The terminals make synaptic contact with the neurons but some show lysosomal action which is believed to be an early stage of degeneration. It is clear from our results concerning the deep cerebellar nuclei that removal of one of its largest inputs, the Purkinje cell axons, does not cause degeneration of the neurons. No studies of the deep cerebellar nuclei of any of the other cerebellar mutant mice have been undertaken. This result then is very different from the result in pcd and does not support generalizations of the conclusions from that mutant.

4. *Quantitative results in the Lurcher mouse*

(*a*) *Purkinje cells*

Our results have shown that all the Purkinje cells die within the first 12 weeks of life. The only estimate of Purkinje cells in any other mutant mice was by Mullen *et al.* (1976) in the pcd mutant mouse. These estimates were expressed in Purkinje cells per millimetre as a percentage of control values and therefore comparison with our results is not possible. One other mutant called nervous also exhibits Purkinje cell degeneration but no estimates of number of Purkinje cells have been published.

(*b*) *Granule cells*

It would seem that the degeneration of the granule cells in Lurcher is greater than the proliferation and migration from the external granule cell layer since there is never the increase

in cell number seen in the internal granule cell layer of the normal mouse. The cells remaining (10 %) in the Lurcher mouse 730 days old presumably make synaptic contact with the Golgi, stellate and basket cells which remain. We have not made a study of the synapses remaining in the adult Lurcher although the synapses between mossy fibre glomeruli and granule cell dendrites are present and look normal. In a number of the cerebellar mutant mice the granule cells are affected in some way. This loss has not been quantified in these mutant mice (weaver, staggerer and reeler).

(*c*) *Olive neurons*

Although there is a large decrease in the number of olivary neurons in the Lurcher mouse, even in old age (730 days) we would expect nearly 25 % of the climbing fibres to persist. We have not tried to determine whether there are climbing fibre synapses in the cerebellum but it would seem likely that the synapses between climbing fibres and Golgi, granule, basket and stellate cells would be unaffected. The deep cerebellar nuclei also receive collaterals from the climbing fibres (see Armstrong 1974). These two sources could undoubtedly account for the 25 % of remaining olivary neurons.

In none of the other cerebellar mutant mice has the inferior olivary complex been involved.

(*d*) *Deep cerebellar nuclei neurons*

Quantitative analysis of the deep cerebellar nuclei in the Lurcher mouse has shown that no loss of neurons occurs even though the input from the Purkinje cell axons has been removed in this mutant animal.

One difference which was found between the normal and Lurcher mouse deep cerebellar nuclei was the slight difference in their dorsal–ventral and rostral–caudal extent. This decrease in volume means that the cell density in the Lurcher is greater than in the normal. This quite small shrinkage may be due to the lack of the myelinated Purkinje cell axons in the Lurcher mutant mouse.

In none of the other cerebellar mutant mice has any quantitative work been done concerning the number of neurons in the deep cerebellar nuclei.

5. *Experimentally produced lesions and the Lurcher mutation*

The experimentally produced lesions are of interest for the light they may throw on the nature of the hereditary degenerations. A number of experimental approaches have been used as follows.

The Purkinje cells are affected directly if foetal rats are X-irradiated at 15 and 18 days of gestation (Das 1977*a*, *b*); undernourished during the embryonic and suckling period (Barnes & Altman 1973*a*, *b*; McConnel & Berry 1977); treated with ethanol post-natally (Bauer-Moffett & Altman 1975, 1977); or given carbon monoxide to breathe during adult life (Chan-Palay & McCroskey 1976). In these cases the Purkinje cells degenerate to varying degrees. Injections of diphenylhydantoin sodium (Snider & Del Cerro 1967) have been reported to cause formation of sprouts arising from Purkinje cell dendrites.

A number of experimental studies have been done on young post-natal animals and in these cases the experiments destroy the proliferating cells in the external granule cell layer. Therefore the models are testing the effects of destroying to a greater or lesser extent the granule, basket

and stellate cells. The methods that have been used are: X-irradiation (Altman 1973*a*, *b*, 1976*a*, *b*, *c*; Altman & Anderson 1971, 1972, 1973; Altman *et al.* 1968); undernutrition (Barnes & Altman 1973*a*, *b*; Neville & Chase 1971); injections of methylazoxymethanol (Bradley & Berry 1978; Woodward *et al.* 1975) and injections of panleukopenia virus infected cerebellum (Herndon *et al.* 1971*a*, *b*; Llinás *et al.* 1973).

Removal of granule cells results in malformation of Purkinje cell dendritic trees and abnormalities in the location and orientation of Purkinje cells. Destruction of basket cells affects the vertical growth of the primary dendrites of Purkinje cells.

The elimination of the climbing fibres with 3-acetylpyridine (Bradley & Berry 1976) results in new spines on Purkinje cell dendrites where previously climbing fibres had formed synapses, and diminution of the Purkinje cell dendritic tree.

In the above experiments either Purkinje cells, inferior olivary neurons or granule cells have been completely or partially destroyed. In none of these experimental conditions was the scale of degeneration found in Lurcher seen.

In the Lurcher mutant mouse we are interested, among other things, in finding out whether or not a unique primary location for the effect of the mutant gene can be identified. Our quantitative results have led us to conclude that at 8 days after birth there is a reduction in the number of granule cells in the Lurcher. If this was the only place where the mutant gene was acting in destroying the granule cells then one would expect similar degeneration to that occurring in animals where most of the granule cells are destroyed experimentally. In these animals degeneration of Purkinje cells does not occur and nobody has described retrograde degeneration of olivary neurons. The cerebellar mutant mice which have degenerating granule cells (weaver, staggerer and reeler) have unusual shaped Purkinje cell dendritic trees but these cells do not all die as in Lurcher. If the granule cell death is the primary lesion then from our results it seems that normal granule cell numbers are reached, in the internal granule cell layer, at 4 days after birth but that thereafter the granule cells die before, during, or after migration, or a mixture of any of these, coupled with a reduction in the rate of proliferation of granule cells.

The other cell type which degenerates in the Lurcher mutant mouse is the olive neuron. In view of the present evidence of effects caused by destruction of the olive it would seem that this would not be the seat of a primary and unique location for the action of the mutant gene. Inferior olivary degeneration has not been described in any of the other cerebellar mutant mice.

If the primary lesion is not in the granule cell or the olive neuron then it might be the Purkinje cell. This it would seem would be the most likely since all the Purkinje cells in the Lurcher degenerate whereas all of the other two cell types do not. This would explain why many but not all granule cells and olive neurons degenerate. The granule cells having Purkinje cells as their primary targets would be now redundant while other granule cell axons contacting Golgi, stellate and basket cells would survive. The olive neurons whose climbing fibres synapse only with Purkinje cells, assuming such cells exist, would degenerate while those climbing fibres going to the deep cerebellar nuclei would remain intact. As described above various experimental procedures have been found to reduce the number of Purkinje cells. Most of these experiments also cause reduction in the granule cell numbers but this degeneration is most probably a direct effect of the procedure rather than a secondary result.

6. *Ratio of neuron numbers*

The ratio of Purkinje cells to deep cerebellar nuclei neurons in the normal adult mouse shows that the Purkinje cells outnumber the deep cerebellar nuclei neurons by about 10:1. Since according to Chan-Palay (1977) the Purkinje cell axons branch profusely on entering the deep cerebellar nuclei to contact a wide variety of neurons it follows that there is considerable divergence at this point and that each deep cerebellar nucleus cell would be expected to receive synaptic contacts from very many more than ten Purkinje cells.

The ratio results for olive neurons to deep cerebellar nuclei neurons have to be regarded as hypothetical since we are not sure whether there are climbing fibres which project exclusively to the deep cerebellar nuclei. If this were the case then the ratios for the Lurcher represent a maximum ratio since the granule and Golgi cells also receive synapses from climbing fibres.

It is perhaps more likely that the synapses between climbing fibres and granule cells, Golgi cells, and deep cerebellar nuclei neurons are collaterals of climbing fibres to the Purkinje cell and that only these climbing fibres degenerate (in the Lurcher), due to lack of targets.

The ratio of granule cells to Purkinje cells in the adult normal mouse of about 170 again gives a quantitative measure of the degree of convergence in this part of the cortex. However, we have not measured the length of a parallel fibre and so cannot calculate how many Purkinje cells might be contacted by one granule cell. Nevertheless we do know the density of Purkinje cells in the cortex (20 cells/mm) and can thus estimate the number of cells contacted; if the parallel fibres were for example 2 mm long then the number of Purkinje cells contacted would be 40.

In so far as Lurcher is concerned the interesting result is that the ratios of Purkinje cells to olive cells do not diverge from the normal until 17 days after-birth. A similar time course is found for the ratio of granule cells to Purkinje cells for normal and Lurcher. This means that the degeneration of the Purkinje cells, granule cells and olive neurons run parallel to each other, at least until 17 days after birth and does not resolve the question of which cell type if any has primacy.

7. *Concluding remarks*

In pursuance of this investigation we have found it necessary to make a detailed study of the normal cerebellum as well as that of the mutant animal. These normal results are of interest in themselves for the light they shed on the rates of development and cell death and for the measures they provide of the dimensions of the neuronal networks in and associated with the mouse cerebellum.

In regard to the Lurcher mutant we have reached no firmly established conclusion about the primary lesion. At present it is our tentative conclusion that the fault lies within the Purkinje cell.

This work was supported by M.R.C. Program Grant G975/952. K. W. T. Caddy was a Wellcome Trust Research Training Scholar.

References

Abercrombie, M. 1946 Estimation of nuclear population from microtome sections. *Anat. Rec.* **94**, 239–247.

Altman, J. 1972 Postnatal development of the cerebellar cortex in the rat. I. The external germinal layer and the the transitional molecular layer. *J. comp. Neurol.* **145**, 353–397.

Altman, J. 1973*a* Experimental reorganization of the cerebellar cortex. III. Regeneration of the external germinal layer and granule cell ectopia. *J. comp. Neurol.* **149**, 153–179.

Altman, J. 1973*b* Experimental reorganization of the cerebellar cortex. IV. Parallel fiber reorientation following regeneration of the external germinal layer. *J. comp. Neurol.* **149**, 181–191.

Altman, J. 1976*a* Experimental reorganization of the cerebellar cortex. V. Effects of X-irradiation schedules that allow or prevent the acquisition of basket cells. *J. Comp. Neurol.* **165**, 31–47.

Altman, J. 1976*b* Experimental reorganization of the cerebellar cortex. VI. Effects of X-irradiation schedules that allow or prevent cell acquisition after basket cells are formed. *J. comp. Neurol.* **165**, 49–63.

Altman, J. 1976*c* Experimental reorganization of the cerebellar cortex. VII. Effects of late X-irradiation schedules that interfere with cell acquisition after stellate cells are formed. *J. comp. Neurol.* **165**, 65–75.

Altman, J. & Anderson, W. J. 1971 Irradiation of the cerebellum in infant rats with low-level X-ray: histological and cytological effects during infancy and adulthood. *Expl Neurol.* **30**, 492–509.

Altman, J. & Anderson, W. J. 1972 Experimental reorganization of the cerebellar cortex. I. Morphological effects of elimination of all microneurones with prolonged X-irradiation started at birth. *J. comp. Neurol.* **146**, 355–405.

Altman, J. & Anderson, W. J. 1973 Experimental reorganization of the cerebellar cortex. II. Effects of elimination of most microneurones with prolonged X-irradiation started at 4 days. *J. comp. Neurol.* **144**, 123–151.

Altman, J., Anderson, W. J. & Wright, K. A. 1968 Gross morphological consequences of irradiation of the cerebellum in infant rats with repeated doses of low-level X-ray. *Expl Neurol.* **21**, 69–91.

Armstrong, D. M. 1974 Functional significance of connections of the inferior olive. *Physiol. Rev.* **54**, 358–417.

Armstrong, D. M. & Schild, R. F. 1970 A quantitative study of the Purkinje cells in the cerebellum of the albino rat. *J. comp. Neurol.* **139**, 449–456.

Barnes, D. & Altman, J. 1973*a* Effects of different schedules of early undernutrition on the preweaning growth of the rat cerebellum. *Expl Neurol.* **38**, 406–419.

Barnes, D. & Altman, J. 1973*b* Effects of two levels of gestational-lactational undernutrition on the postweaning growth of the rat cerebellum. *Expl Neurol.* **38**, 420–428.

Bauer-Moffett, C. & Altman, J. 1975 Ethanol-induced reductions in cerebellar growth of infant rats. *Expl Neurol.* **48**, 378–382.

Bauer-Moffett, C. & Altman, J. 1977 The effect of ethanol chronically administered to preweaning rats on cerebellar development: a morphological study. *Brain Res.* **119**, 249–268.

Bell, C. C. & Dow, R. S. 1967 Cerebellar circuitry. *Neurosci. Res. Prog. Bull.* **5**, 121–122.

Blinkov, S. M. & Glezer, I. I. 1968 *The human brain in figures and tables*, p. 159. New York: Basic Books.

Bradley, P. & Berry, M. 1976 Quantitative effects of climbing fibre deafferentiation on the adult Purkinje cell dendritic tree. *Brain Res.* **112**, 133–140.

Bradley, P. & Berry, M. 1978 Quantitative effects of methylazoxymethanol acetate on Purkinje cell dendritic growth. *Brain Res.* **143**, 499–511.

Braitenberg, V. & Atwood, R. P. 1958 Morphological observations on the cerebellar cortex. *J. comp. Neurol.* **109**, 1–33.

Caddy, K. W. T. & Biscoe, T. J. 1975 Preliminary observations on the cerebellum in the mutant mouse Lurcher. *Brain Res.* **91**, 276–280.

Caddy, K. W. T. & Biscoe, T. J. 1976 The number of Purkinje cells and olive neurones in the normal and Lurcher mutant mouse. *Brain Res.* **111**, 396–398.

Caddy, K. W. T., Martin, M. R. & Biscoe, T. J. 1977 The identification of mossy fibres and their cells of origin in the normal and Lurcher mutant mouse. *J. neurol. Sci.* **34**, 121–129.

Cammermeyer, J. 1967 Artifactual displacement of neuronal nucleoli in paraffin sections. *J. Hirnforsch.* **9**, 209–224.

Chan-Palay, V. 1977 *Cerebellar dentate nucleus, organization, cytology and transmitters*. Berlin, Heidelberg: Springer-Verlag.

Chan-Palay, V. & McCroskey, L. 1976 The effects of carbon monoxide on neurons of the cerebellum. *Neuropath. appl. Neurobiol.* **2**, 293–312.

Courville, J. & Cooper, C. W. 1970 The cerebellar nuclei of Macaca mulatta; a morphological study. *J. comp. Neurol.* **140**, 241–254.

Das, G. D. 1977*a* Experimental analysis of embryogenesis of cerebellum in rat. I. Subnormal growth following X-ray irradiation on day 15 of gestation. *J. comp. Neurol.* **176**, 419–433.

Das, G. D. 1977*b* Experimental analysis of embryogenesis of cerebellum in rat. II. Morphogenetic malformations following X-ray irradiation on day 18 of gestation. *J. comp. Neurol.* **176**, 435–451.

Desclin, J. C. 1974 Histological evidence supporting the inferior olive as the major source of cerebellar climbing fibers in the rat. *Brain Res.* **77**, 365–384.

Escobar, A., Sampedro, E. D. & Dow, R. S. 1968 Quantitative data on the inferior olivary nucleus of man, cat and vampire bat. *J. comp. Neurol.* **132**, 397–403.

Floderus, S. 1944 Untersuchungen über den Bau der menschlichen Hypophyse mit besonderer Berücksichtigung der quantitativen mikromorphologischen Verhältnisse. *Acta path. microbiol. scand., Suppl.* **53**, 1–276.

Fox, C. A. & Barnard, J. W. 1957 A quantitative study of the Purkinje cell dendritic branchlets and their relationship to afferent fibres. *J. Anat.* **91**, 299–313.

Fujita, S. 1967 Quantitative analysis of cell proliferation and differentiation in the cortex of the postnatal mouse cerebellum. *J. Cell Biol.* **32**, 277–287.

Fujita, S., Shimada, M. & Nakamura, T. 1966 H^3-thymidine autoradiographic studies on the cell proliferation and differentiation in the external and internal granular layers of the mouse cerebellum. *J. comp. Neurol.* **128**, 191–207.

Hall, T. C., Miller, A. K. H. & Corsellis, J. A. N. 1975 Variations in the human Purkinje cell population according to age and sex. *Neuropath. appl. Neurobiol.* **1**, 267–293.

Hamburgh, M. 1960 Observations on the neuropathology of 'reeler' a neurological mutation of mice. *Experientia* **16**, 460–461.

Hamburgh, M. 1963 Analysis of the postnatal developmental effects of 'reeler', a neurological mutation in mice. A study in developmental genetics. *Devl Biol.* **8**, 165–185.

Hanley, T. 1974 'Neuronal fall-out' in the aging brain: a critical review of the quantitative data. *Age & Aging* **3**, 133–151.

Hanna, R. B., Hirano, A. & Pappas, G. D. 1976 Membrane specializations of dendritic spines and glia in the weaver mouse cerebellum, a freeze fracture study. *J. Cell. Biol.* **68**, 403–410.

Heidary, H. & Tomasch, J. 1969 Neuron numbers and perikaryan areas in the human cerebellar nuclei. *Acta anat.* 74, 290–296.

Herndon, R. M., Margolis, G. & Kilham, L. 1971*a* The synaptic organisation of the malformed cerebellum induced by perinatal infection with the feline panleukopenia virus (PLV). I. Elements forming the cerebellar glomeruli. *J. Neuropath. exp. Neurol.* **30**, 196–205.

Herndon, R. M., Margolis, G. & Kilham, L. 1971*b* The synaptic organisation of the malformed cerebellum induced by perinatal infection with the feline panleukopenia virus (PLV). II. The Purkinje cell and its afferents. *J. Neuropath. exp. Neurol.* **30**, 557–570.

Hirano, A. & Dembitzer, H. M. 1973 Cerebellar alterations in the weaver mouse. *J. Cell. Biol.* **56**, 478–486.

Hirano, A. & Dembitzer, H. M. 1975 The fine structure of staggerer cerebellum. *J. Neuropath. exp. Neurol.* **34**, 1–11.

Hollingworth, T. & Berry, M. 1975 Network analysis of dendritic fields of pyramidal cells in neocortex and Purkinje cells in the cerebellum of the rat. *Phil. Trans. R. Soc. Lond.* B **270**, 227–264.

Inukai, T. 1928 On the loss of Purkinje cells, with advancing age, from the cerebellar cortex of the albino rat. *J. comp. Neurol.* **45**, 1–31.

Johnson, H. A. & Erner, S. 1972 Neuron survival in the aging mouse. *Expl Geront.* **7**, 111–117.

Jones, R. L. 1937 Split nucleoli as a source of error in nerve cell counts. *Stain Tech.* **12**, 91–95.

Landis, D. M. D. & Reese, T. S. 1977 Structure of the Purkinje cell membrane in staggerer and weaver mutant mice. *J. comp. Neurol.* **171**, 247–260.

Landis, S. C. 1973*a* Ultrastructural changes in the mitochondria of cerebellar Purkinje cells of nervous mutant mice. *J. Cell Biol.* **57**, 782–797.

Landis, S. C. 1973*b* Changes in neuronal mitochondrial shape in brains of nervous mutant mice. *J. Hered.* **64**, 193–196.

Landis, S. C. & Mullen, R. J. 1977 The development and degeneration of Purkinje cells in pcd mutant mice. *J. comp. Neurol.* **177**, 125–143.

Lange, W. 1975 Cell number and cell density in the cerebellar cortex of man and some other mammals. *Cell Tiss. Res.* **157**, 115–124.

Larramendi, L. M. H. 1969 Analysis of synaptogenesis in the cerebellum of the mouse. In *Neurobiology of cerebellar evolution and development* (ed. R. Llinás), pp. 803–843. Chicago, Ill.: A.M.A.

Larramendi, L. M. H. 1970 Morphological characteristics of extrinsic and intrinsic nerve terminals and their synapses in the cerebellar cortex of the mouse. In *The cerebellum in health and disease* (eds W. S. Fields & W. D. Willis, Jr), pp. 63–110. St Louis: Warren M. Green.

Larramendi, L. M. H. & Lemkey-Johnston, N. 1970 The distribution of recurrent Purkinje collateral synapses in the mouse cerebellar cortex: an electron microscopic study. *J. comp. Neurol.* **138**, 451–482.

Larramendi, L. M. H. & Victor, T. 1967 Synapses of the Purkinje cell spines in the mouse. An electron microscopic study. *Brain Res.* **5**, 15–30.

Larsell, O. 1970 *The comparative anatomy and histology of the cerebellum from monotremes through apes* (ed. J. Jansen). The University of Minnesota Press.

Larsell, O. & Jansen, J. 1972 *The comparative anatomy and histology of the cerebellum: the human cerebellum, cerebellar connections, and cerebellar cortex.* University of Minnesota Press.

Llinás, R., Hillman, D. E. & Precht, W. 1973 Neuronal circuit reorganization in mammalian agranular cerebellar cortex. *J. Neurobiol.* **4**, 69–94.

Mariani, J., Crepel, F., Mikoshiba, K., Changeux, J. P. & Sotelo, C. 1977 Anatomical, physiological and biochemical studies of the cerebellum from reeler mutant mouse. *Phil. Trans. R. Soc. Lond.* B **281**, 1–28.

Martin, M. R. & Caddy, K. W. T. 1977 Electrophysiological studies on interpositus neurones in the normal and Lurcher mutant mouse. *Expl Brain. Res.* **29**, 275–281.

Martin, M. R., Caddy, K. W. T. & Biscoe, T. J. 1977 Numbers and diameters of motoneurons and myelinated axons in the facial nucleus and nerve of the albino rat. *J. Anat.* **123**, 579–587.

Martinez, A. & Sirlin, J. L. 1955 Neurohistology of the Agitans mouse. *J. comp. Neurol.* **103**, 131–137.

McConnel, P. & Berry, M. 1977 The effects of undernutrition on Purkinje cell dendritic growth in the rat. *J. comp. Neurol.* **177**, 159–171.

Miale, I. L. & Sidman, R. L. 1961 An autoradiographic analysis of histogenesis in the mouse cerebellum. *Expl Neurol.* **4**, 277–296.

Mlonyeni, M. 1973 The number of Purkinje cells and inferior olivary neurones in the cat. *J. comp. Neurol.* **147**, 1–9.

Moatamed, F. 1966 Cell frequencies in the human inferior olivary nuclear complex. *J. comp. Neurol.* **128**, 109–116.

Mullen, R. J., Eicher, E. M. & Sidman, R. L. 1976 Purkinje cell degeneration, a new neurological mutation in the mouse. *Proc. natn. Acad. Sci. U.S.A.* **73**, 208–212.

Neville, H. E. & Chase, H. P. 1971 Undernutrition and cerebellar development. *Expl Neurol.* **33**, 485–497.

Okamoto, M. 1968 Anatomy of olivary nucleus and the surrounding areas. *Adv. neurol. Sci.* **12**, 341–367.

Palay, S. L., Billings-Gagliardi, S. & Chan-Palay, V. 1974 Neuronal perikarya with dispersed, single ribosomes in the visual cortex of Macaca Mulatta. *J. Cell Biol.* **63**, 1074–1089.

Palay, S. L. & Chan-Palay, V. 1974 *Cerebellar cortex, cytology and organization.* Berlin, Heidelberg: Springer-Verlag.

Palkovits, M., Magyar, P. & Szentágothai, J. 1971*a* Quantitative histological analysis of the cerebellar cortex in the cat. I. Number and arrangement in space of the Purkinje cells. *Brain Res.* **32**, 1–13.

Palkovits, M., Magyar, P. & Szentágothai, J. 1971*b* Quantitative histological analysis of the cerebellar cortex in the cat. II. Cell numbers and densities in the granular layer. *Brain Res.* **32**, 15–30.

Palkovits, M., Magyar, P. & Szentágothai, J. 1971*c* Quantitative histological analysis of the cerebellar cortex in the cat. III. Structural organisation of the molecular layer. *Brain Res.* **34**, 1–18.

Palkovits, M., Mezey, E., Hámori, J. & Szentágothai, J. 1977 Quantitative histological analysis of the cerebellar nuclei in the cat. I. Numerical data on cells and on synapses. *Expl Brain Res.* **28**, 189–210.

Pasternak, J. F. & Woolsey, T. A. 1975 On the 'selectivity' of the Golgi–Cox method. *J. comp. Neurol.* **160**, 307–312.

Phillips, R. J. S. 1960 Lurcher, a new gene in linkage group XI of the house mouse. *J. Genet.* **57**, 35–42.

Rakic, P. 1975*a* Cell migration and neuronal ectopias in the brain. In *Morphogenesis and malformation of the brain and face* (eds J. Langman & D. Bergsma), pp. 95–129. March of Dimes Monograph.

Rakic, P. 1975*b* Synaptic specificity in the cerebellar cortex: Study of anomalous circuits induced by single gene mutations in mice. *Cold Spring Harbor Symp. quant. Biol.* **40**, 333–346.

Scheibel, M. E. & Scheibel, A. B. 1955 The inferior olive. A Golgi study. *J. comp. Neurol.* **102**, 77–131.

Scheibel, M., Scheibel, A., Walberg, F. & Brodal, A. 1956 Areal distribution of axonal and dendritic patterns in inferior olive. *J. comp. Neurol.* **106**, 21–49.

Schild, R. F. 1970 On the inferior olive of the albino rat. *J. comp. Neurol.* **140**, 255–259.

Schild, R. F. 1972 Aspects of the relationship between the inferior olivary nucleus and the cerebellum in the rat and the cat. Ph.D. thesis, Bristol University.

Sholl, D. A. 1953 Dendritic organisation in the neurons of the visual and motor cortices of the cat. *J. Anat.* **87**, 387–406.

Sidman, R. L. 1976 Cell surface properties and the expression of inherited brain diseases in mice. In *Membranes and disease* (eds L. Bolis, J. F. Hoffman & A. Leaf), pp. 379–386. New York: Raven Press.

Sidman, R. L., Green, M. C. & Appel, S. H. 1965 *Catalogue of the neurological mutants of the mouse.* Cambridge, Massachusetts: Harvard University Press.

Sidman, R. L., Lane, P. W. & Dickie, M. M. 1962 Staggerer, a new mutation in the mouse affecting the cerebellum. *Science, N.Y.* **137**, 610–612.

Sidman, R. L. & Miale, I. 1959 Histogenesis of the mouse cerebellum studied by autoradiography with tritiated thymidine. *Anat. Rec.* **133**, 429–430.

Sidman, R. L. & Rakic, P. 1973 Neuronal migration, with special reference to developing human brain: a review. *Brain Res.* **62**, 1–35.

Smolyaninov, V. V. 1971 Some special features of organization of the cerebellar cortex. In *Models of the structural–functional organization of certain biological systems* (eds I. M. Gelfand, V. S. Gurfinkel, S. V. Fornin & M. L. Tsetlin), pp. 251–325. Massachusetts: MIT Press. Originally published as *Modeli strukturno–funktionalnoy organisatsii nyekotoyh biologichyeskikh sistem.* Moscow (1966).

Snider, R. S. & Del Cerro, M. P. 1967 Drug-induced dendritic sprouts on Purkinje cells in the adult cerebellum. *Expl Neurol.* **17**, 466–480.

Sotelo, C. 1973 Permanence and fate of paramembranous synaptic specializations in 'mutants' and experimental animals. *Brain Res.* **62**, 345–351.

Sotelo, C. 1975*a* Dendritic abnormalities of Purkinje cells in the cerebellum of neurologic mutant mice (weaver and stagger). *Adv. Neurol.* **12**, 335–351.

Sotelo, C. 1975*b* Anatomical, physiological and biochemical studies of the cerebellum from mutant mice. II. Morphological study of cerebellar cortical neurons and circuits in the weaver mouse. *Brain Res.* **94**, 19–44.

Sotelo, C. & Changeux, J. P. 1974*a* Transsynaptic degeneration 'en cascade' in the cerebellar cortex of staggerer mutant mice. *Brain Res.* **67**, 519–526.

Sotelo, C. & Changeux, J. P. 1974*b* Bergmann fibers and granular cell migration in the cerebellum of homozygous weaver mutant mouse. *Brain Res.* **77**, 484–491.

Swisher, D. A. & Wilson, D. B. 1975 Cerebellar dysplasia in Lurcher (Lc) mutant mice. *Anat. Rec.* **181**, 489.

Swisher, D. A. & Wilson, D. B. 1977 Cerebellar histogenesis in the Lurcher (Lc) mutant mouse. *J. comp. Neurol.* **173**, 205–217.

Taber Pierce, E. 1973 Time of origin of neurones in the brain stem of the mouse. *Prog. Brain Res.* **40**, 53–65.

Vijayan, V. K. & Wilson, D. B. 1975 Acetylcholesterase activity in the cerebellum of the Lurcher (Lc) mutant mouse. *Neurobiology* **5**, 228–234.

Wilson, D. B. 1975 Brain abnormalities in the Lurcher (Lc) mutant mouse. *Experientia* **31**, 220–221.

Wilson, D. B. 1976 Histological defects in the cerebellum of adult Lurcher (Lc) mice. *J. Neuropath. exp. Neurol.* **35**, 40–45.

Woodward, D. J., Bickett, D. & Chanda, R. 1975 Purkinje cell dendritic alterations after transient developmental injury of the external granular layer. *Brain Res.* **97**, 195–214.

Yoon, C. H. 1976 Pleiotropic effect of the staggerer gene. *Brain Res.* **109**, 206–215.

Yoon, C. H. 1977*a* Fine structure of the cerebellum of 'staggerer–reeler', a double mutant of mice affected by staggerer and reeler conditions. II. Purkinje cell anomalies. *J. Neuropath. exp. Neurol.* **36**, 427–439.

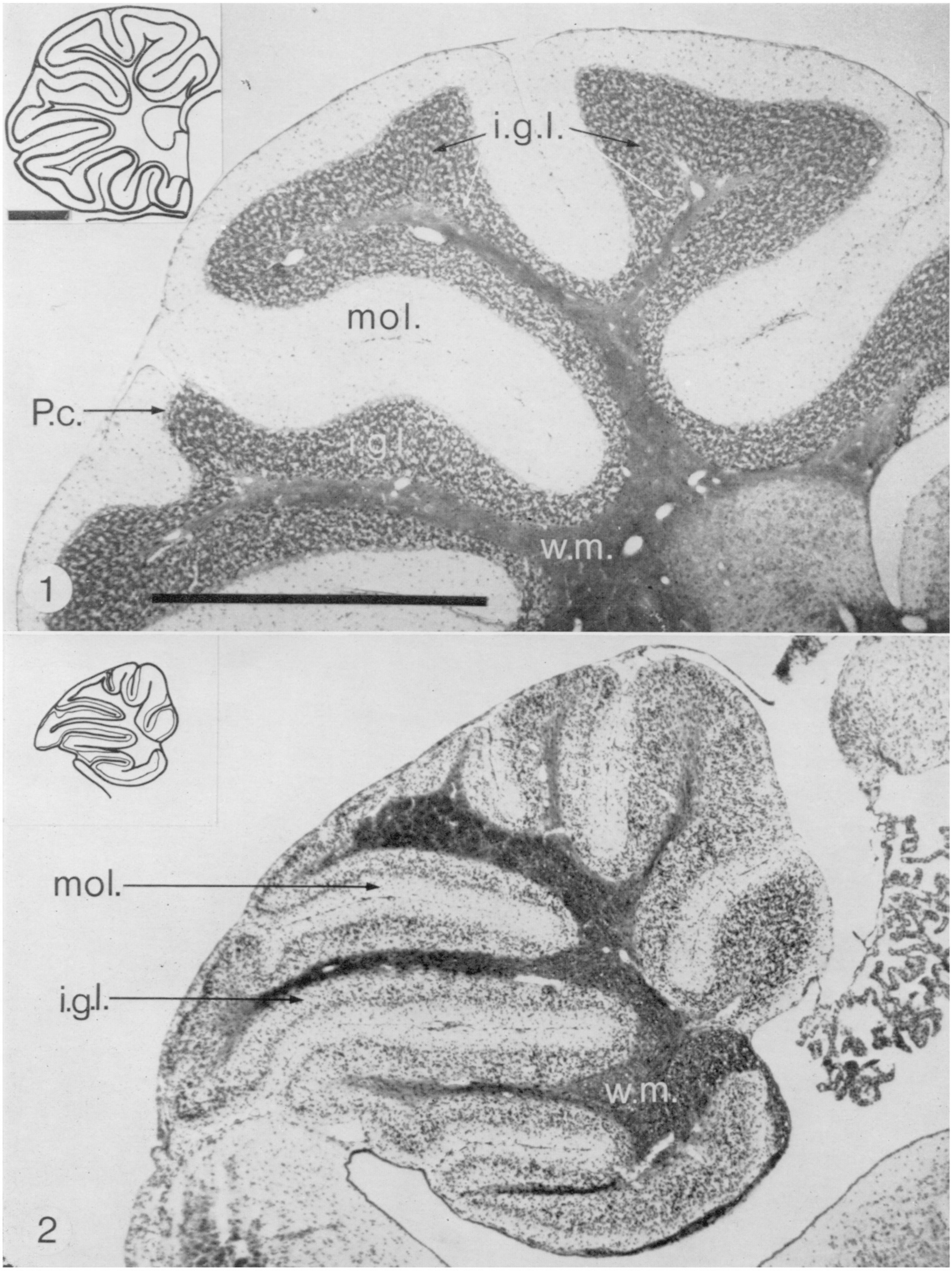

Light micrographs of sagittal sections of cerebellum from adult mice. Inserts show drawings of whole sections to compare size of normal cerebellum with that of the Lurcher mutant mouse. Sections stained with luxol fast blue and cresyl violet. Figures 1 and 2 are the same magnification as are the inserts; calibration bars for all photographs = 1 mm. Abbreviations: mol., molecular layer; i.g.l., internal granule cell layer; P.c., Purkinje cell layer; w.m., white matter.

FIGURE 1. The different layers of the cerebellum in the normal mouse are easily seen in this figure. Section taken from an animal 77 days old.

FIGURE 2. The loss of Purkinje and granule cells in this section of a Lurcher mouse cerebellum is obvious but the overall laminated structure is still maintained. Section from an animal 50 days old.

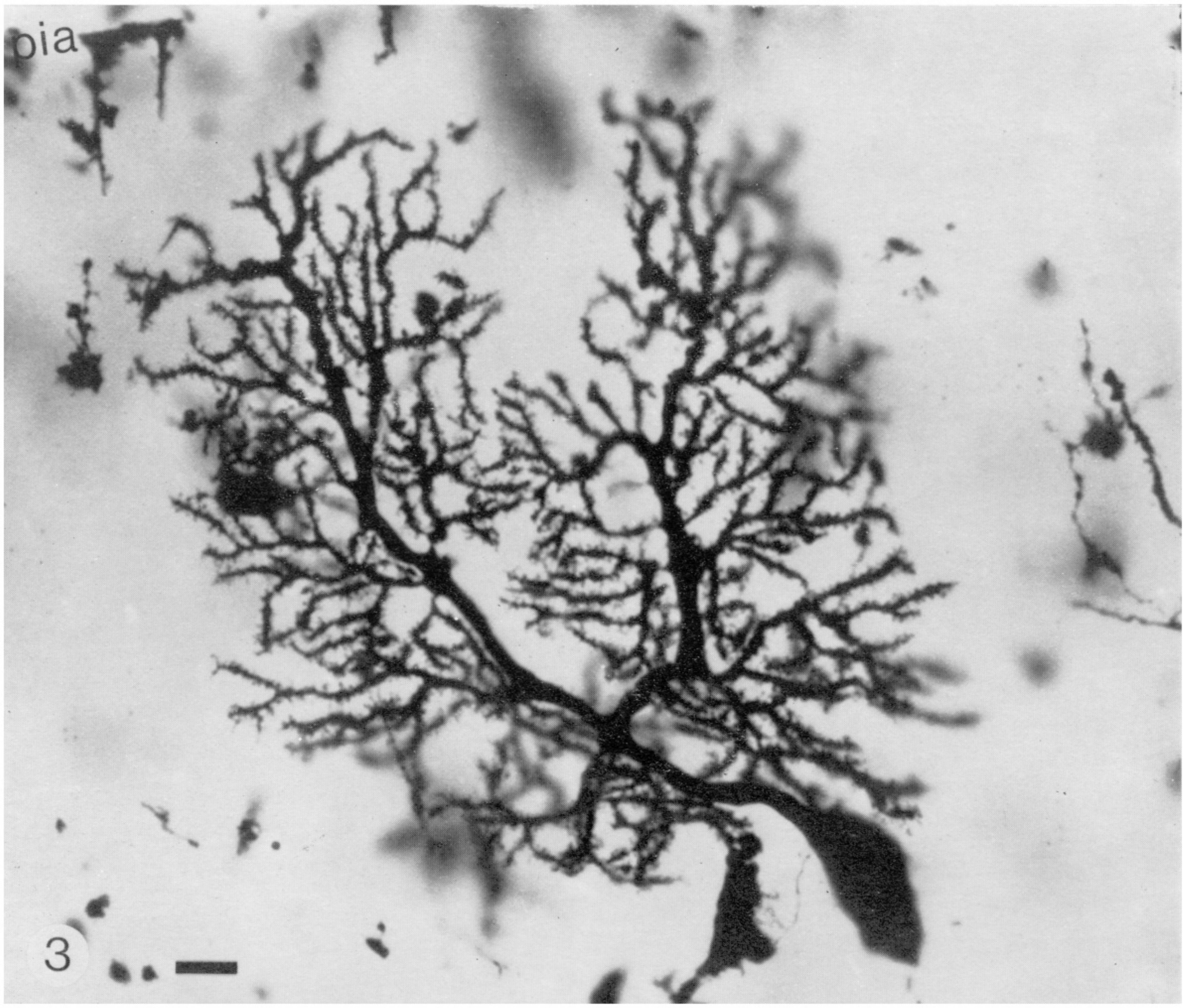

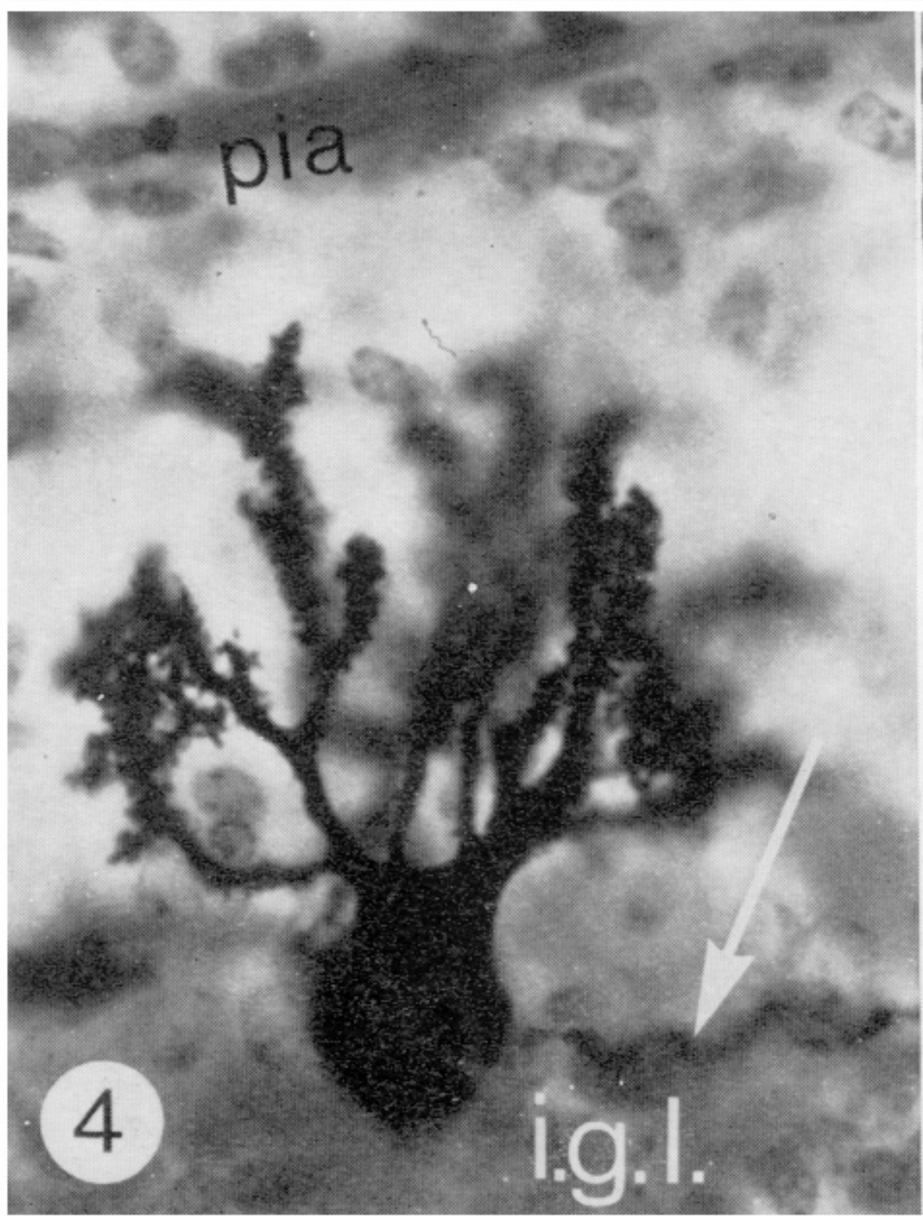

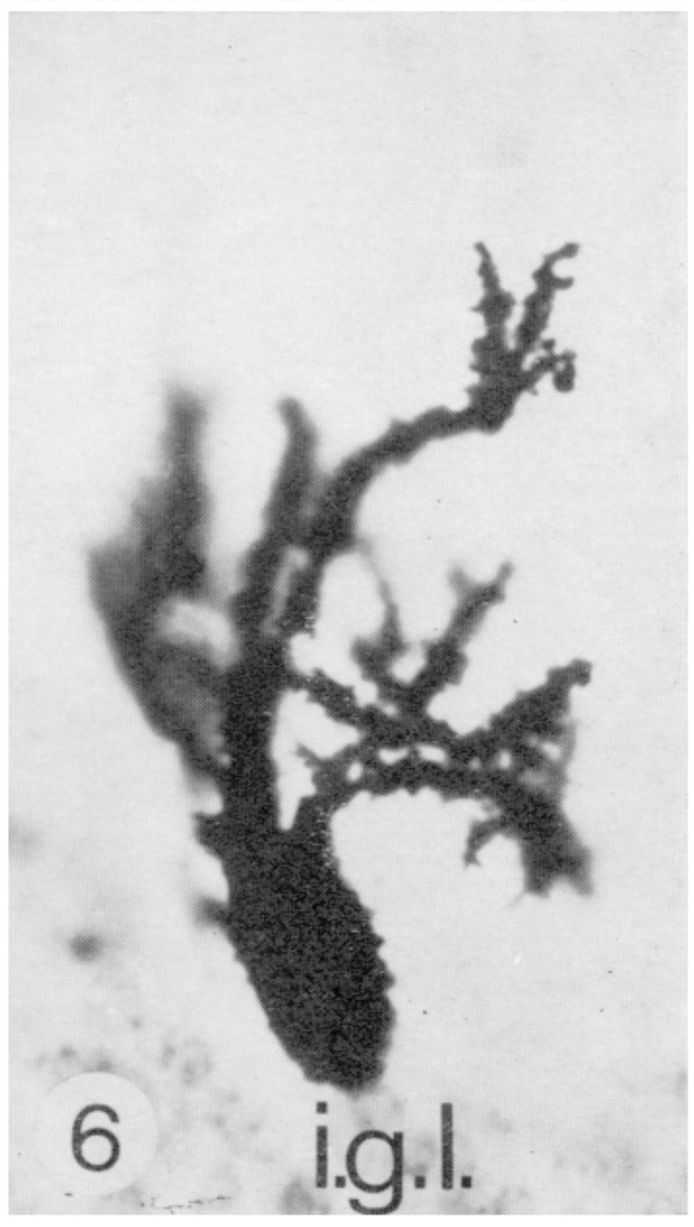

Light micrographs of Golgi–Cox impregnated tissue showing Purkinje cells from normal and Lurcher mice. Calibration bar = 10 μm for all micrographs.

FIGURE 3. Cell from a 15 day post-natal normal cerebellum showing the pial surface (pia) in the top left-hand corner. The smooth primary and secondary dendrites and spines on the more distal dendrites are easily seen. The section is 100 μm thick and fortunately the majority of this dendritic tree is in the plane of focus.

FIGURES 4–6. Examples of Purkinje cells seen in a 14 day post-natal Lurcher mouse. Spines can be seen on the dendrites and also on the soma of the Purkinje cell in 6. Axons are arrowed in 4 and 5. These sections are counterstained with cresyl violet and therefore the internal granule cell layer is visible (i.g.l.).

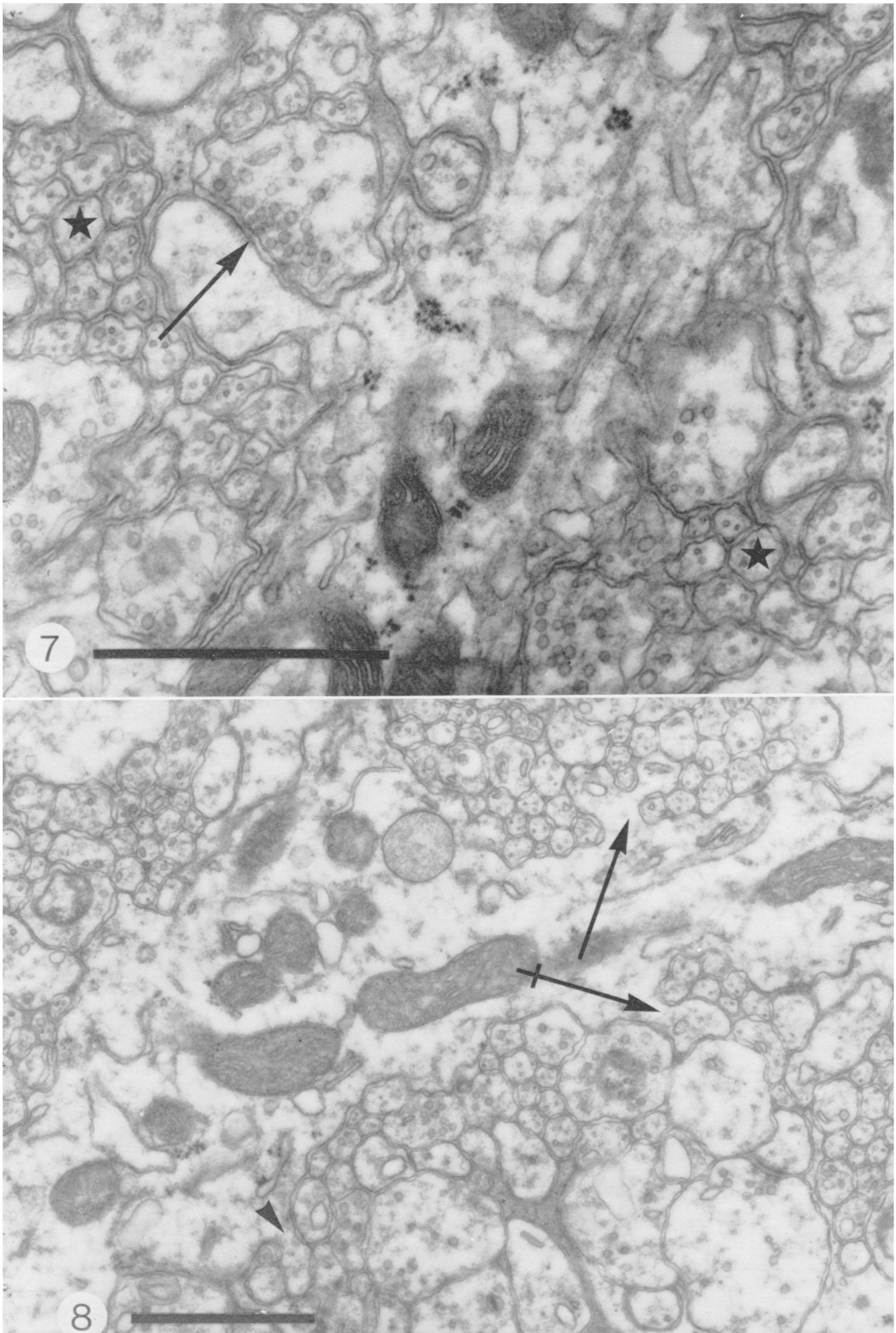

Electron micrographs of Purkinje cell dendrites from normal mice. Calibration bar = 1 μm for both micrographs.

FIGURE 7. Dendrite from a mouse 14 days old, surrounded by parallel fibres (stars) cut in cross section. A parallel fibre is seen synapsing with a dendritic spine (arrow).

FIGURE 8. Dendrite from a mouse 13 days old with three different spines. None of these spines is in synaptic contact with a parallel fibre although fibres surround them.

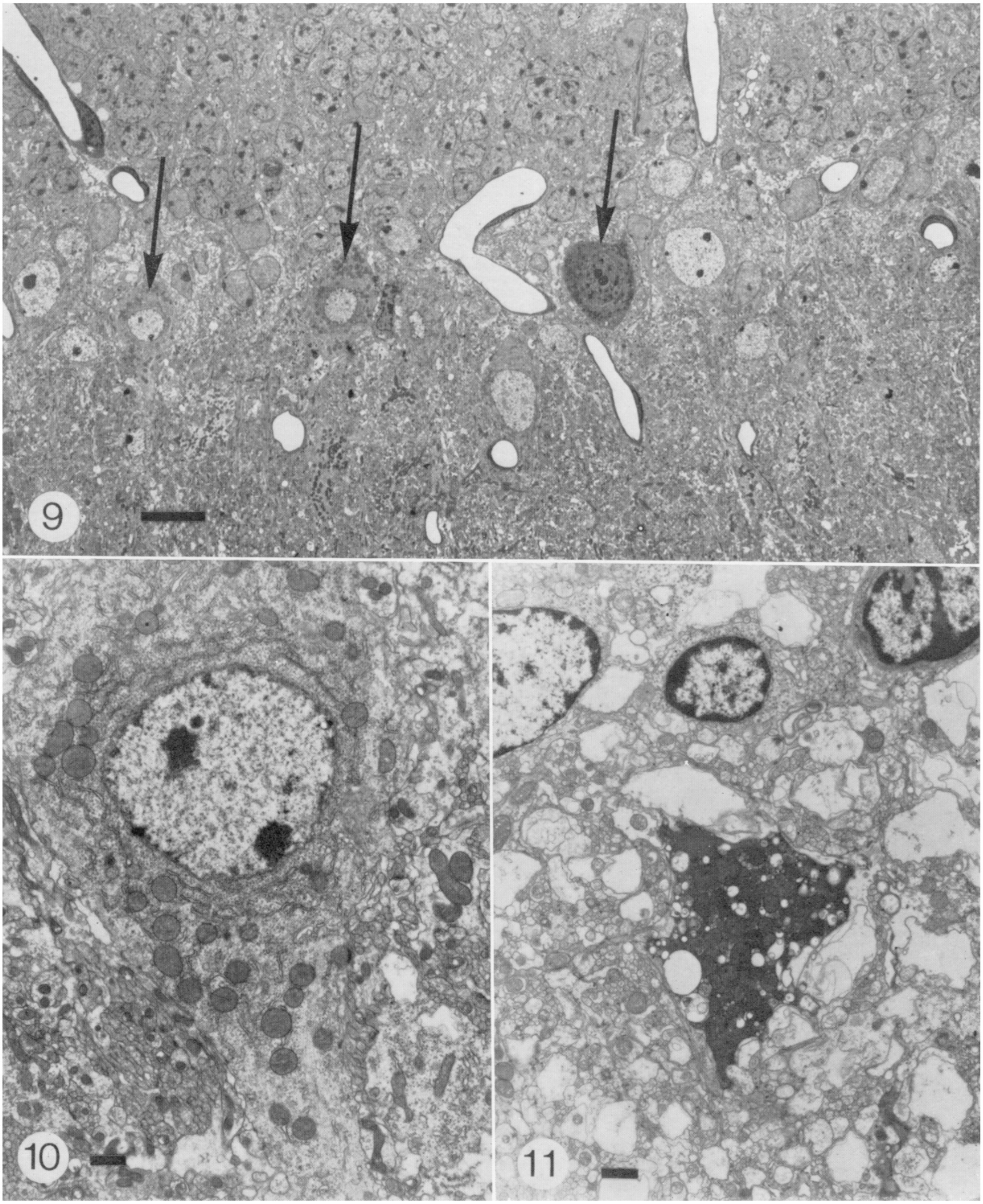

Electron micrographs from Lurcher mutant mice 15 days old.

FIGURE 9. Low power electron micrograph showing the internal granule cell layer (i.g.l.), the Purkinje cell layer (P.c.), and the molecular layer (mol.). Three Purkinje cells in different stages of degeneration are arrowed. Calibration bar = 10 μm.

FIGURE 10. Purkinje cell arrowed far left in figure 9. This higher power electron micrograph shows the rounded up mitochondria and the disrupted endoplasmic reticulum. Calibration bar = 1 μm.

FIGURE 11. Purkinje cell in an advanced stage of degeneration. The rounded profiles of mitochondria are visible. Calibration bar = 1 μm.

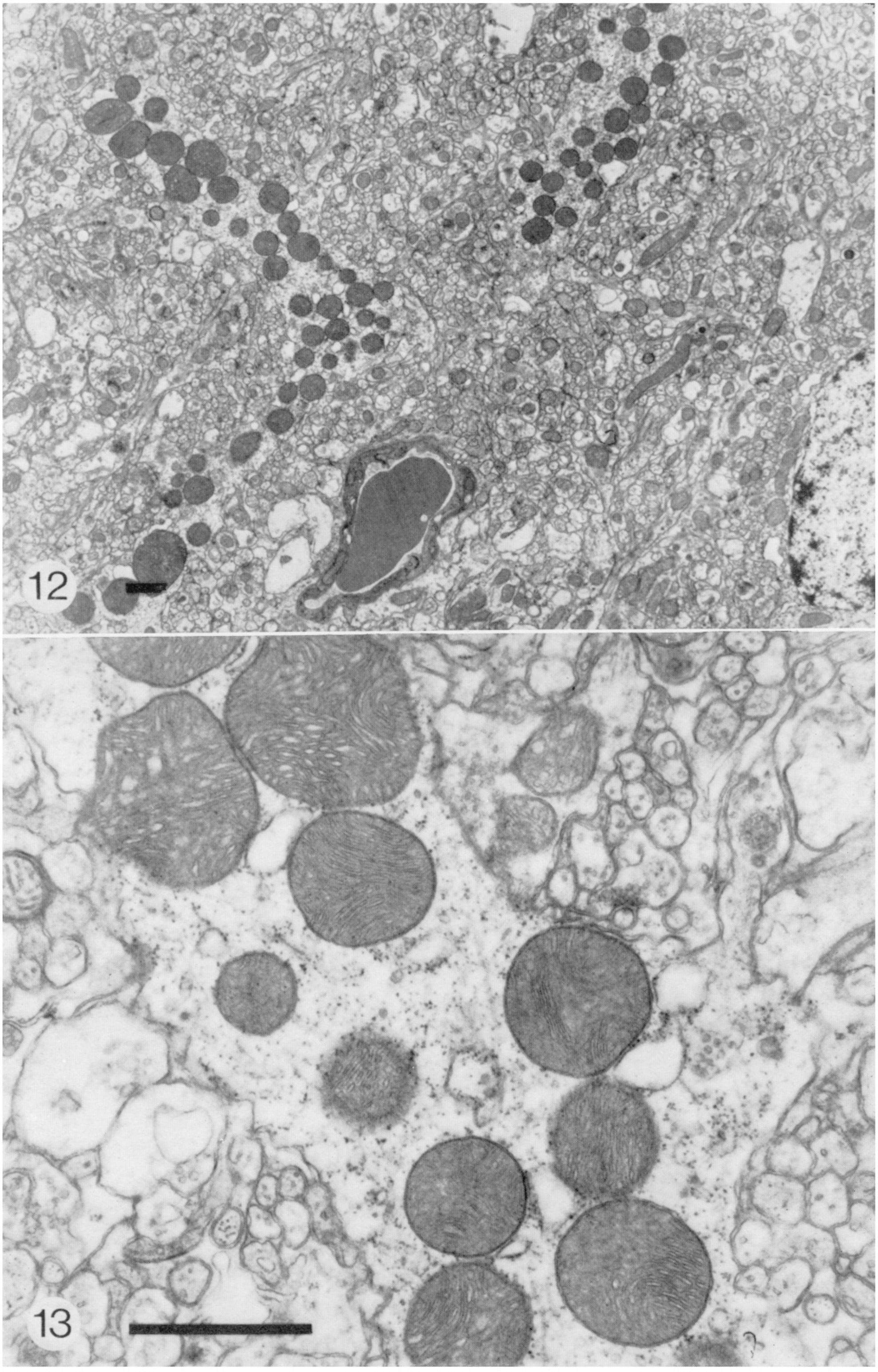

Electron micrographs of Purkinje cell dendrites from a Lurcher mouse 17 days old. Calibration bars = 1 μm.

FIGURE 12. Two portions of a dendrite can be seen. They are almost full of spherical mitochondria.

FIGURE 13. Higher magnification micrograph of figure 12 to show the unusual pattern of cristae in the spherical mitochondria.

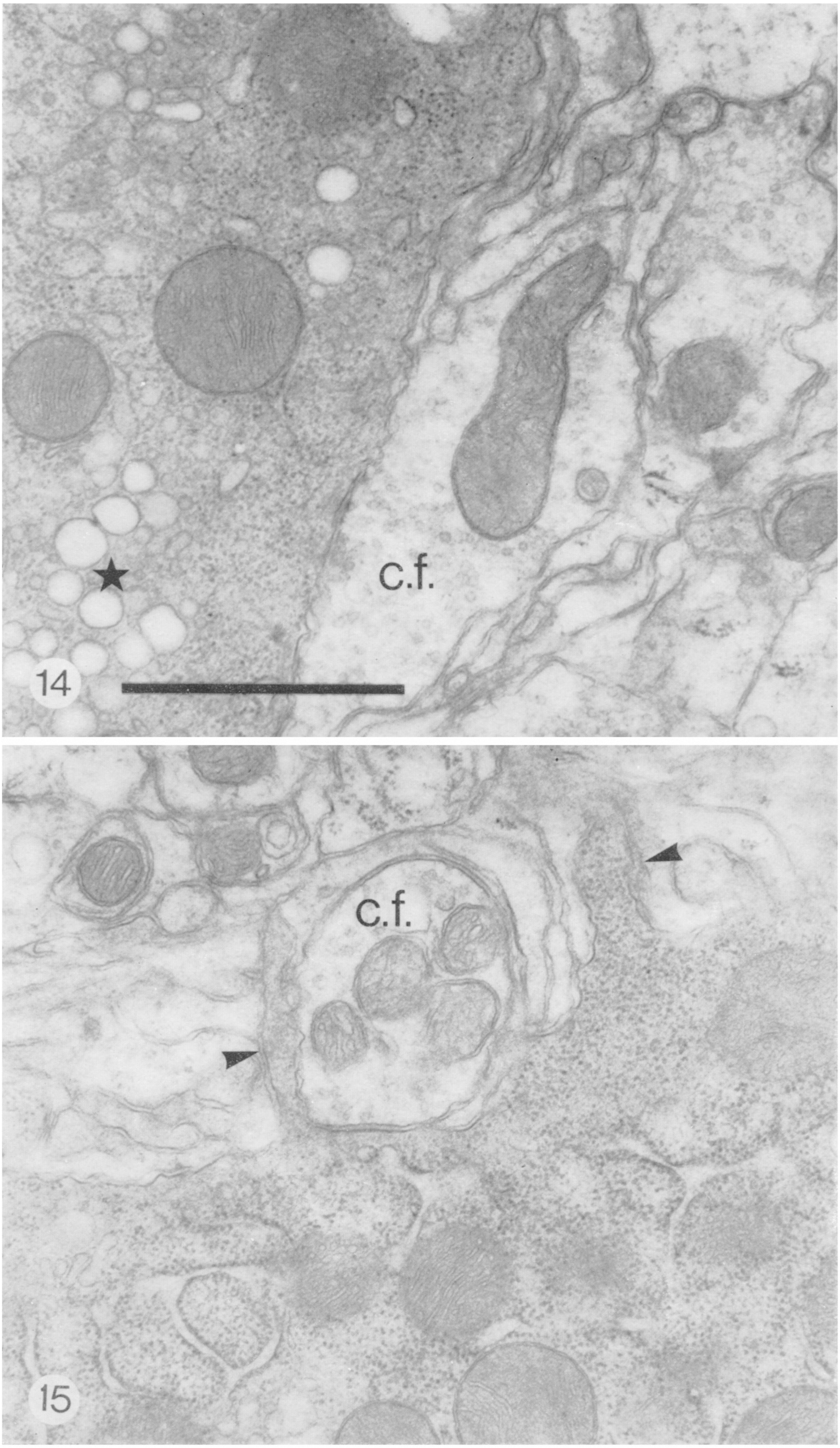

Electron micrographs of Purkinje cell dendrites from a Lurcher mouse 15 days old.
Calibration bar = 1 μm for both micrographs.

FIGURE 14. Dendrite on left in an advanced state of degeneration. Vacuoles (star) are present in the cytoplasm and a climbing fibre (c.f.) is in close apposition to the dendrite.

FIGURE 15. Two slender spines (arrowheads) emerge from the dendrite at the bottom of the field. A climbing fibre (c.f.) is closely apposed to one of these spines.

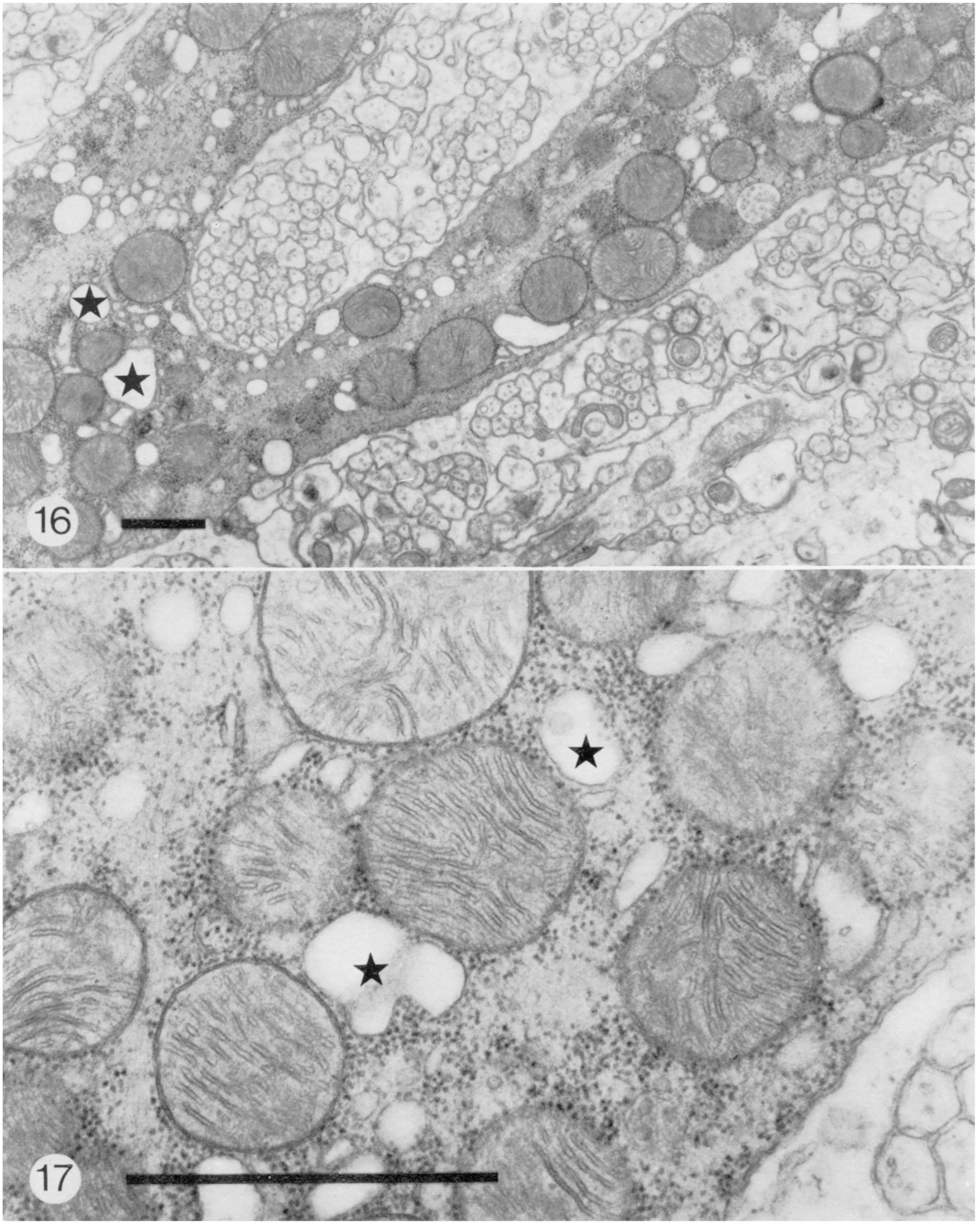

Electron micrographs of the Purkinie cell dendrites from a Lurcher mouse 17 days old. Calibration bars = 1 μm.

FIGURE 16. A dendrite in a very advanced state of degeneration. Neurofilaments and vacuoles (stars) can be seen in an electron-dense matrix which fills the dendrite.

FIGURE 17. Higher power micrograph of figure 16 showing the cristae patterns in the mitochondria, the vacuoles (stars) and the increased density of ribosomes.

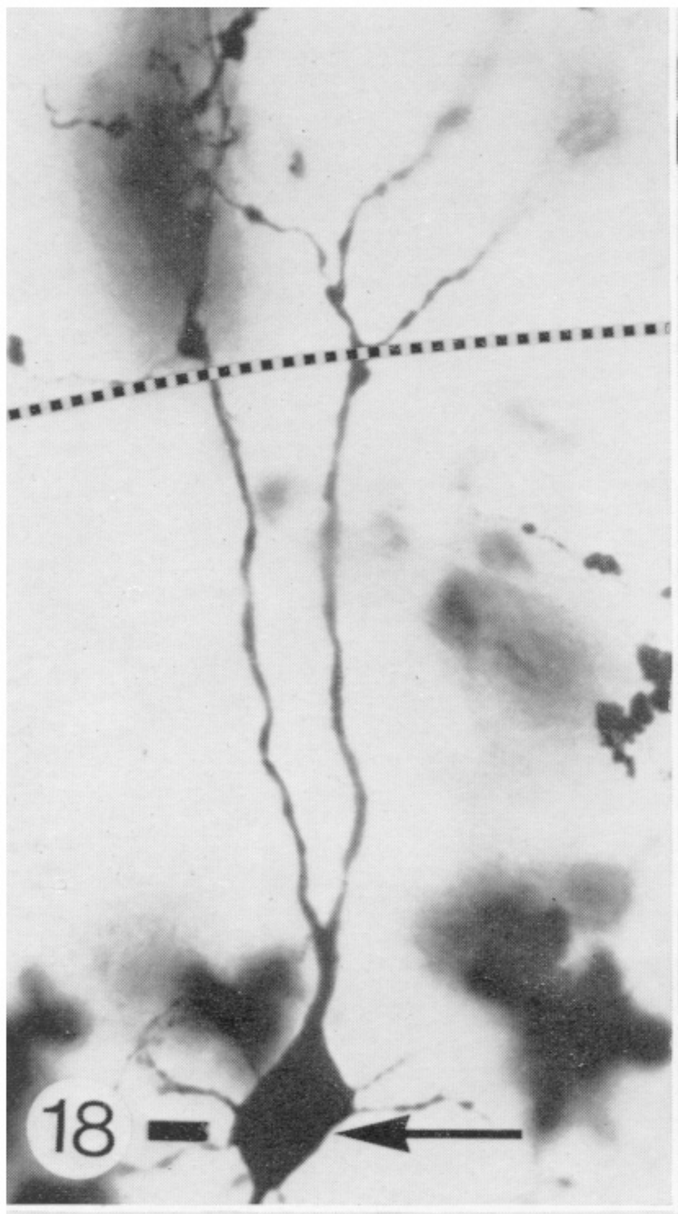

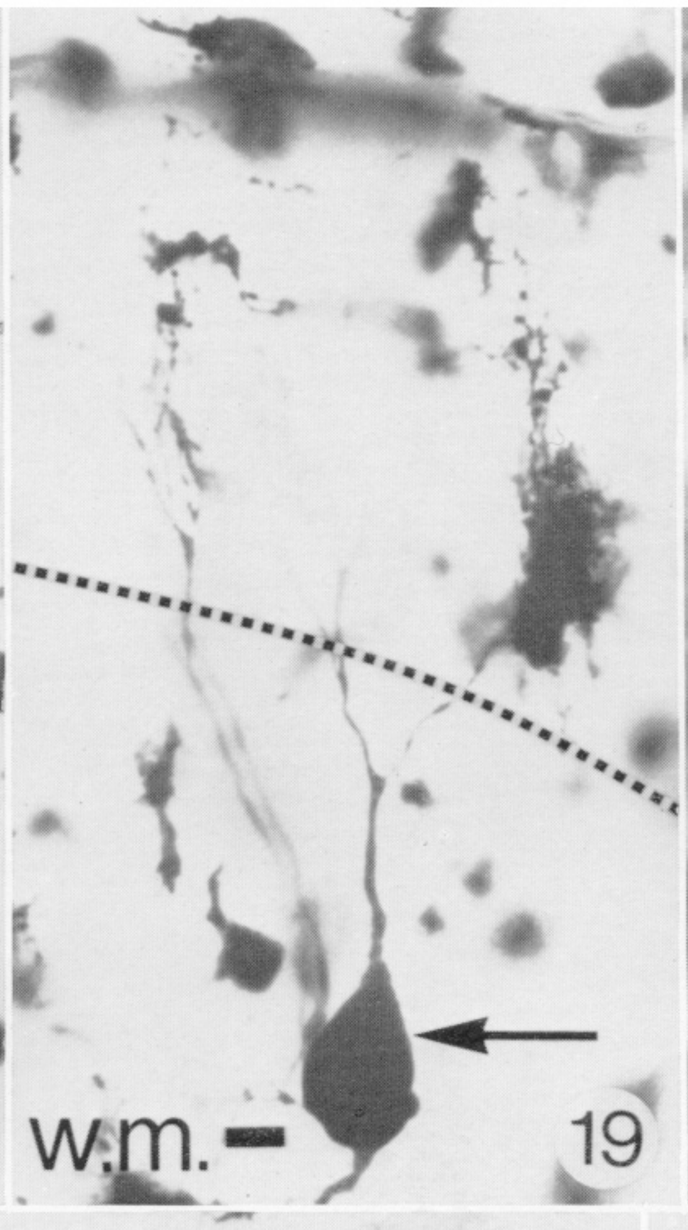

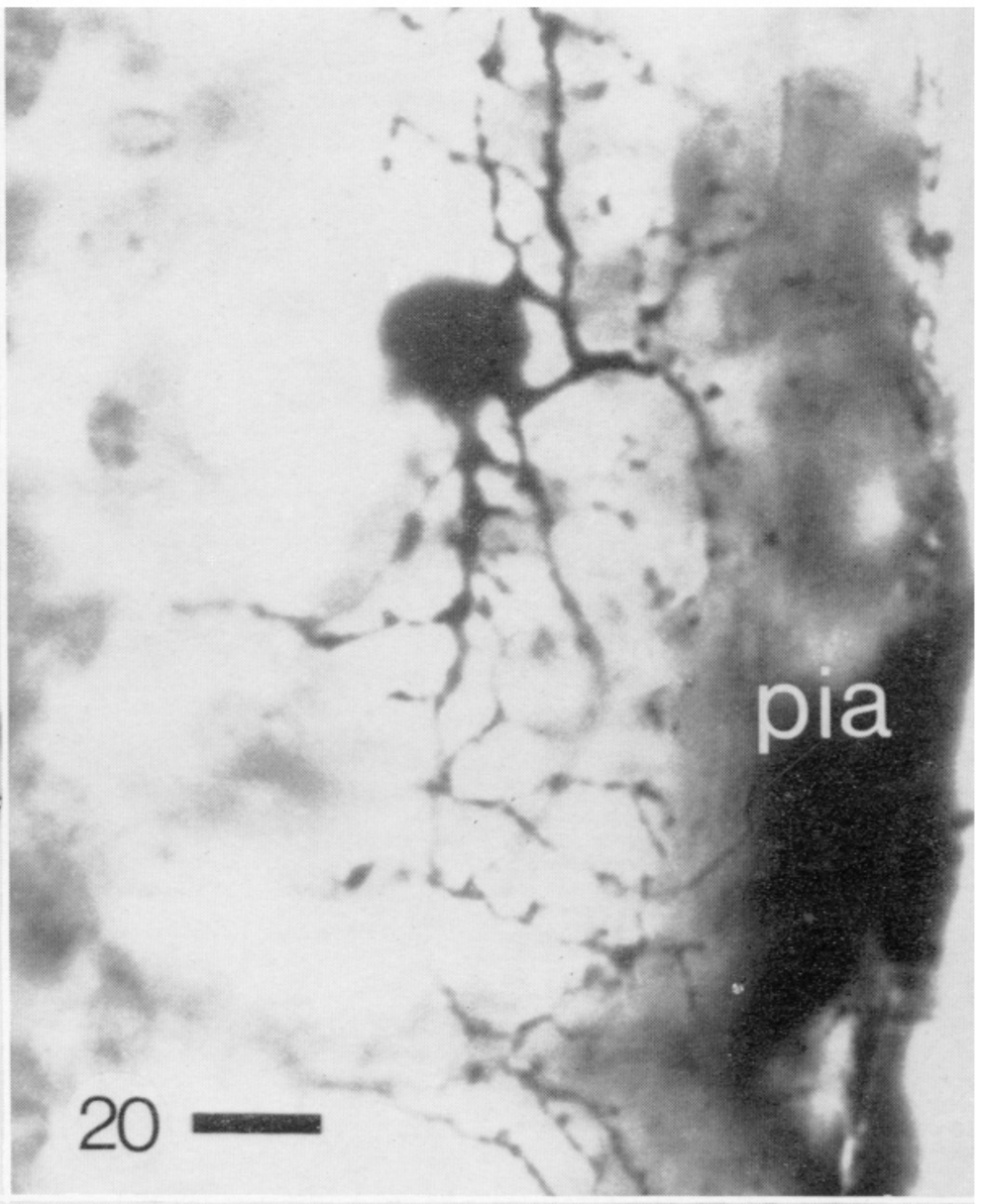

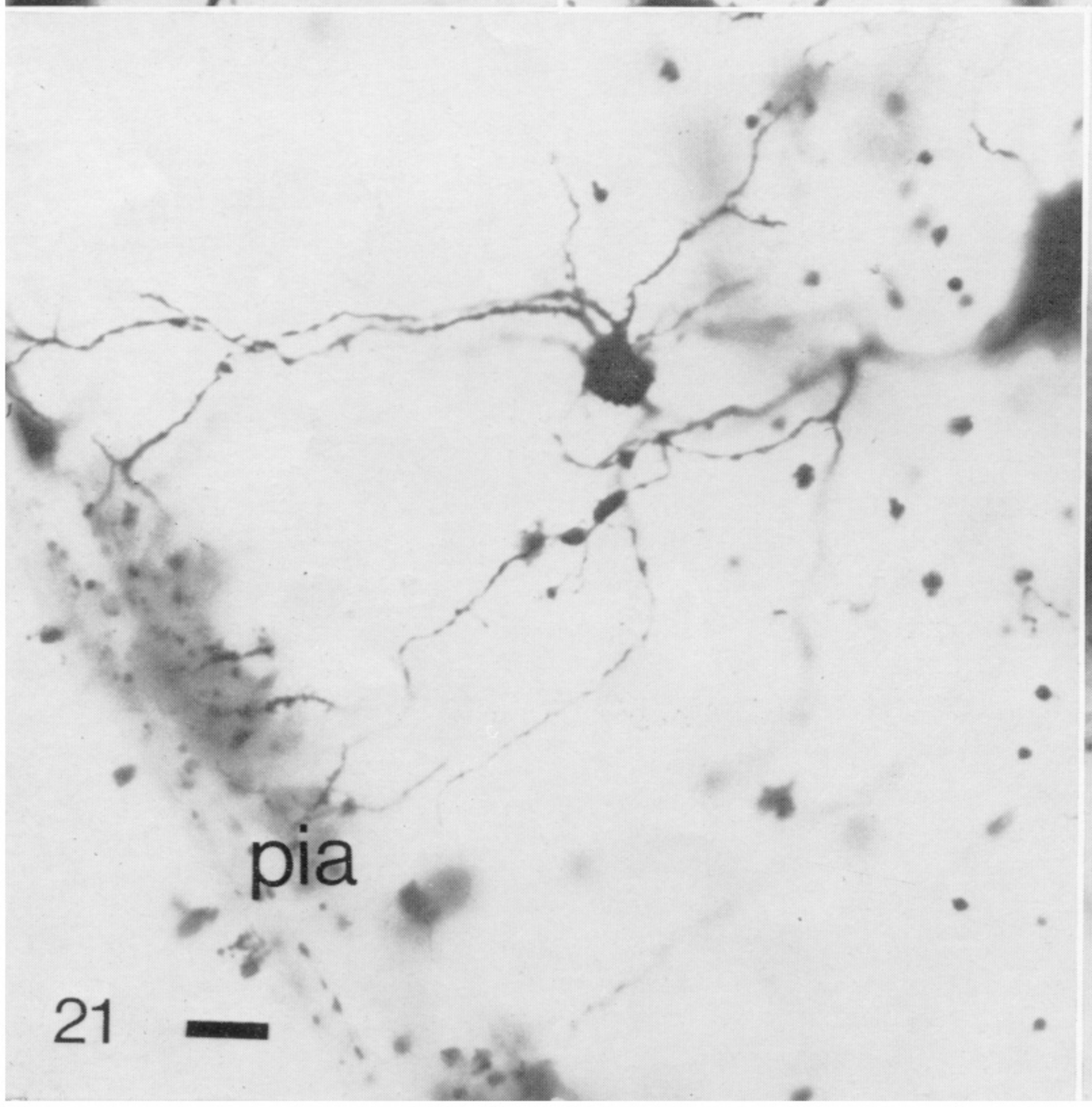

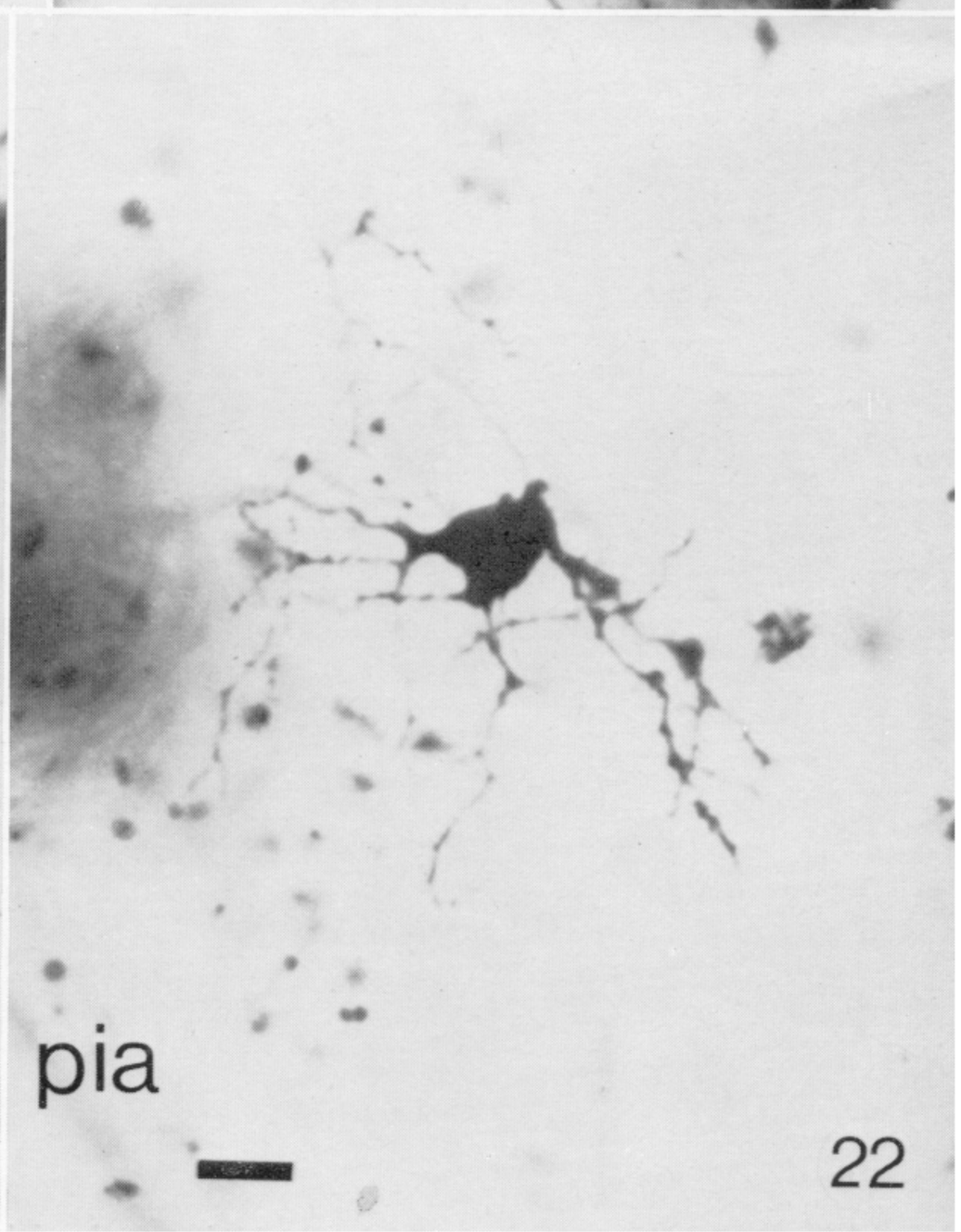

Light micrographs of Golgi–Cox impregnated tissue showing stellate cells, Golgi cells and a basket cell from normal and Lurcher mice. Sections are 100 μm thick except figure 22 which is 60 μm thick and counterstained with cresyl violet. Calibration bars = 10 μm.

FIGURE 18. Golgi cell from a normal mouse 429 days old showing two long main dendrites stretching towards the molecular layer where they branch profusely. Dashed line represents the level of the Purkinje cells.

FIGURE 19. Golgi cell from a Lurcher mouse 380 days old cerebellum showing essentially the same features as in figure 18.

FIGURE 20. A basket cell from a Lurcher mouse 14 days old is seen in the molecular layer close to the pial surface (pia). Most of the branching axons are rising towards the pial surface rather than descending towards the Purkinje cell layer. No Purkinje cells are in the area shown in this micrograph.

FIGURE 21. A stellate cell from a normal mouse 15 days old is shown with dendrites extending from pial surface to Purkinje cell layer.

FIGURE 22. A stellate cell from a Lurcher mouse 14 days old is shown. Its soma is closer to the Purkinje cell layer than in figure 18 and hence its dendritic tree extends in the direction of the pial surface.

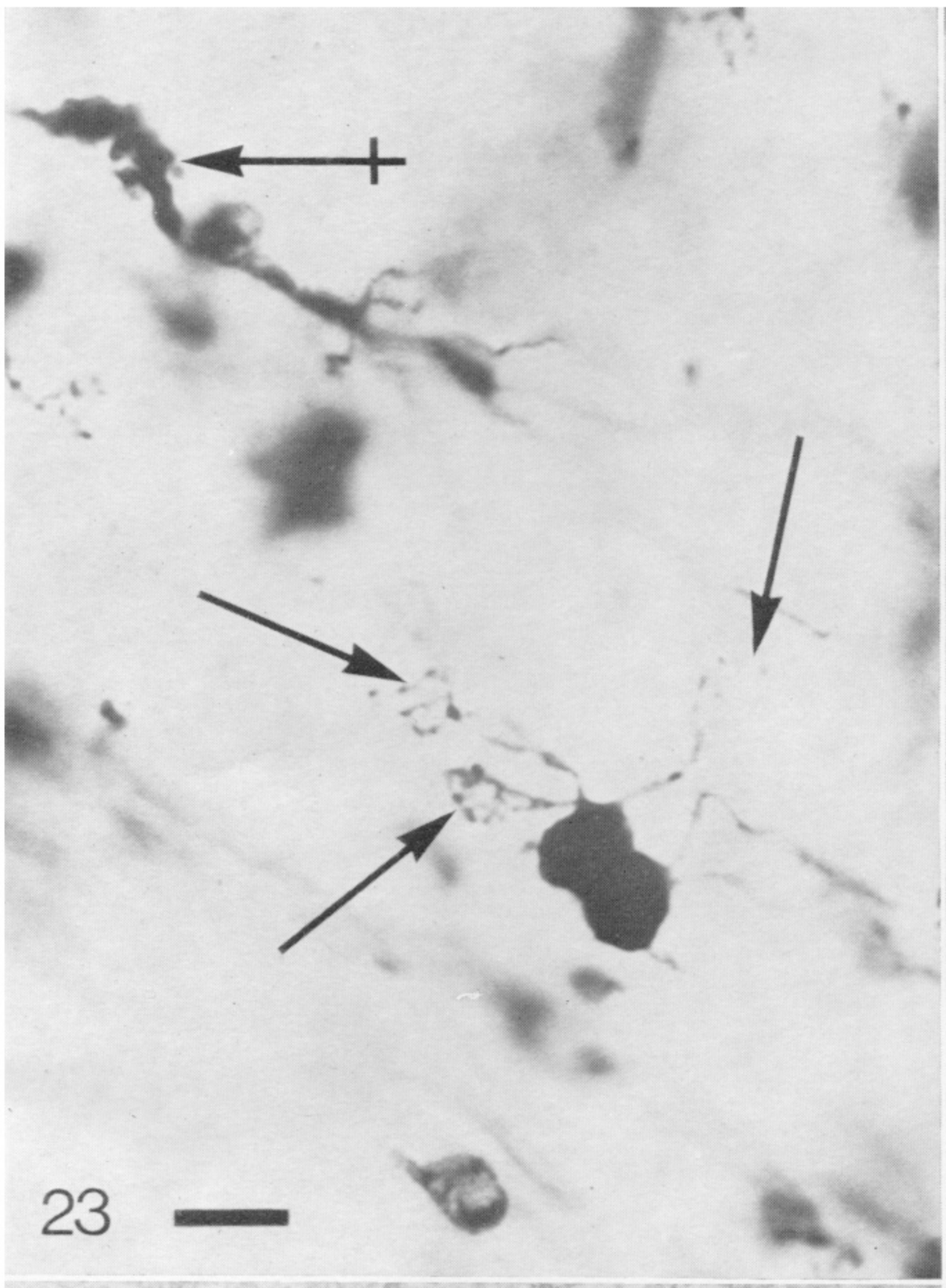

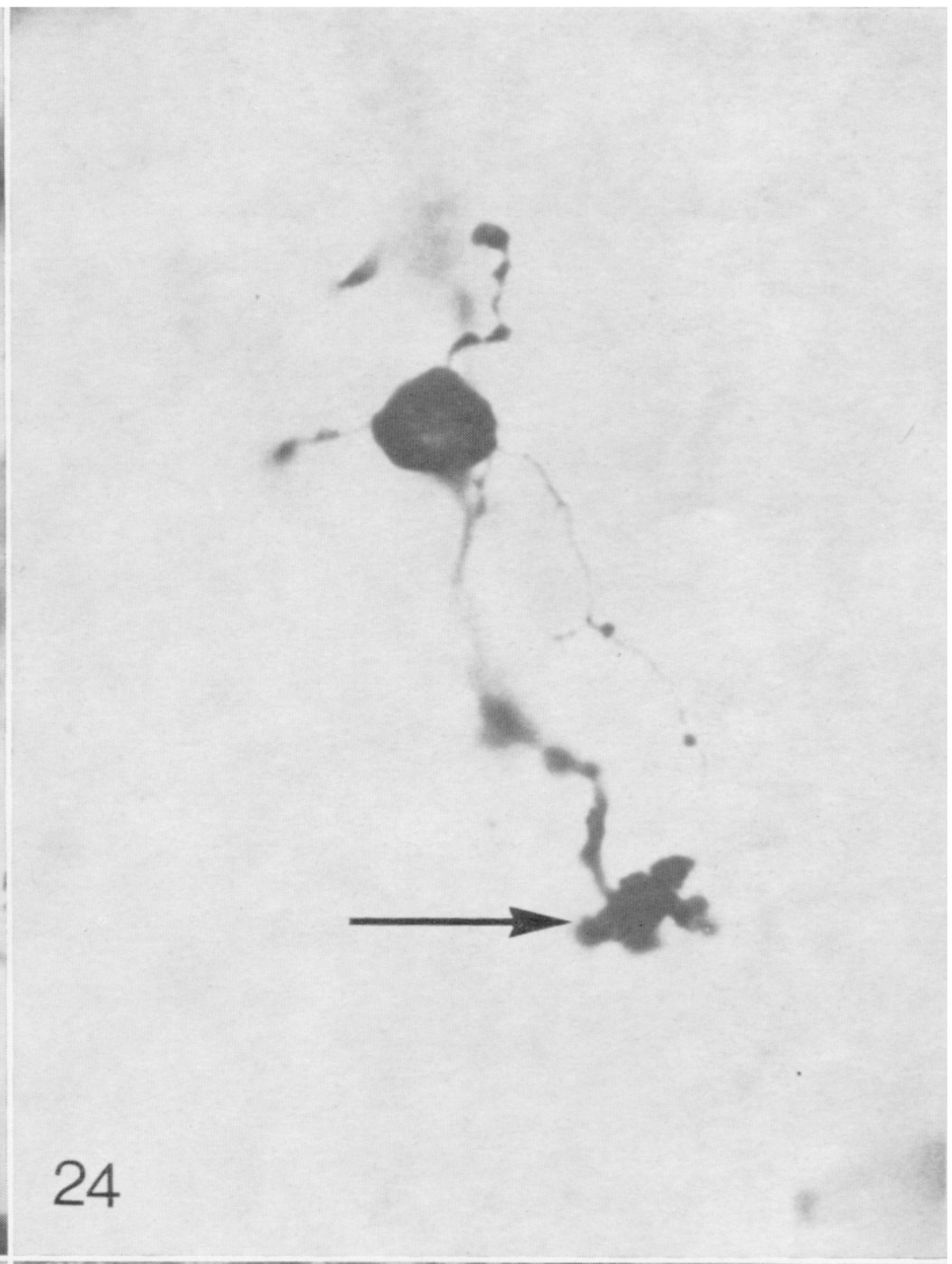

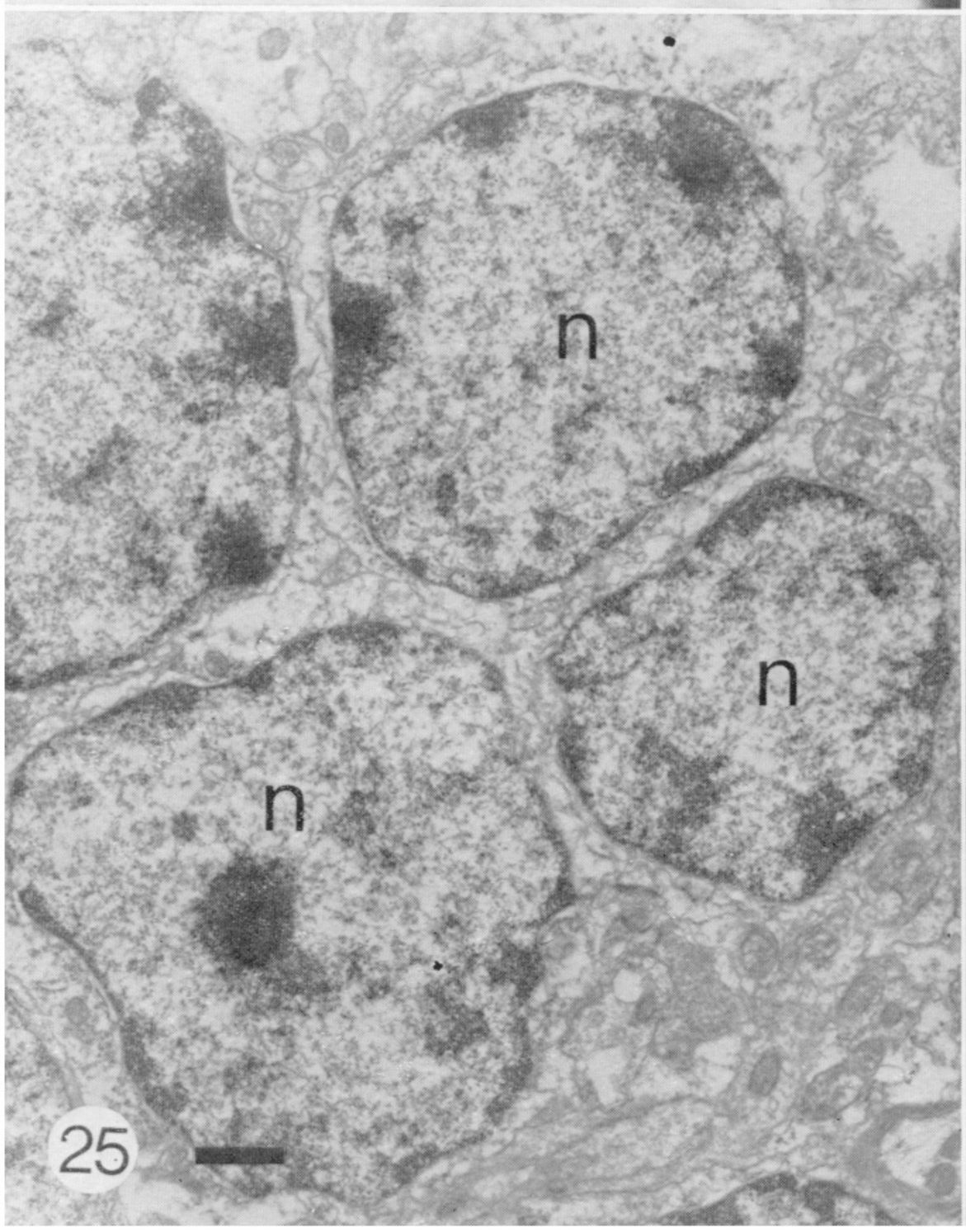

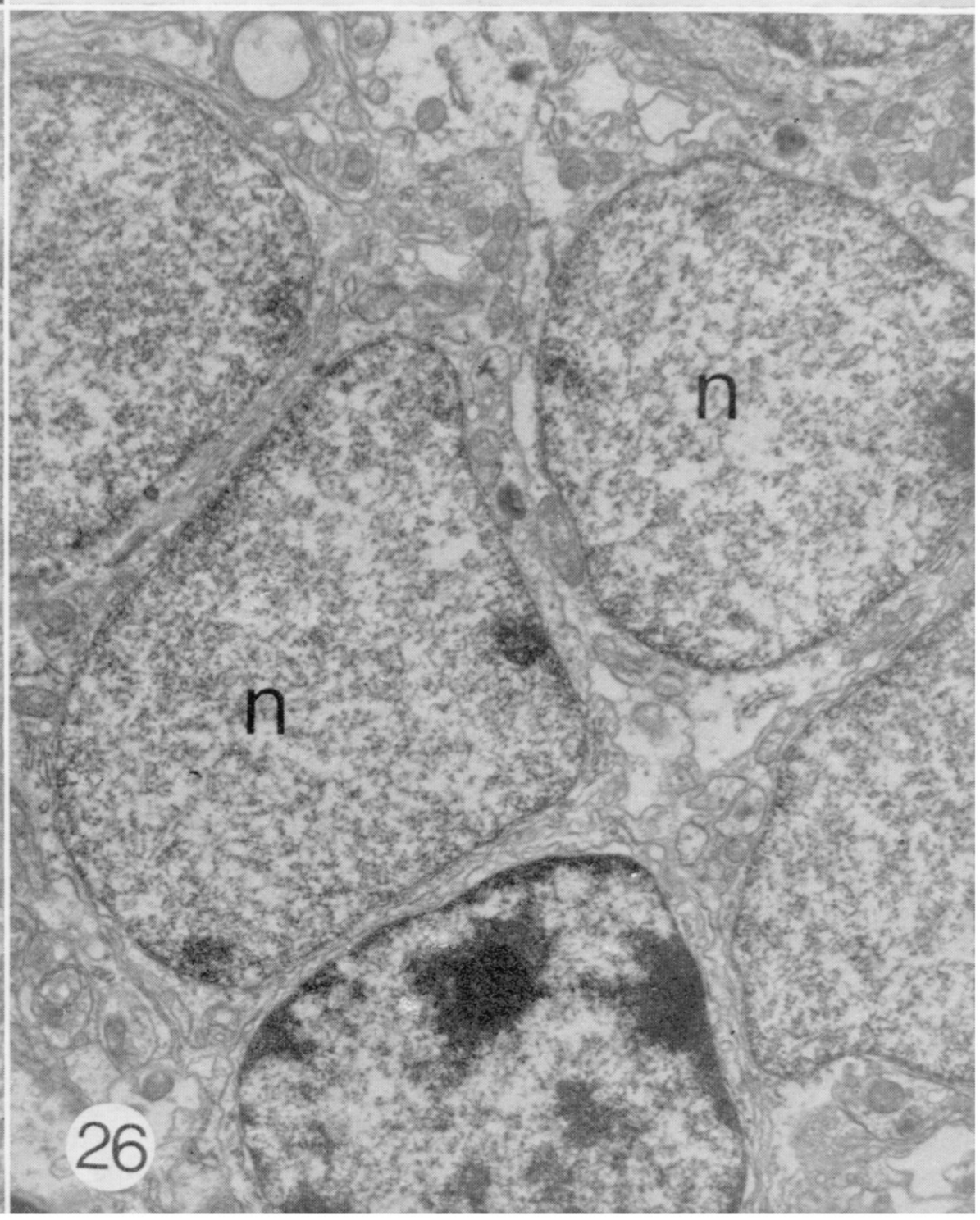

FIGURES 23–26. For description see opposite.

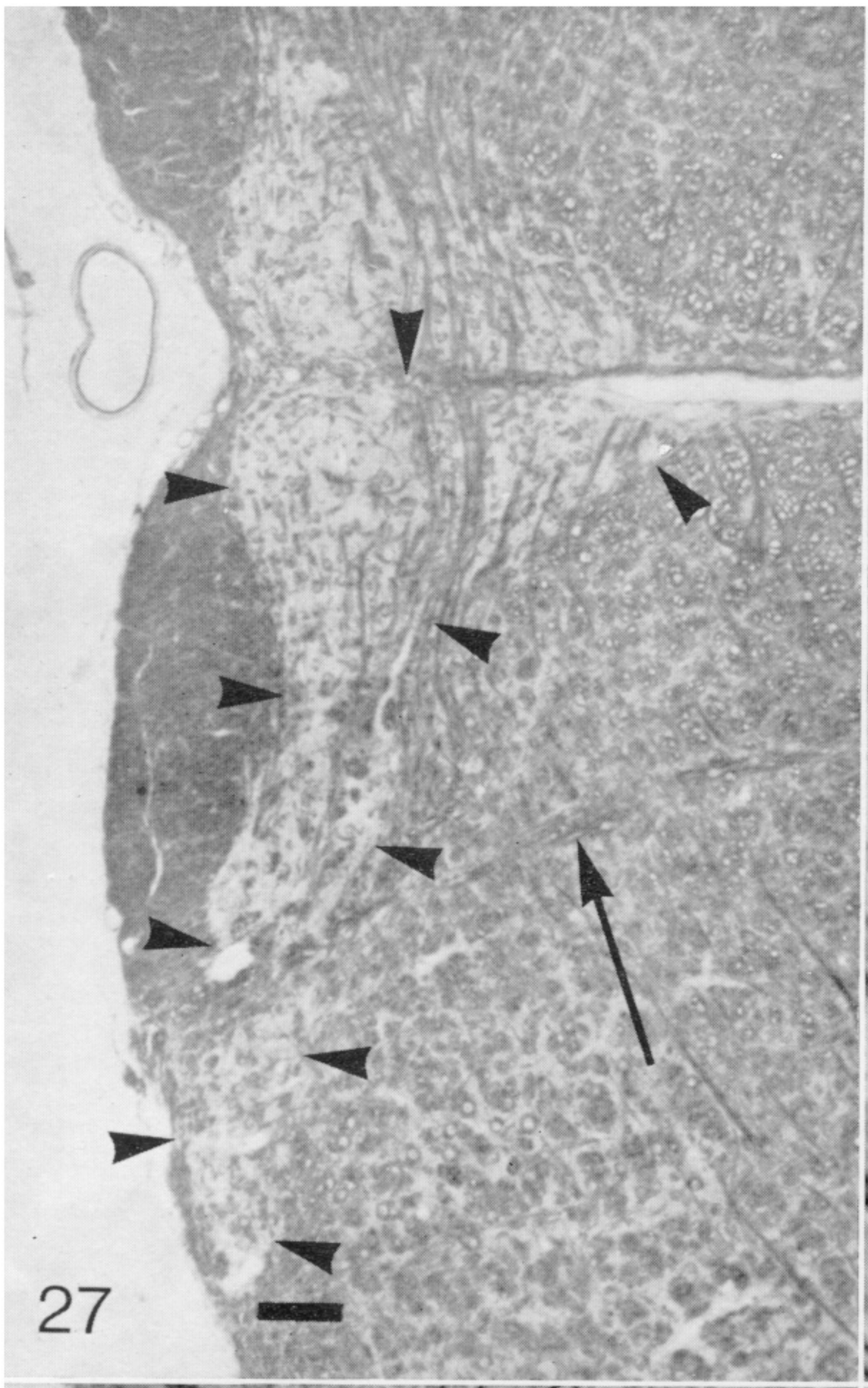

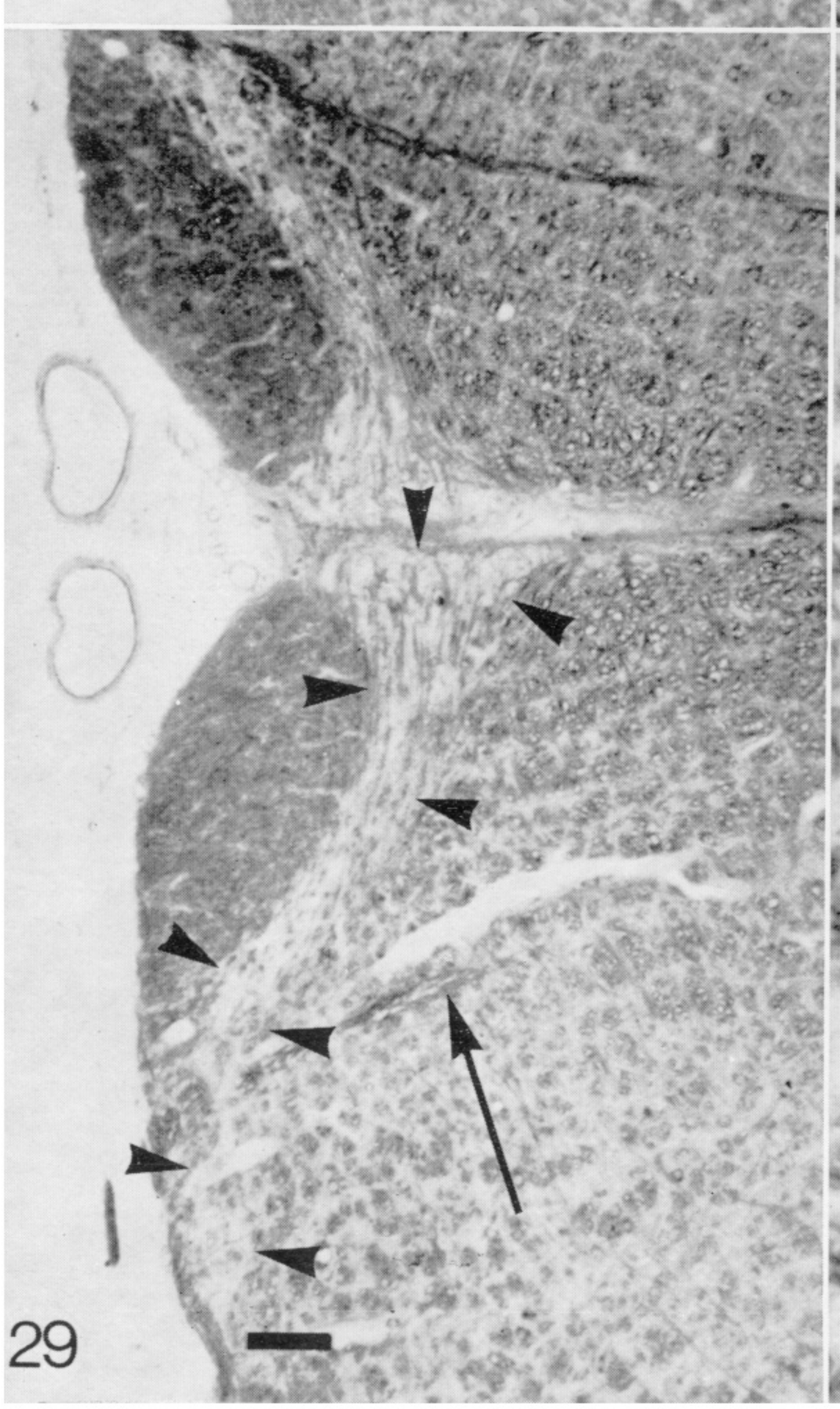

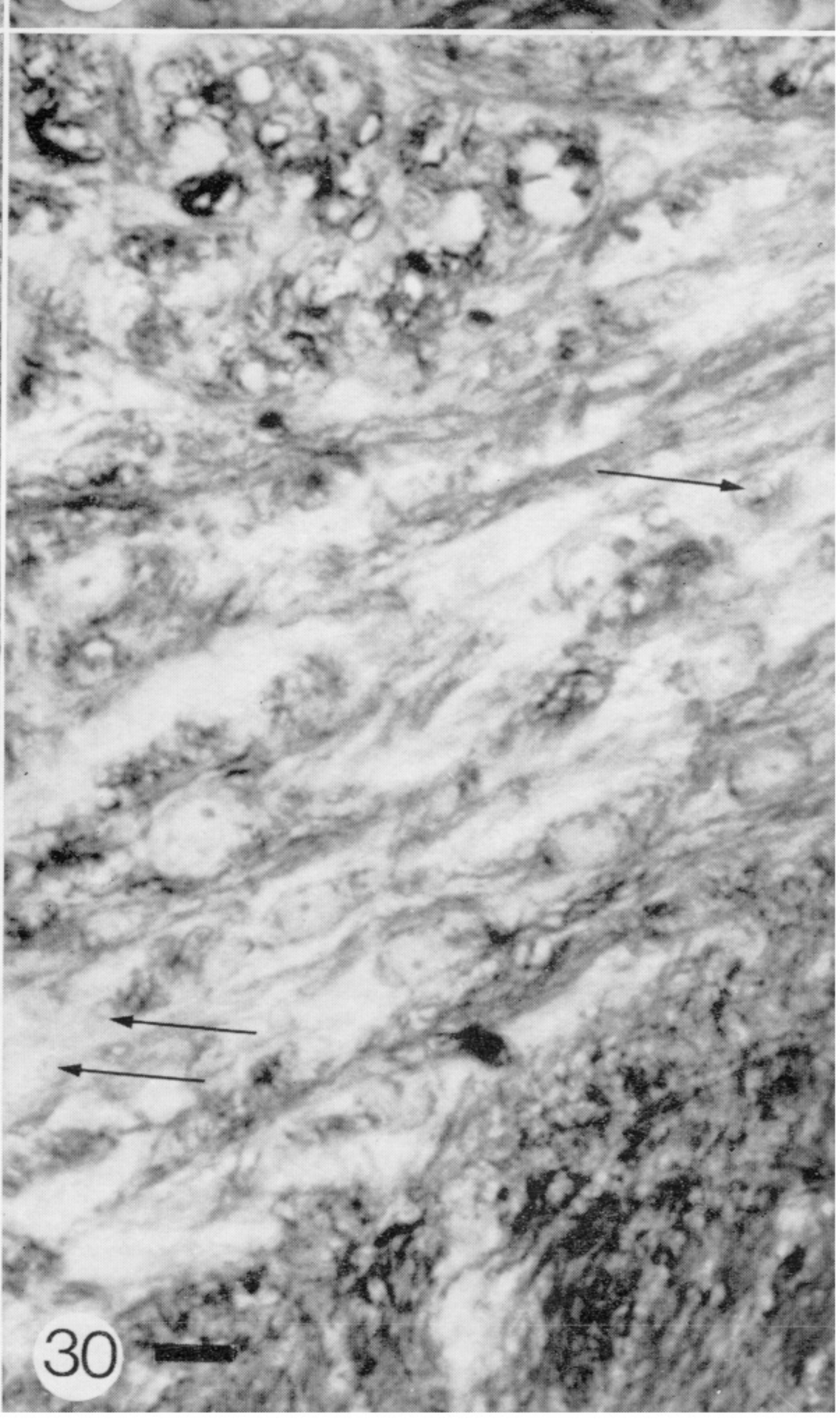

FIGURES 27–30. For description see opposite.

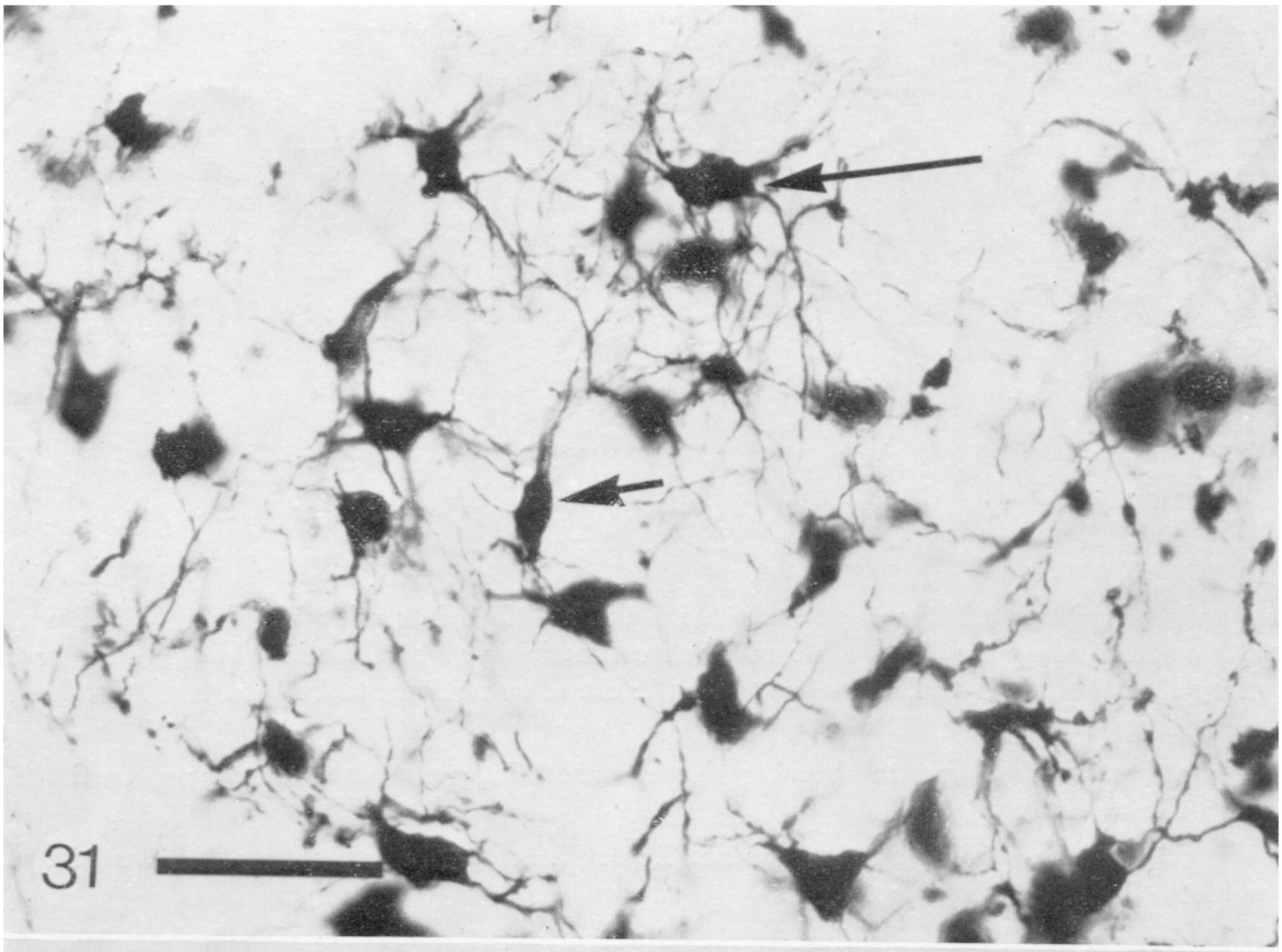

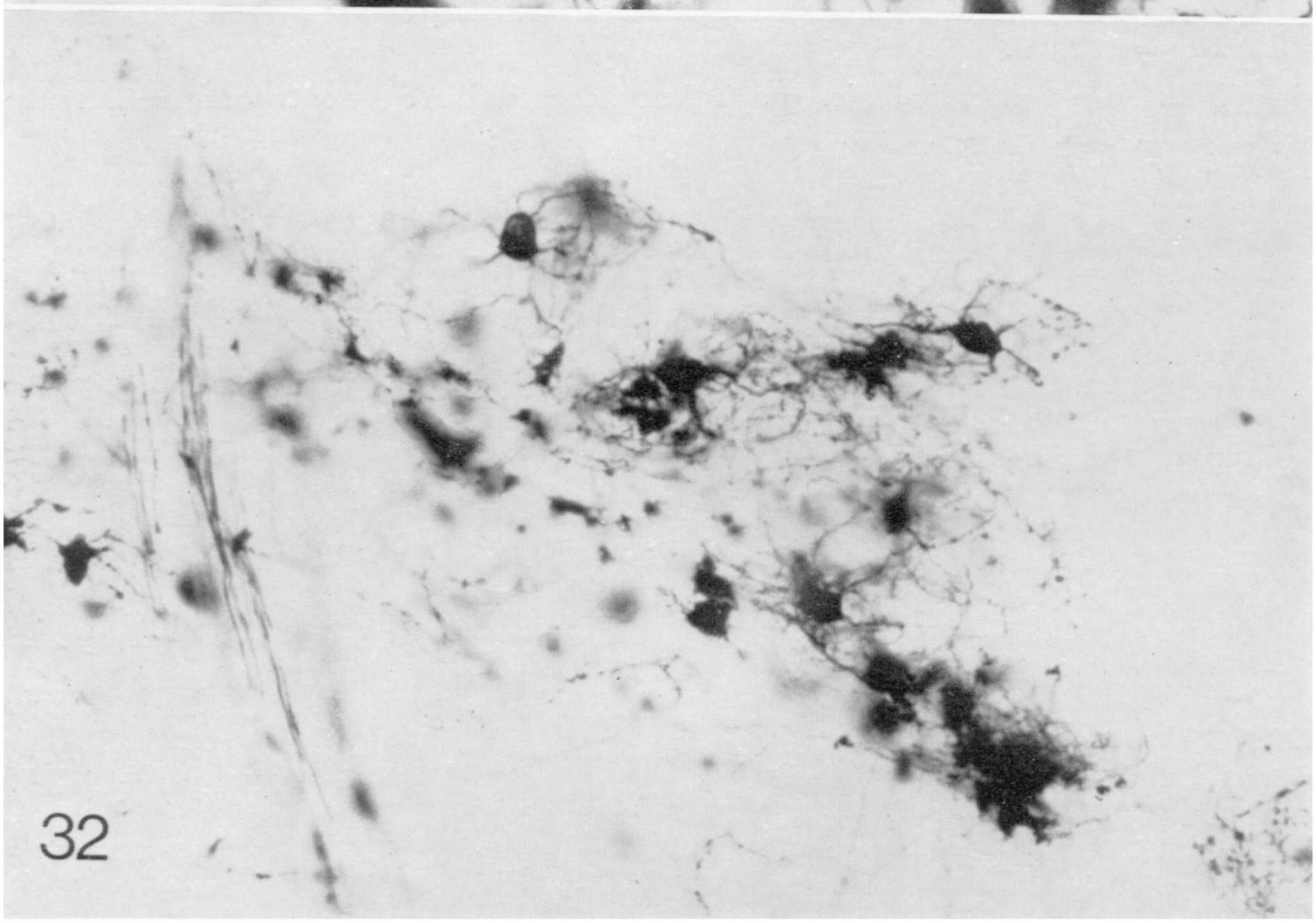

Light micrographs of Golgi–Cox impregnated inferior olivary nucleus from normal and Lurcher mice. Sections are 100 μm thick. Calibration bar = 100 μm for both micrographs.

FIGURE 31. Neurons from a mouse 429 days old showing some cells with simple dendritic patterns (short arrows) and one with highly ramified spherical dendrites (long arrow).

FIGURE 32. Neurons from a Lurcher mouse 14 days old showing only cells with highly ramified spherical dendrites.

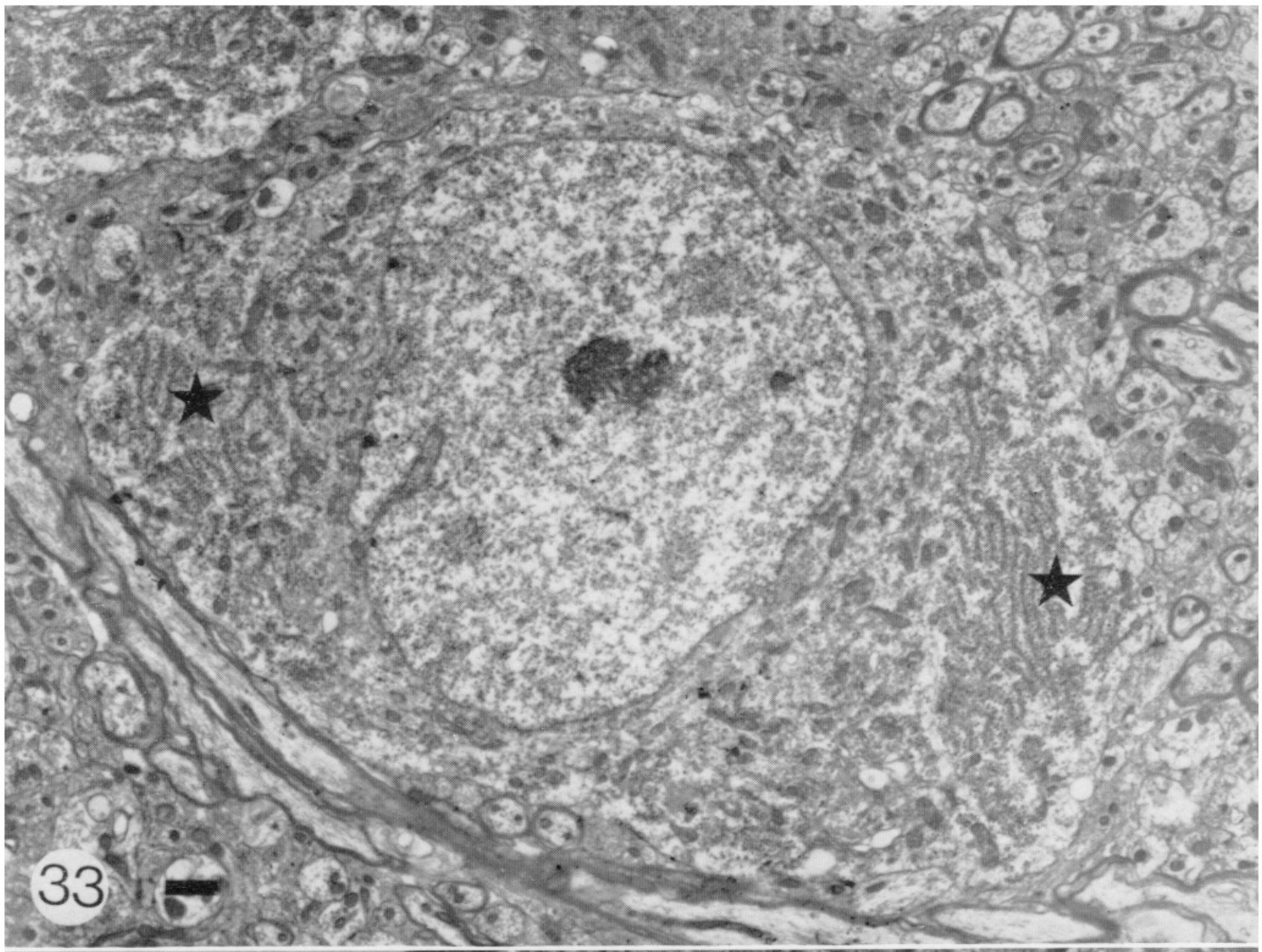

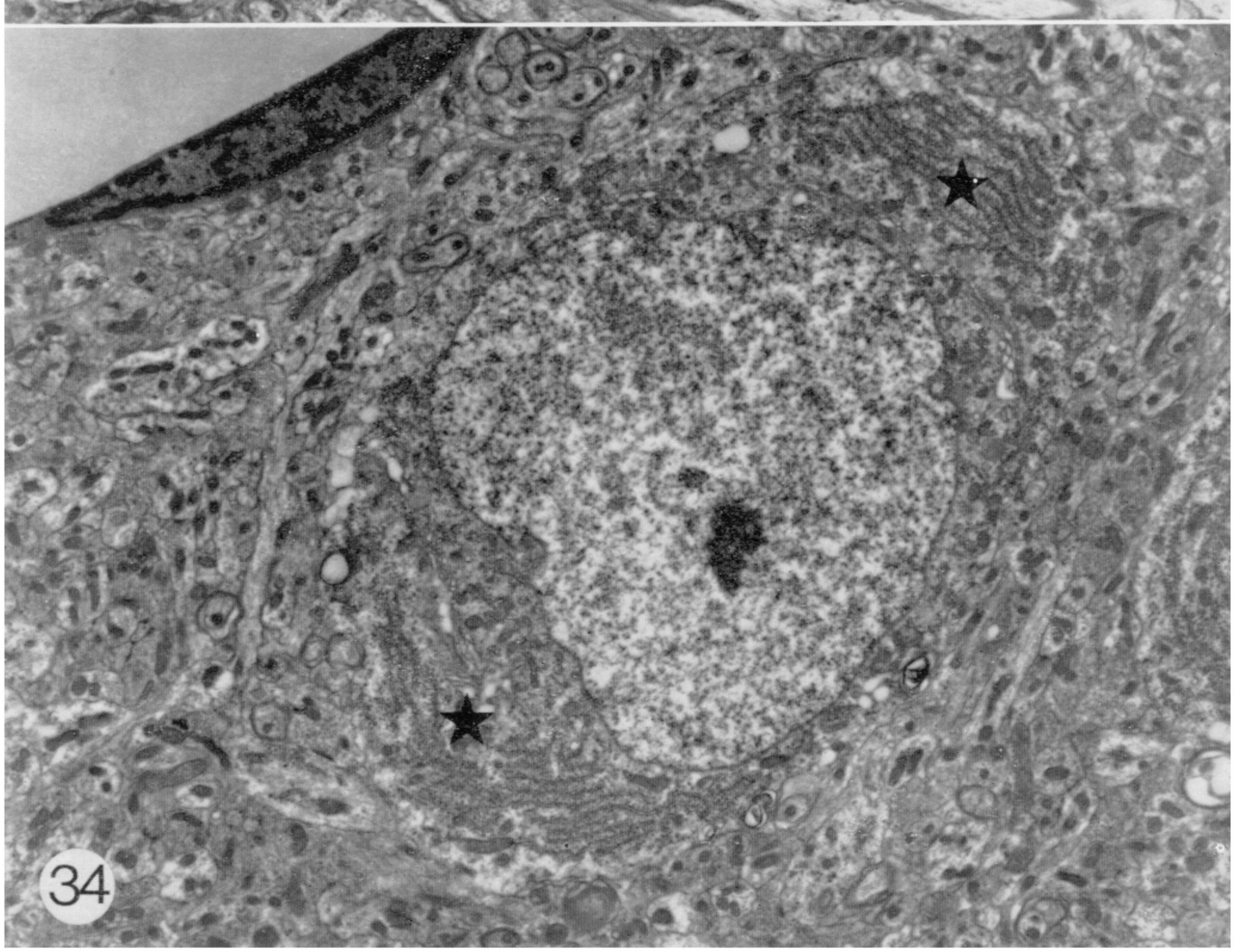

Electron micrographs from normal and Lurcher mice 17 days old showing olive neurons. Nissl bodies are indicated by stars. Calibration bar = 1 μm for both micrographs.

FIGURE 33. Normal mouse olive neuron.

FIGURE 34. Lurcher mutant mouse olive neuron.

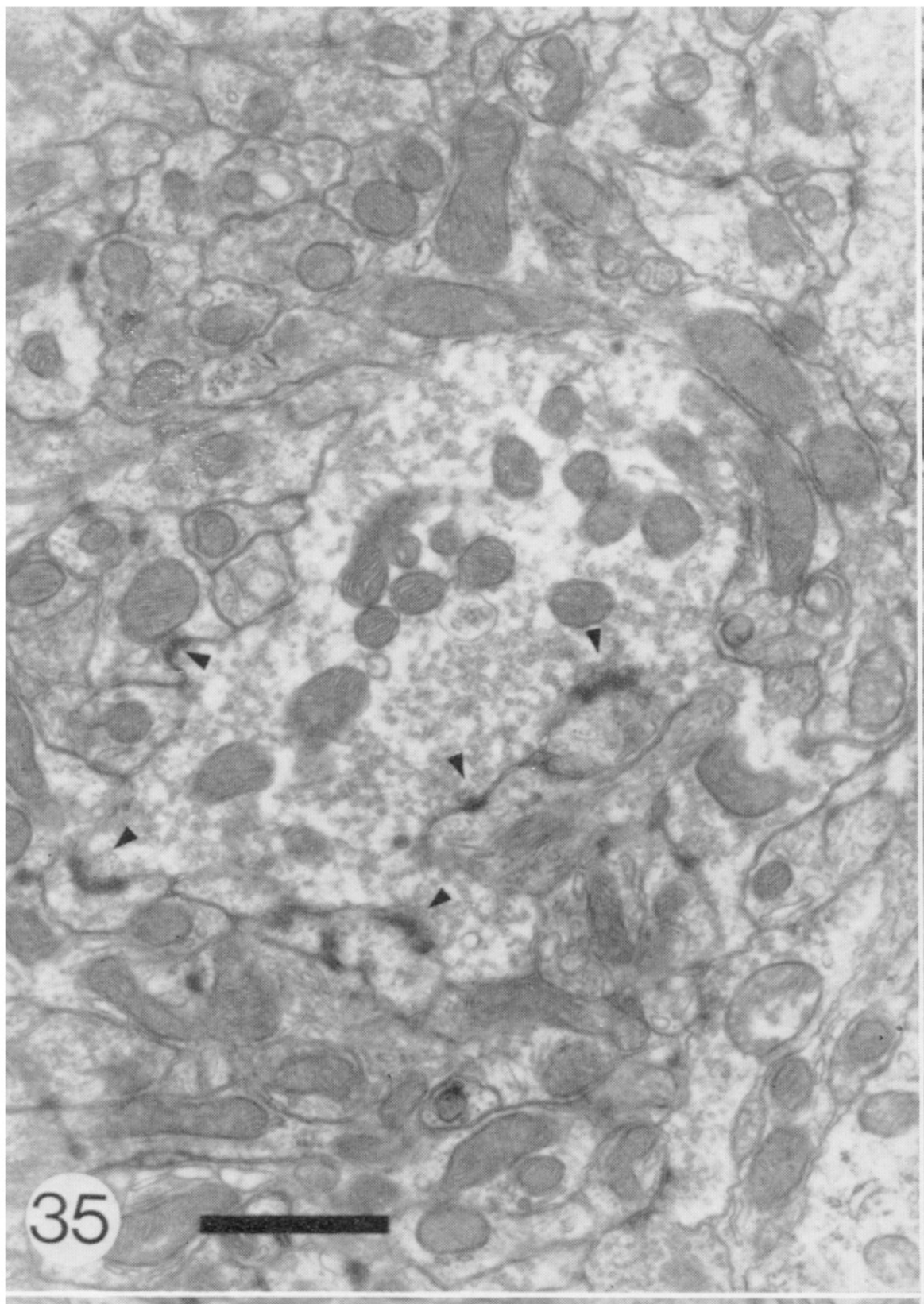

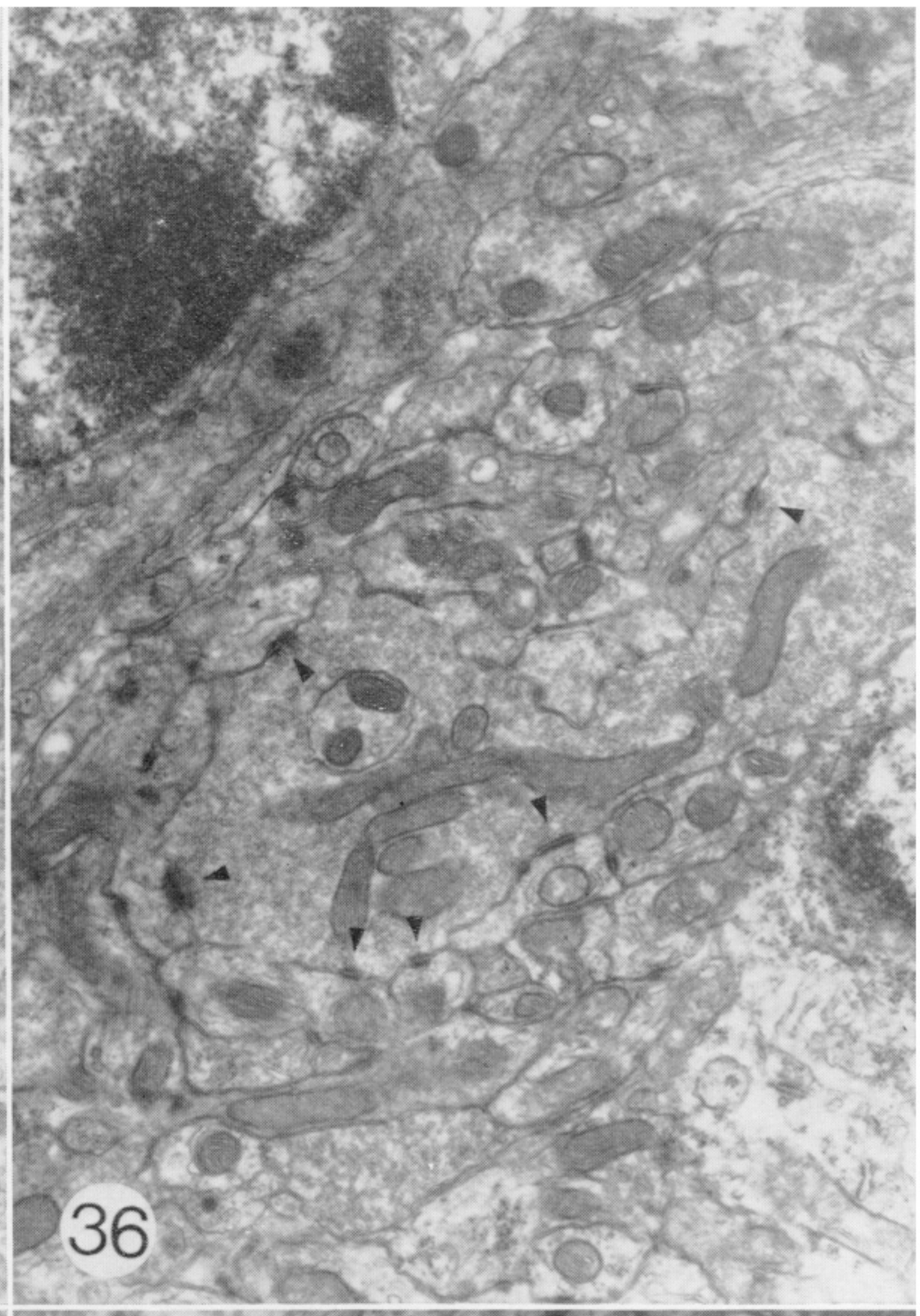

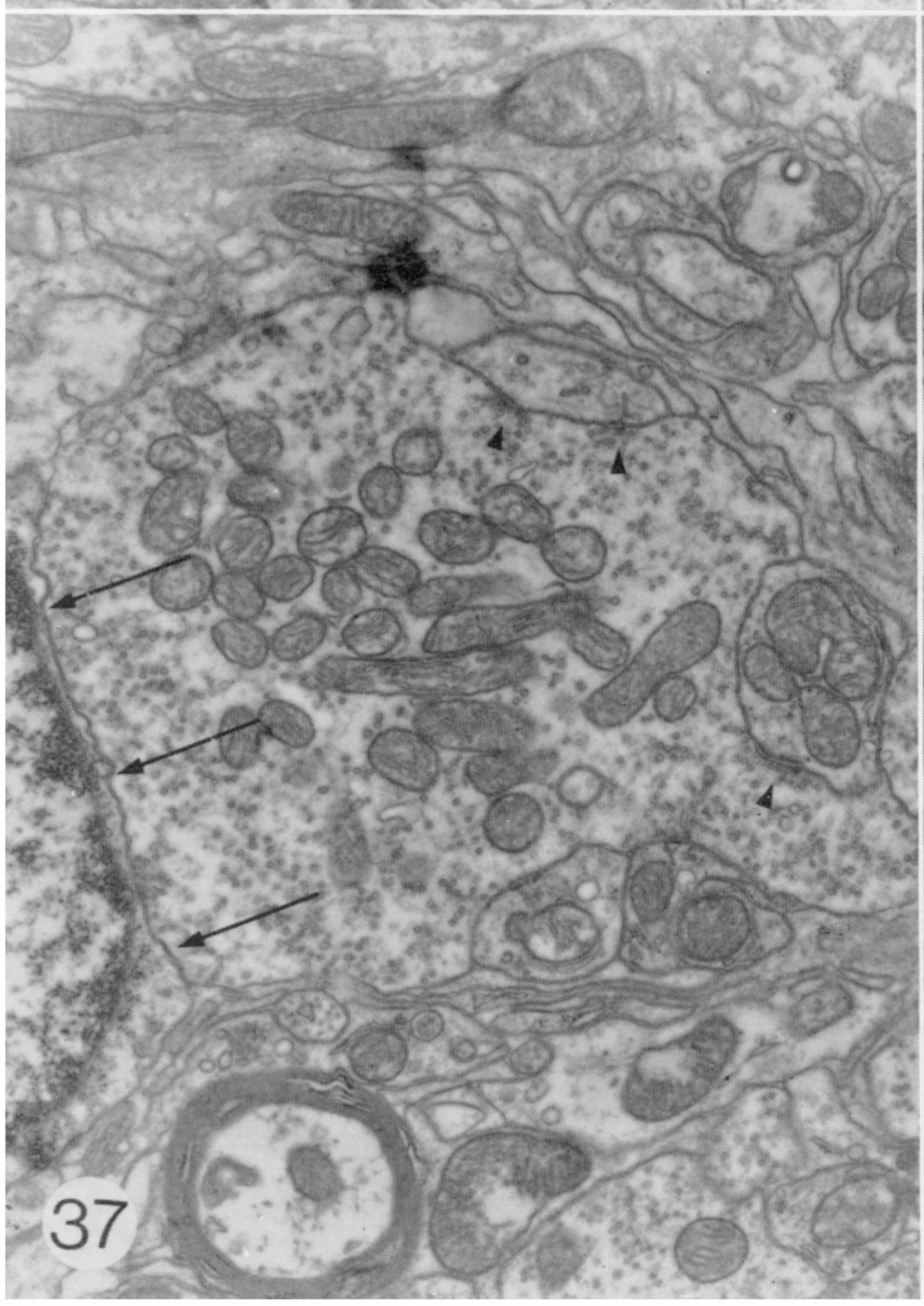

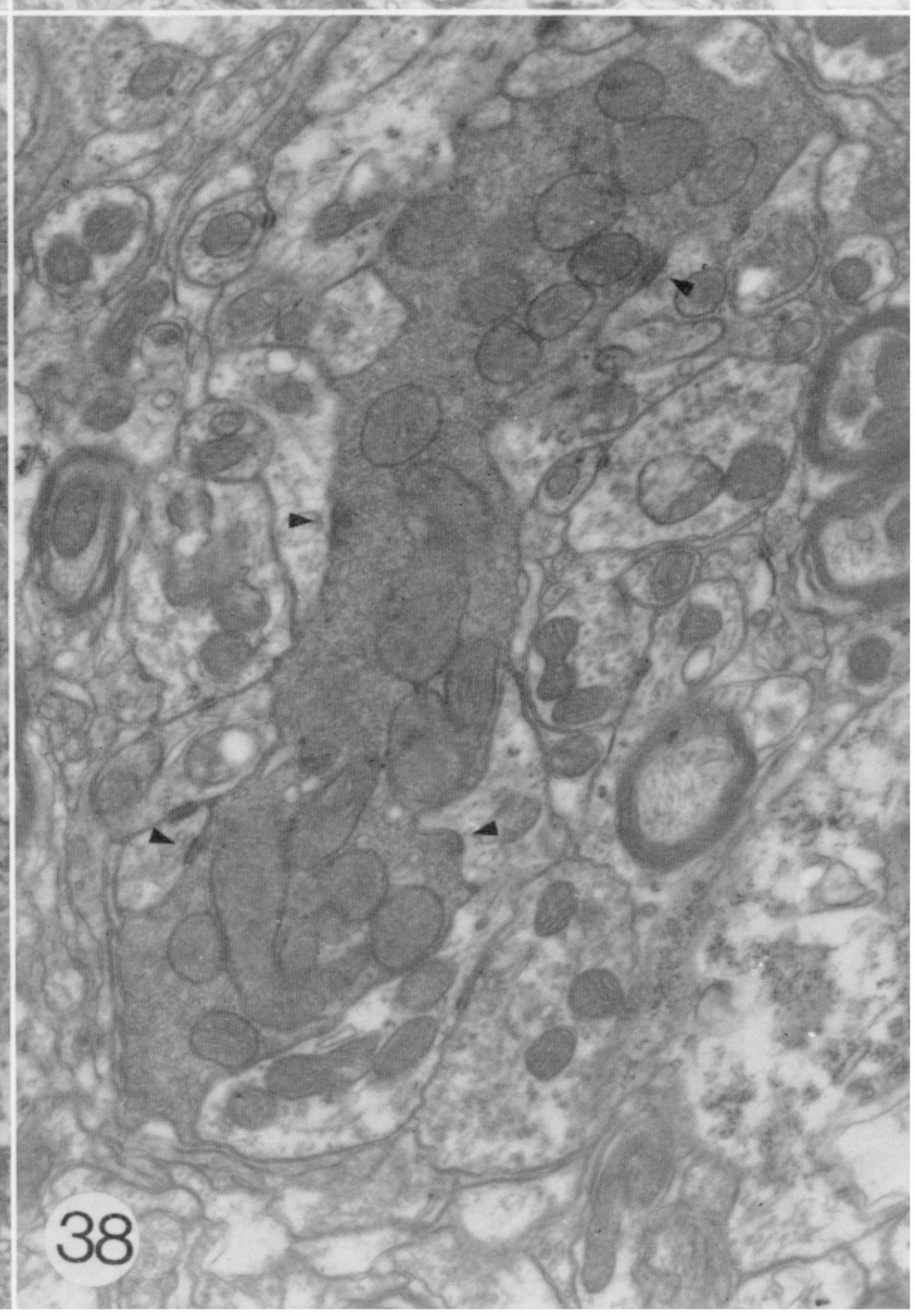

Electron micrographs of mossy and climbing fibre glomeruli from normal and Lurcher mutant mice. Arrowheads show synapses with granule cell dendrites and Golgi cell axons. Calibration bar = 1 μm for all micrographs.

FIGURE 35. A mossy fibre glomerulus from a normal mouse 15 days old. Note the fairly low density of synaptic vesicles.

FIGURE 36. A climbing fibre glomerulus from a normal mouse 15 days old. Note the higher density of synaptic vesicles when compared with figure 35.

FIGURE 37. A mossy fibre glomerulus from a Lurcher mouse 63 days old. The low packing density of synaptic vesicles is shown and a granule cell in close apposition to the glomerulus can be seen (arrows).

FIGURE 38. A climbing fibre glomerulus from a Lurcher mouse 19 days old. The packing density should be compared to that in figure 37.

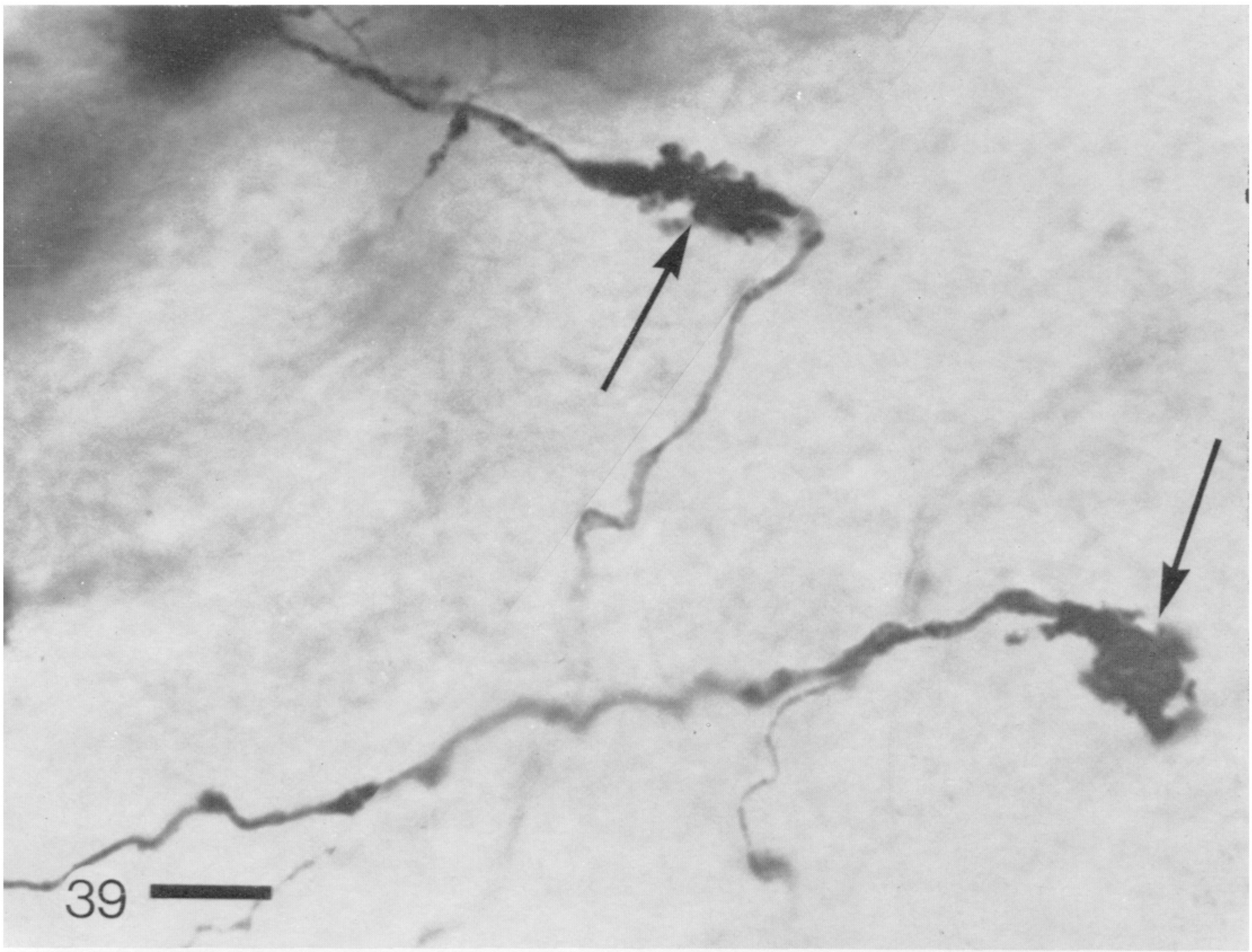

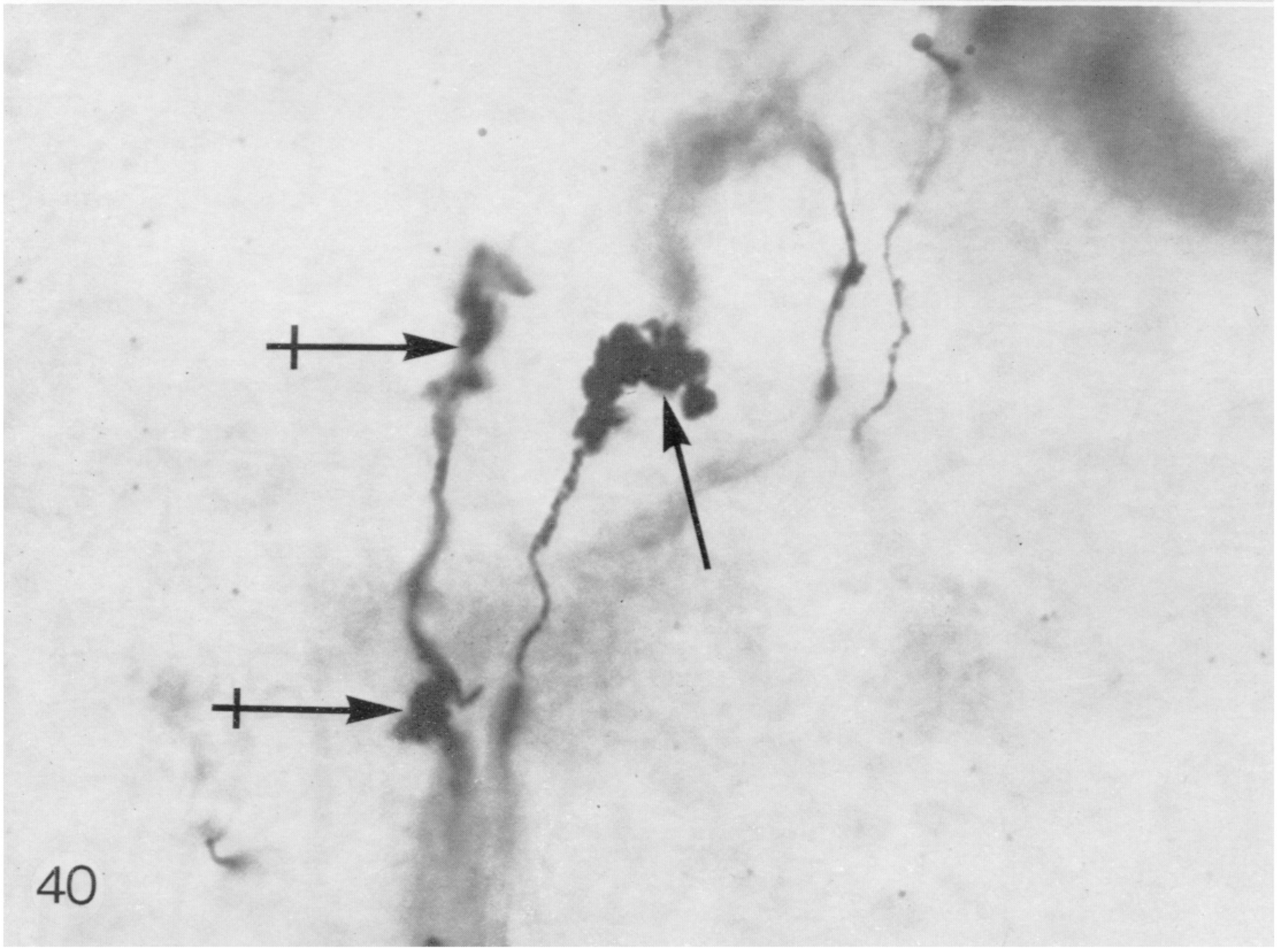

Light micrographs of Golgi–Cox impregnated mossy fibre glomeruli from adult normal and Lurcher mice. The glomeruli are arrowed. The photographs were taken in the internal granule cell layer. Sections are 100 μm thick. Calibration bar = 10 μm for both micrographs.

FIGURE 39. This is a photomontage to show two mossy fibre glomeruli of the complex type in a normal mouse 429 days old.

FIGURE 40. Three mossy fibre glomeruli in a Lurcher mouse 380 days old. These are also of the complex type although it is difficult to see those at the crossed arrows because they are out of the plane of focus.

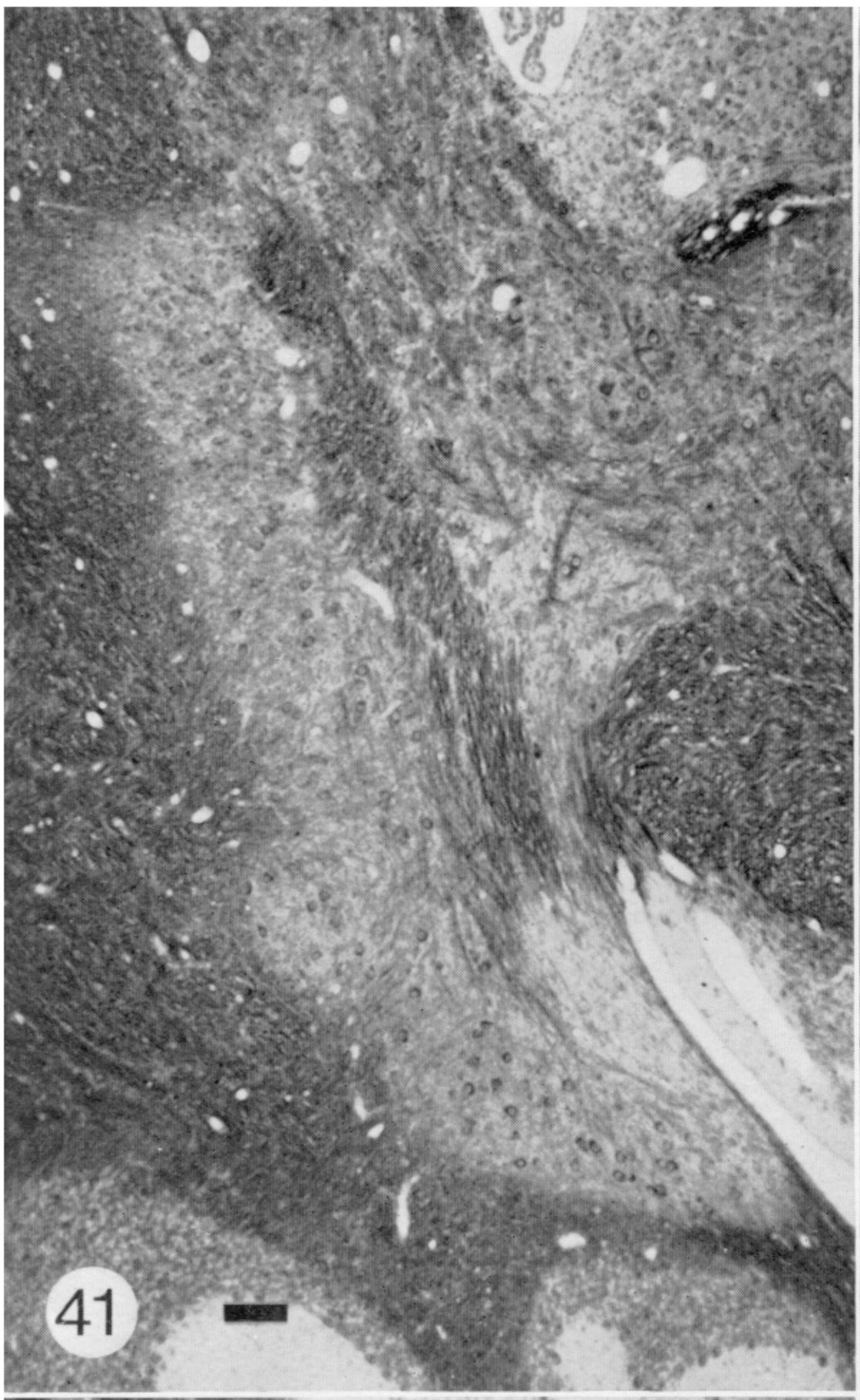

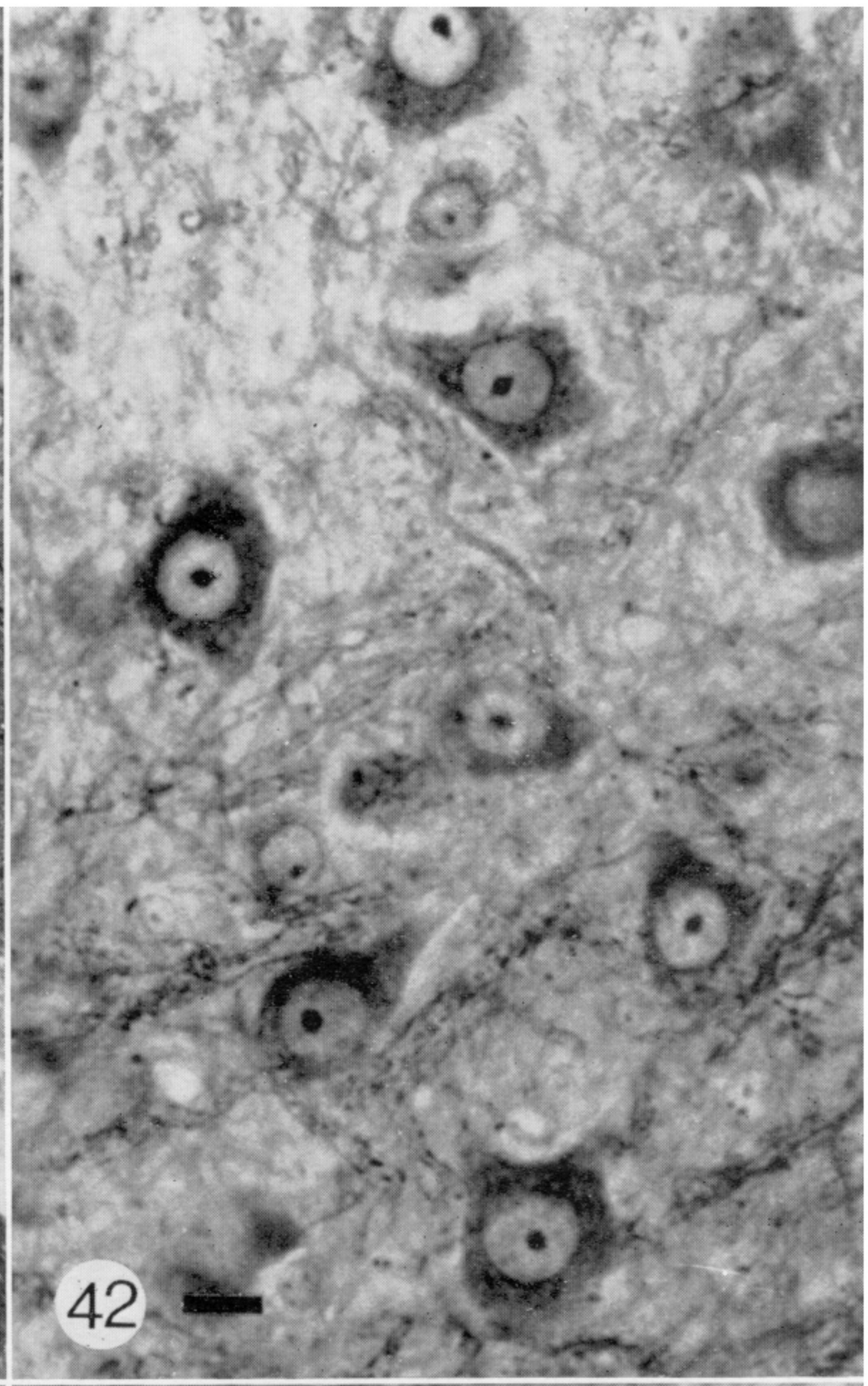

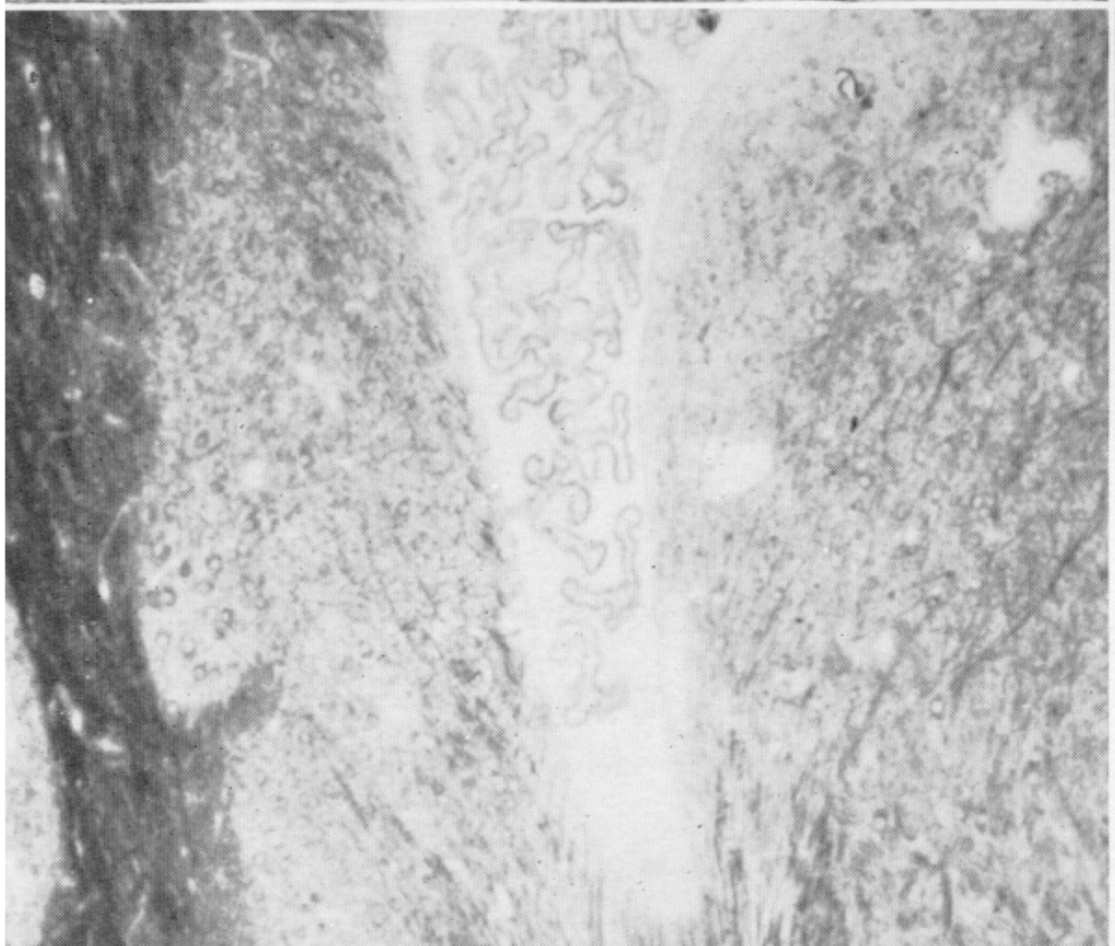

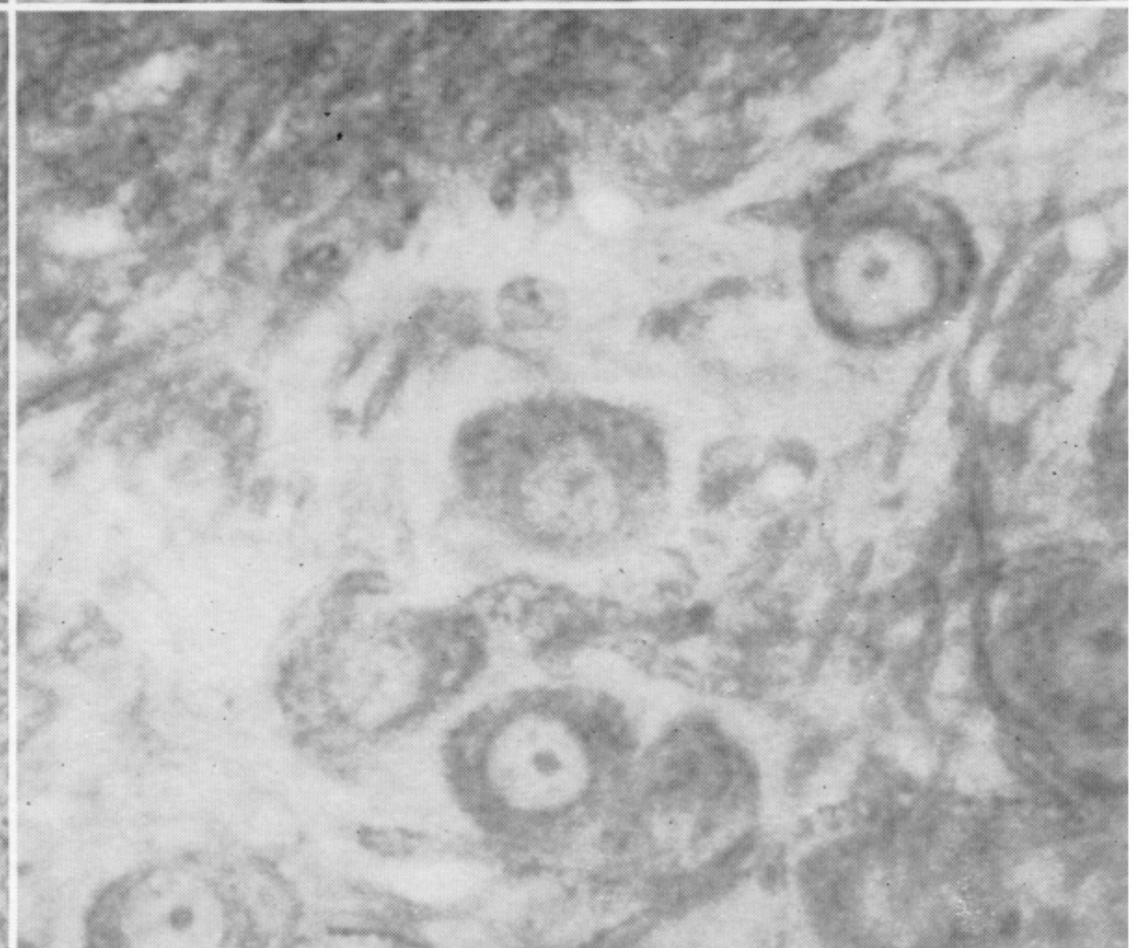

FIGURES 41–44. For description see opposite.